UNIVERSITÀ DEGLI STUDI DI TRIESTE

A Triazolotriazine-Based Dual GSK-3β/CK-1δ Ligand as a Potential Neuroprotective Agent Presenting Two Different Mechanisms of Enzymatic Inhibition

This is the peer reviewed (post-print) version of the following article:

Original
A Triazolotriazine-Based Dual GSK-3β/CK-1δ Ligand as a Potential Neuroprotective Agent Presenting Two Different Mechanisms of Enzymatic Inhibition / Redenti, S., Marcovich, I., De Vita, T., Pérez, C., De Zorzi, R., Demitri, N., Perez, D.I., Bottegoni, G., Bisignano, P., Bissaro, M., Moro, S., Martinez, A., Storici, P., Spalluto, G., Cavalli, A., Federico, S.. - In: CHEMMEDCHEM. - ISSN 1860-7179. - STAMPA. - 14:3(2019), pp. 310-314. [10.1002/cmdc.201800778]

Availability:
This version is available at: 11368/2935106 since: 2019-02-07T09:33:26Z
Publisher:

Published
DOI:10.1002/cmdc.201800778
Terms of use:

Some rights reserved. More details in the PostPrint rights section below.

License:
Digital Rights Management not defined

Publisher copyright

-.-

(Article begins on next page)

21 October 2026

arTs Università degli Studi di Trieste
Archivio della ricerca – postprint

Supporting Information

A Triazolotriazine-Based Dual GSK-3β/CK-1δ Ligand as a Potential Neuroprotective Agent Presenting Two Different Mechanisms of Enzymatic Inhibition

Sara Redenti,[a] Irene Marcovich,[a] Teresa De Vita,[b] Concepción Pérez,[c] Rita De Zorzi,[a] Nicola Demitri,[d] Daniel I. Perez,[c] Giovanni Bottegoni,[e] Paola Bisignano,[f] Maicol Bissaro,[g] Stefano Moro,[g] Ana Martinez,[c] Paola Storici,[d] Giampiero Spalluto,[a] Andrea Cavalli,*[b] and Stephanie Federico*[a]

SUPPORTING INFORMATION

Table of Contents

Experimental Procedures 2
Results and discussion 10
Spectra of tested compound 24

Experimental Procedures

Chemistry

General material and methods used in the synthetic process. Reagents were obtained from commercial suppliers and used without further purification. Reactions were monitored by TLC, on precoated silica gel plates (Macherey-Nagel, SIL G UV_{254}). Final compounds and intermediates were purified by flash chromatography using silica gel as stationary phase (Macherey-Nagel, silica 60, 230-400 mesh). Light petroleum ether refers to the fractions boiling at 40-60°C. Melting points were determined with a Stuart SMP10 melting point apparatus and were not corrected. The ^{1}H NMR and ^{13}C NMR spectra were determined in $CDCl_3$ or DMSO-d_6 solutions and recorded on Jeol GX 270 MHz, Jeol 400 MHz, Varian 400 MHz or Varian 500 MHz spectrometers; chemical shifts (δ scale) are reported in parts per million (ppm) and referenced to residual solvent peak, splitting patterns are abbreviated to: s (singlet), d (doublet), dt (doublet of triplets), q (quartet), t (triplet), m (multiplet) and bs (broad singlet). Coupling constants (*J*) are given in Hz. MS-ESI analysis were performed using ESI Bruker 4000 Esquire spectrometer and compounds were dissolved in methanol; accurate mass spectra of compound **12** in methanol was recorded on micrOTOF-Q – Bruker.Purity of tested compounds were determined by HPLC-DAD (*Waters* 515 HPLC pump; *Waters* PDA 2998 Detector) using Luna C8(2) HPLC column (150 x 4.6 mm, particle size 3 µm). Isocratic elution was performed for 40 min at a flow rate of 300 µL/min in water-methanol 30:70 either containing 2 mM ammonium acetate. UV absorption was detected from 200 to 400 nm using a diode array detector; purity was determined at maximum absorption wavelength of compound and at 254 nm. All compounds showed a purity >95% at the detected wavelengths.

Synthesis of compounds **1-5**

*Synthesis of 2,4,6-triphenoxy-[1,3,5]triazine (**17**).*[1] 2,4,6-Trichloro-[1,3,5]triazine (**16**) (184.4 g, 1.0 mol) was dissolved in phenol (3.0-4.0 mol) and refluxed for 5 h. The hot reaction was extracted with methanol and a white solid (253.7 g) was obtained. Yield 71%; mp 235 °C (EtOAc-light petroleum); ^{1}H NMR (400 MHz, $CDCl_3$): δ 7.40–7.30 (m, 6H), 7.25–7.18 (m, 3H), 7.17–7.10 (m, 6H). ^{13}C NMR (101 MHz, $CDCl_3$) δ 173.80, 151.71, 129.58, 126.18, 121.52.

*Synthesis of (4,6-diphenoxy-[1,3,5]triazin-2-yl)-hydrazine (**18**).*[2] To a solution of 2,4,6-triphenoxy-[1,3,5]triazine (**17**) (20 g, 0.056 mol) in DCM (200 mL), hydrazine monohydrate (3.3 mL, 0.067 mol) in 20 mL of THF was added dropwise and the reaction was stirred overnight. The solvent was removed, the residue suspended in 10 mL of methanol/EtOAc (1:1), then 100 mL of light petroleum were added and the solid was filtered and used in the next step without further purification (yield 72%, 23.0 g). ^{1}H NMR (400 MHz, DMSO-d_6) δ 9.20 (s, 1H), 7.50 – 7.32 (m, 4H), 7.32 – 7.07 (m, 6H), 4.33 (s, 2H).

*Synthesis of N'-(4,6-diphenoxy-[1,3,5]triazin-2-yl)-formohydrazide (**19**).* Formic acid (15.5 mL, 0.41 mol) was added dropwise to a solution of compound **18** (12.0 g, 0.041 mol) in toluene (50 mL). The biphasic mixture was stirred for 4 h at room temperature, then volatiles were removed under vacuum and the residue was purified by gradient elution flash chromatography (DCM to DCM-MeOH 98:2). Yield 69% (9.2 g); white solid; mp 192-193°C (EtOEt-light petroleum); ^{1}H NMR (400 MHz, DMSO-d_6): δ 10.05 (s, 1H), 9.92 (s, 1H), 8.00 (s, 1H), 7.47–7.36 (m, 4H), 7.35–7.09 (m, 6H). ES-MS (methanol) m/z: 324.1 $[M+H]^+$, 346.1 $[M+Na]^+$.

*Synthesis of 5,7-diphenoxy-[1,2,4]triazolo[1,5-a][1,3,5]triazine (**20**).*[3] A mixture of phosphorous pentoxide (0.045 mol) and hexamethyldisiloxane (0.045 mol) in anhydrous xylene (150 mL) was heated to 90°C over 1.5 h and then stirred for 1 h at 90°C, under argon atmosphere. The well-dried *N'*-(4,6-diphenoxy-[1,3,5]triazin-2-yl)-formohydrazide (**19**) (4.85 g, 0.015 mol) was then added to the clear solution, heated under reflux and stirred for 2-3 h. The solvent was then removed, the residue dissolved in DCM (300 mL) and the resulting solution was washed with water (3x100 mL). The organic layer was concentrated, dried over anhydrous sodium sulfate and purified on silica plug (3-4 cm length) in light petroleum-EtOAc 6.5:3.5. Yield 25% (1.1 g); white solid; mp 120-121 °C (EtOEt-light petroleum); ^{1}H NMR (400 MHz, acetone-d_6): δ 8.41 (s, 1H), 7.60–7.49 (m, 4H), 7.48-7.40 (m, 3H), 7.31-7.21 (m, 3H). ^{13}C NMR (101 MHz, acetone-d_6): δ 165.6, 161.1, 157.6, 156.5, 153.3, 151.9, 130.8, 130.4, 128.1, 126.8, 122.36, 122.30. ES-MS (acetonitrile) m/z: 306.1 $[M+H]^+$, 328.1 $[M+Na]^+$.

*Synthesis of 5-phenoxy-[1,2,4]triazolo[1,5-a][1,3,5]triazin-7-amine (**21**).* A solution of the 5,7-diphenoxy-[1,2,4]triazolo[1,5-*a*][1,3,5]triazine derivative (**20**) (0.611 g, 2 mmol) in methanol (20 mL) with methanolic ammonia 7 N (1.7 mL, 12 mmol) was stirred for 3 h at room temperature. The solvent was removed under reduced pressure, the residue was then suspended in a EtOEt-light petroleum mixture and filtered to afford the desired compound **21**. Yield 86% (0.39 g); white solid; mp 130-131 °C (EtOEt-light petroleum); ^{1}H NMR (400 MHz, DMSO-d_6) δ: 9.15-8.77 (bd, 2H), 8.34 (s, 1H), 7.50-7.41 (m, 2H), 7.31-7.20 (m, 3H). ^{13}C NMR (68 MHz, DMSO-d_6): δ 165.2, 158.7, 155.5, 152.7, 152.5, 129.9, 125.7, 122.1. ES-MS (methanol) m/z: 229.4 $[M+H]^+$, 251.4 $[M+Na]^+$, 267.4 $[M+K]^+$.

*Synthesis of N-cyclohexyl-5-phenoxy-[1,2,4]triazolo[1,5-a][1,3,5]triazine-7-amine (**22**).* A solution of 5,7-diphenoxy-[1,2,4]triazolo[1,5-*a*][1,3,5]triazine (**20**) (0.611 g, 2 mmol) and cyclohexylamine (688 µL, 6 mmol) in ethanol (20 mL) was stirred at 50°C for 3 h. The solvent was removed under reduced pressure and the residue was purified by flash chromatography (eluent: EtOAc-light petroleum 7:3) to afford the desired compound as a solid. Yield 94% (0.583 g); sticky foam; ^{1}H NMR (270 MHz; DMSO-d_6): δ 9.26-9.21 (m, 1H), 8.36 (s, 1H), 7.48-7.42 (m, 2H), 7.31-7.23 (m, 3H), 3.92-3.77 (m, 1H), 1.88-1.71 (m, 4H), 1.64-1.42 (m, 3H), 1.33-1.00 (m, 3H). ^{13}C

NMR (101 MHz, DMSO-d_6): δ 165.2, 158.7, 155.3, 152.7, 149.9, 129.8, 125.9, 122.3, 51.1, 31.9, 25.3. ES-MS (methanol) m/z: 311.0 $[M+H]^+$, 333.0 $[M+Na]^+$, 348.9 $[M+K]^+$.

*Synthesis of [1,2,4]triazolo[1,5-a][1,3,5]triazine-5,7-diamine (**1**).* 5,7-diphenoxy-[1,2,4]triazolo[1,5-*a*][1,3,5]triazine (***20***) (0.120 g, 0.39 mmol) was dissolved in methanol (3 mL) and methanolic ammonia 7 N (1.68 mL, 3.9 mmol) was added. The mixture was heated at 75 °C in sealed tube for 12 h. When the reaction was completed, the white precipitate was filtered and washed with methanol. Yield 48.5% (29 mg); white solid; mp >300 °C (methanol). ^{1}H NMR (400 MHz; DMSO-d_6): δ 8.29-7.89 (m, 3H), 6.91-6.78 (bs, 2H). ^{13}C NMR (101 MHz; DMSO-d_6): δ 163.1, 159.3, 154.6, 151.1. ES-MS (methanol/water) m/z: 151.9 $[M+H]^+$, 173.9 $[M+Na]^+$.

*Synthesis of N^5-cyclohexyl-[1,2,4]triazolo[1,5-a][1,3,5]triazin-5,7-diamine (**2**).* A mixture of 5-phenoxy-[1,2,4]triazolo[1,5-*a*][1,3,5]triazin-7-amine (**21**) (68.5 mg, 0.3 mmol) and cyclohexylamine (103 µL, 0.9 mmol) in absolute ethanol (3-4 mL) was poured into a sealed tube and heated at 90 °C for 72 h. When the reaction was completed, the solvent was removed under reduced pressure, the residue was purified by flash chromatography (eluent: EtOAc-light petroleum 5.5:4.5) to afford the desired compound **2**. Yield 34% (24 mg); white solid; mp 223 °C (EtOEt-light petroleum); ^{1}H NMR (400 MHz, DMSO-d_6) δ: 8.33-7.99 (m, 3H), 7.27 + 7.20 (d, J = 8.0 Hz, 1H), 3.76-3.65 (m, 1H), 1.83-1.55 (m, 5H), 1.31-1.06 (m, 5H). ^{13}C NMR (101 MHz; DMSO-d_6): δ 160.2, 158.9, 154.0, 150.1, 49.2, 32.3, 25.3, 24.9. ES-MS (acetonitrile) m/z: 234.5 $[M+H]^{+,}$ 256.5 $[M+Na]^+$, 272.4 $[M+K]^+$.

*Synthesis of N^7-cyclohexyl-[1,2,4]triazolo[1,5-a][1,3,5]triazine-5,7-diamine (**3**).* Compound **3** was obtained applying the same procedure used to obtain compound **2**, using 0.3 mmol of *N*-cyclohexyl-5-phenoxy-[1,2,4]triazolo[1,5-*a*][1,3,5]triazine-7-amine (**22**) (93 mg) and 0.9 mmol of methanolic ammonia 7 N (129 µL). Flash chromatography eluent: EtOAc-light petroleum 7:3. Yield 40% (28 mg); white solid; mp 225 °C (EtOEt-light petroleum); ^{1}H NMR (400 MHz; DMSO-d_6): δ 8.25 (d, J = 8.5 Hz, 1H), 8.03 (s, 1H), 6.91 (s, 2H), 3.92-3.87 (m, 1H), 1.87-1.67 (m, 4H), 1.59 (d, J = 12.5 Hz, 1H), 1.44 (qd, J = 12.5 Hz, J = 3.0 Hz, 2H), 1.33-1.17 (m, 2H), 1.17-1.02 (m, 1H). ^{13}C NMR (101 MHz; DMSO-d_6): δ 162.8, 159.0, 154.1, 148.6, 49.8, 32.1, 25.3, 25.2. ES-MS (methanol) m/z: 234.0 $[M+H]^+$, 255.9 $[M+Na]^+$, 271.9 $[M+K]^+$.

*Synthesis of N^5-N^7-dicyclohexyl-[1,2,4]triazolo[1,5-a][1,3,5]triazine-5,7-diamine (**4**)*. A mixture of 5,7-diphenoxy-[1,2,4]triazolo[1,5-*a*][1,3,5]triazine (0.120 g, 0.39 mmol) and cyclohexylamine (**20**) (0.450 mL, 3.9 mmol) in absolute ethanol (3 mL) was poured into a sealed tube and heated at 95 °C for 12 h. The solvent was removed under reduced pressure and the crude product was purified by flash chromatography (EtOAc–light petroleum 6.5:3.5) to afford the final compound **4**. Yield 64.5% (79 mg); white solid; mp 201-203 °C (EtOEt-light petroleum); ^{1}H NMR (400 MHz; DMSO-d_6): δ 8.42 + 8.20 (d, J = 8.7 Hz, 1H), 8.05 + 8.03 (s, 1H), 7.39-7.33 (m, 1H), 4.02-3.86 (m, 1H), 3.82-3.62 (m, 1H), 1.96-1.39 (m, 12H), 1.37-0.99 (m, 8H). ^{13}C NMR (101 MHz; DMSO-d_6): δ 160.1, 158.7, 153.8, 147.8, 50.6+49.3, 32.4+32.3, 31.8+31.5, 25.3+25.1, 25.1+24.9. ES-MS (methanol) m/z: 316.1 $[M+H]^+$, 338.0 $[M+Na]^+$, 354.0 [M+K]+.

*Synthesis of N^5-benzyl-[1,2,4]triazolo[1,5-a][1,3,5]triazin-5,7-diamine (**5**).* Compound **5** was obtained applying the same procedure used to obtain compound **2**, using 0.9 mmol of benzylamine (98 µL). Flash chromatography eluent: EtOAc-light petroleum 6:4. Yield 46% (33 mg); white solid; mp 263-267 °C (EtOEt-light petroleum); ^{1}H NMR (400 MHz, DMSO-d_6) δ: 8.59-7.95 (m, 3H), 7.89 (t, J = 6.0 Hz, 1H), 7.34-7.27 (m, 4H), 7.26-7.17 (m, 1H), 4.57-4.45 (m, 2H). ^{13}C NMR (101 MHz; DMSO-d_6): δ 161.2, 159.7, 154.1, 150.3, 139.9, 128.2, 127.0, 127.6, 43.7. ES-MS (methanol) m/z: 242.5 $[M+H]^+$, 264.4 $[M+Na]^+$.

Synthesis of compound **6**

*Synthesis of 5-(methylthio)-[1,2,4]triazolo[1,5-a][1,3,5]triazin-7-amine (**24**).*[3] 3-Amino-1,2,4-triazole (**23**) (1.0 g, 11.89 mmol) and dimethyl-*N*-cyanodithioiminocarbonate (1.913 g, 13.08 mol) were mixed in a three-neck round bottom flask and stirred at 170 °C for 1 h in a stream of argon until the two powders melted. The reaction mixture was then cooled and refluxed in a mixture of DCM and methanol for 1 h. The solvent was removed under reduced pressure and the resulting solid was dissolved in ethyl ether (500 mL) and washed with water (5x150 mL). Yield 21% (0.455 g); white solid; mp 261-263 °C (EtOEt); ^{1}H NMR (270 MHz; DMF-d_7): δ 9.06 (s, 1H), 8.81 (s, 1H), 8.40 (s, 1H), 2.55 (s, 3H). ^{13}C NMR (101 MHz; DMSO-d_6): δ 173.5, 157.2, 155.0, 150.2, 14.0. ES-MS (methanol/water) m/z: 182.9 $[M+H]^+$, 204.8 $[M+Na]^+$, 220.8 $[M+K]^+$.

*Synthesis of 5-methylsulfinyl-[1,2,4]triazolo[1,5-a][1,3,5]triazin-7-amine (**25**).*[3] A solution of *meta*-chloroperoxybenzoic acid (*m*-CPBA) (1.1562 g, 6.6 mmol) in 10 mL of DCM was added dropwise to a cooled suspension of compound **24** (0.4 g, 2.2 mmol) in 15 mL of DCM. The resulting mixture was stirred for 12 h at room temperature, the solvent was evaporated and ethanol was added to the residue. The solid was collected by filtration, washed with cool ethanol and dried. Yield 58% (0.253 g); white solid; mp 232-235 °C; ^{1}H NMR (270 MHz; DMSO-d_6): δ 9.59 + 9.23 (bs, 2H), 8.60 (s, 1H), 2.87 (s, 3H). ES-MS (methanol/acetonitrile) m/z: 220.8 $[M+Na]^+$, 236.8 $[M+K]^+$.

*Synthesis of N^5-phenyl-[1,2,4]triazolo[1,5-a][1,3,5]triazin-5,7-diamine (**6**).*[4] To 0.260 g (1.31 mmol) of 5-methylsulfinyl-[1,2,4]triazolo[1,5-*a*][1,3,5]triazin-7-amine (**25**) suspended in acetonitrile, aniline (0.884 mL, 10.48 mmol) was added. The mixture was heated in a sealed tube at 80 °C for 48 h. The solvent was then removed under reduced pressure and the residue was purified by flash chromatography (DCM-MeOH 95:5). Yield 47% (140 mg); white solid; mp 286 °C (EtOEt-light petroleum). ^{1}H NMR (400 MHz; DMSO-d_6): δ 9.62 (s, 1H), 8.38 (bd, 2H), 8.19 (s, 1H), 7.78 (d, J = 7.7 Hz, 2H), 7.38-7.24 (m, 2H), 7.00 (t, J = 7.3 Hz, 1H). ^{13}C NMR (101 MHz; DMSO-d_6): δ 159.1, 158.3, 154.5, 150.5, 139.8, 128.4, 122.2, 120.0. ES-MS (methanol/acetonitrile) m/z: 228.0 $[M+H]^+$, 249.9 $[M+Na]^+$, 265.9 $[M+K]^+$.

Synthesis of compounds **8-11**

*Synthesis of ethyl 3-cyano-benzoate (**27**).* Concentrated sulfuric acid (0.5 mL) was added dropwise to a solution of 3-cyanobenzoic acid (**26**) (10 g, 68 mmol) in absolute ethanol (500 mL), and the reaction mixture was refluxed for 12 h. Solvent was removed and the residue dissolved in EtOAc (300 mL) and washed with saturated $NaHCO_3$ solution and water 1:1 (3x100 mL). The organic phases are dried upon anhydrous sodium sulfate, filtered, the solvent removed and the resulting ethyl ester derivative used without any further purification. Quantitative yield (11.7 g); white solid; mp 55-56 °C (EtOEt-light petroleum); ^{1}H NMR (400 MHz, $CDCl_3$): δ 8.33-8.32 (m, 1H), 8.27 (dt, J = 7.8, 1.4 Hz, 1H), 7.83 (dt, J = 7.8, 1.4 Hz, 1H), 7.58 (t, J = 7.8 Hz, 1H), 4.41 (q, J = 7.1 Hz, 2H), 1.41 (t, J = 7.1 Hz, 3H). ES-MS (methanol) m/z: 148.0 $[M+H-(CH_2CH_3)]^+$ 176.0 $[M+H]^+$, 198.0 $[M+Na]^+$.

*Synthesis of 3-cyano-benzohydrazide (**28**).* To a solution of compound **27** (17.5 g, 0.1 mol) in ethanol (500 mL), hydrazine hydrate (52 mL, 0.5 mol) was added and the solution heated under reflux for 48 h. Then, the solvent was removed under reduced pressure and the residue purified by flash chromatography (eluent: EtOAc). Yield 60% (9.7 g); pale pink solid; mp 171-174°C (EtOEt-light petroleum); ^{1}H NMR (400 MHz, DMSO-d_6) δ: 9.96 (s, 1H), 8.19-8.09 (m, 2H), 7.97 (dt, *J* = 7.8, 1.4 Hz, 1H), 7.67 (t, *J* = 7.8 Hz, 1H), 4.56 (s, 2H). ES-MS (methanol) m/z: 162.0 $[M+H]^+$.

*Synthesis of 3-cyano-N'-(4,6-diphenoxy-1,3,5-triazin-2-yl)benzohydrazide (**29**).*[5] 2,4,6-triphenoxy-[1,3,5]triazine (**17**, 10.0 g, 0.028 mol) and 3-cyano-benzohydrazide (**28**) (7.66 g, 0.0476 mol) were dissolved in anhydrous THF (200 mL) while DBU (7.1 mL, 0.0476 mmol) was added dropwise at 0°C. The mixture was stirred at room temperature for 12 h. The solvent was then removed, the residue was dissolved in DCM (300 mL), and the resulting solution washed with water (3x100 mL). The organic layer was concentrated, dried over anhydrous sodium sulphate and purified by flash chromatography (eluent: DCM-MeOH 99:1). Yield 56.5% (6.7 g); white solid; mp 213-215 °C (EtOEt-light petroleum); ^{1}H NMR (400 MHz, DMSO-d_6) δ: 10.57 (bs, 1H), 10.15 (bs, 1H), 8.05-7.96 (m, 3H), 7.69 (m, 1H), 7.45-7.41 (m, 2H), 7.28-7.08 (m, 8H). ES-MS (methanol) m/z: 425.1 $[M+H]^+$, 447.1 $[M+Na]^+$.

*Synthesis of 3-(7-amino-5-phenoxy-[1,2,4]triazolo[1,5-a][1,3,5]triazin-2-yl)benzonitrile (**30**).*[3] The mixture of phosphorous pentoxide (10.6 g, 0.075 mol) and hexamethyldisiloxane (16.0 mL, 0.075 mol) in anhydrous xylene (150 mL) was heated to 90 °C over 1.5 h and then stirred for 1 hour at 90°C, under argon atmosphere. The well-dried 3-cyano-*N*'-(4,6-diphenoxy-1,3,5-triazin-2-yl)benzohydrazide (**29**) (6.36 g, 0.015 mol) was then added to the clear solution and the reaction was heated under reflux and stirred for 2-3 h. The solvent was then removed, the residue dissolved in DCM (300 mL) and the resulting solution was washed with water (3x100 mL). The organic layer was dried over anhydrous sodium sulphate, concentrated and readily used in the next step without purification due to stability problems. In the second step, the product was dissolved in methanol (20 mL) and methanolic ammonia 7 N (1.7 mL, 12 mmol) was added to the solution, which was stirred for 3 h at room temperature. The solvent was removed under reduced pressure and the residue was then suspended in a EtOEt-light petroleum mixture and filtered to afford the desired compound **30**. Overall yield 19% (125 mg); white solid; mp 295-297 °C (EtOEt-light petroleum); ^{1}H NMR (400 MHz, DMSO-d_6) δ: 9.18 + 8.80 (bs, 2H), 8.41-8.37 (m, 2H), 8.01-7.96 (m, 1H), 7.76 (t, *J* = 7.8 Hz, 1H), 7.45 (t, *J* = 7.8 Hz, 2H), 7.29-7.23 (m, 3H). ^{13}C NMR (101 MHz; DMSO-d_6): δ 165.4, 162.4, 159.7, 152.8, 152.5, 134.4, 131.9, 131.5, 130.9, 130.4, 130.0, 125.9, 122.2, 118.7, 112.6. ES-MS (methanol) m/z: 330.1 $[M+H]^+$, 352.1 $[M+Na]^+$.

*Synthesis of 3-(7-amino-5-(cyclohexylamino)-[1,2,4]triazolo[1,5-a][1,3,5]triazin-2-yl) benzonitrile (**10**).* Compound **10** was obtained applying the same procedure used to obtain compound **2**, using 0.3 mmol of 3-(7-amino-5-phenoxy-[1,2,4]triazolo[1,5-*a*][1,3,5]triazin-2-yl)benzonitrile (**30**) (99 mg) and 0.9 mmol of cyclohexylamine (103 µL). Flash chromatography eluent: DCM-MeOH 98:2. Yield 47.5% (0.476 g); white solid; mp 297-299 °C (EtOEt-light petroleum); ^{1}H NMR (400 MHz, DMSO-d_6) δ: 8.71-8.31 (m, 2H), 8.29-7.87 (m, 3H), 7.86-7.64 (m, 1H), 7.45 +7.37 (d, *J* = 8.0 Hz, 1H), 3.90-3.61 (m, 1H), 1.96-1.79 (m, 2H), 1.79-1.66 (m, 2H), 1.66-1.50 (m, 1H), 1.47-0.99 (m, 5H). ^{13}C NMR (101 MHz; DMSO-d_6): δ 160.7, 160.3, 159.6, 150.0, 133.4, 132.1, 130.9, 130.2, 129.8, 118.4, 111.9, 49.4, 32.6+32.3, 25.3+24.9. ES-MS (methanol) m/z: 335.2 $[M+H]^+$, 357.2 $[M+Na]^+$.

*Synthesis of 3-(7-amino-5-(benzylamino)-[1,2,4]triazolo[1,5-a][1,3,5]triazin-2-yl)benzonitrile (**11**).* Compound **11** was obtained applying the same procedure used to obtain compound **2**, using 0.3 mmol of 3-(7-amino-5-phenoxy-[1,2,4]triazolo[1,5-*a*][1,3,5]triazin-2-yl)benzonitrile (**30**) (99 mg) and 0.9 mmol of benzylamine (98 µL). Flash chromatography eluent: DCM-MeOH 98:2. Yield 54% (0.555 g); white solid; mp 288-289 °C (EtOEt-light petroleum); ^{1}H NMR (400 MHz, DMSO-d_6) δ: 8.69-7.90 (m, 6H), 7.75 (t, *J* = 7.8 Hz, 1H), 7.44-7.27 (m, 4H), 7.27-7.18 (m, 1H), 4.66-4.32 (m, 2H). ^{13}C NMR (101 MHz; DMSO-d_6): δ 161.3, 160.8, 159.5, 150.1, 139.8, 133.5, 132.1, 130.9, 130.2, 129.8, 128.2, 127.1, 126.6, 118.3, 111.9, 43.8. ES-MS (methanol) m/z: 341.0 $[M-H]^-$.

*Synthesis of 3-(7-amino-5-(cyclohexylamino)-[1,2,4]triazolo[1,5-a][1,3,5]triazin-2-yl)benzamide (**8**).*[6] A solution of nitrile derivative **10** (67 mg, 0.2 mmol) in a mixture of TFA-H_2SO_4 (375 µL, 4:1, v/v) was stirred at 70 °C for three h. Once completed, the reaction was quenched with ice-cold water (2 mL). The precipitate was filtered and washed with cold water and methanol. Yield 59% (41 mg); white solid; mp 266-268 °C; ^{1}H NMR (400 MHz, DMSO-d_6) δ: 8.72-8.57 (m, 1H), 8.45-7.94 (m, 5H), 7.79-7.41 (m, 3H), 3.81-3.67 (bs, 1H), 1.92-1.54 (m, 5H), 1.36-1.04 (m, 5H). ^{13}C NMR (101 MHz; DMSO-d_6): δ 185.84, 171.51, 167.41, 160.04, 159.65, 135.08, 129.16, 128.86, 126.27, 49.89, 32.18, 24.84. ES-MS (methanol) m/z: 353.2 $[M+H]^+$.

*Synthesis of 3-(7-amino-5-(benzylamino)-[1,2,4]triazolo[1,5-a][1,3,5]triazin-2-yl)benzamide (**9**).*[6] Compound **9** was obtained applying the same procedure used to obtain compound **8**, using 0.2 mmol of 3-(7-amino-5-(benzylamino)-[1,2,4]triazolo[1,5-*a*][1,3,5]triazin-2-yl)benzonitrile (**11**) (68 mg). Yield 59% (42 mg); white solid; mp 249-252 °C; ^{1}H NMR (400 MHz, DMSO-d_6) δ: 8.80-7.87 (m, 7H), 7.64-7.13 (m, 7H), 4.58-4.45 (m, 2H). ^{13}C NMR (101 MHz; DMSO-d_6): δ 167.41, 166.67, 161.25, 161.19, 150.04, 139.61, 135.01, 129.17, 128.80, 128.27, 128.23, 127.21, 127.16, 127.08, 126.68, 43.88. ES-MS (methanol) m/z: 361.2 $[M+H]^+$.

Synthesis of compounds **12-15**

*Synthesis of benzyloxy acetic acid (**32**).*[7] A solution of benzyl alcohol (**31**) (21.6 g, 0.2 mol) in dry toluene (40 mL) was added at 0 °C to a stirred suspension of NaH (16.0 g, 60% dispersion in mineral oil, 0.4 mol) in dry toluene (100 mL). After mixing for 1 hour at room temperature, a solution of chloroacetic acid (27.8 g, 0.2 mol) in dry toluene (100 mL) was added. The resulting slurry was stirred at room temperature for 1 h and then at 80°C for 2 h. After cooling at room temperature, water was added (300 mL) and the mixture was washed with diethyl ether (3x100 mL). The aqueous layer was acidified with concentrated HCl (23 mL) to pH 2 and extracted repeatedly with DCM (3x100 mL). The combined organic extracts were dried over anhydrous sodium sulphate, then the solvent was evaporated to give the crude product as pale yellow oil (yield 65%, 24.6 g). ^{1}H NMR (270 MHz; $CDCl_3$): δ 10.17 (bs, 1H), 7.31-7.18 (m, 5H), 4.53 (s, 2H), 4.02 (s, 2H). MS (methanol) m/z: 189.0 $[M+Na]^+$.

*Synthesis of 2-(benzyloxy)-N'-(4,6-diphenoxy-1,3,5-triazin-2-yl)acetohydrazide (**33**).* Benzyloxyacetic acid (**32**) (5.19 g, 30.8 mmol) was dissolved in DCM (50 mL) and oxalyl chloride (3.39 mL, 40.0 mmol) was added at room temperature. The solution was stirred for 4 h under reflux then the solvent was removed by evaporation under reduced pressure to give the corresponding acyl chloride, which was readily directly added dropwise to a solution of (4,6-diphenoxy-[1,3,5]triazin-2-yl)-hydrazine (**18**) (7.0 g, 23.7 mmol) and triethylamine (23.7 mmol) in dry DCM (80 mL). The mixture was stirred for 12h at room temperature.[2] The solvent was removed

under reduced pressure and the crude residue purified by flash chromatography (light petroleum-EtOAc 6.5:3.5) to afford the desired compound. Yield 55% (5.8 g); white solid; mp 147 °C (EtOEt-light petroleum); ^{1}H NMR (270 MHz, DMSO-d_6) δ: 9.94-9.87 (m, 2H), 7.48-7.15 (m, 15H), 4.48 (s, 2H), 3.92 (s, 2H). ES-MS (methanol) m/z: 444.0 [M+H]$^+$, 465.9 [M+Na]$^+$, 481.9 [M+K]$^+$.

*Synthesis of 2-((benzyloxy)methyl)-N^5-N^7-dicyclohexyl-[1,2,4]triazolo[1,5-a][1,3,5]triazine-5,7-amine (**34**).*[3] The mixture of phosphorous pentoxide (12.8 g, 0.045 mol) and hexamethyldisiloxane (9.6 mL, 0.045 mol) in anhydrous xylene (150 mL) was heated to 90 °C over 1.5 h and then stirred for 1 hour at 90°C, under argon atmosphere. The well-dried derivative **33** (6.7 g, 0.015 mol) was then added to the clear solution, heated under reflux and stirred for 2-3 h. The solvent was then removed, the residue dissolved in DCM (300 mL) and the resulting solution was washed with water (3x100 mL). The organic layer was concentrated, dried over anhydrous sodium sulfate and purified to afford the desired 2-((benzyloxy)methyl)-5,7-diphenoxy-[1,2,4]triazolo[1,5-*a*][1,3,5]triazine. Due to stability problems, the crude was roughly purified on silica plug (3-4 cm length) in light petroleum-EtOAc 7:3 and readily used in the next step. In particular, the obtained solid was reacted with a large excess of cyclohexylamine (5 mL) in absolute ethanol (40 mL). Then, reaction was poured into a sealed tube and heated at 95 °C for 24 h. The solvent was removed under reduced pressure, and the crude product was purified by flash chromatography (EtOAc–light petroleum 4:6) to afford the final compound as sticky foam. Overall yield 12.5% (82 mg). ^{1}H NMR (400 MHz): δ 8.49 + 8.26 (d, *J* = 8.7 Hz, 1H), 7.46-7.28 (m, 6H), 4.59 (s, 2H), 4.51 (s, 2H), 3.96-3.65 (m, 2H), 1.90-1.42 (m, 12H), 1.35-1.04 (m, 8H). ^{13}C NMR (101 MHz, DMSO-d_6): δ 160.0, 159.2, 153.6, 151.6, 147.7, 128.2, 127.70, 127.52, 71.6, 65.2, 49.3, 32.9, 31.8, 25.7+25.6, 25.3. ES-MS (methanol) m/z: 436.2 [M+H]$^+$, 458.3 [M+Na]$^+$.

*Synthesis of 2-((benzyloxy)methyl)-5-phenoxy-[1,2,4]triazolo[1,5-a][1,3,5]triazin-7-amine (**35**).* Compound **35** was obtained applying the same procedure used to obtain compound **34** but using a different second step reaction. In detail, the slightly purified solid was dissolved in methanol (20 mL) with methanolic ammonia 7 N (1.7 mL, 12 mmol) and it was stirred for 3 h at room temperature. The solvent was removed under reduced pressure and the residue purified by flash chromatography (eluent: EtOAc-light petroleum 7:3). Desired compound **35** was obtained as a white solid (1.57 g, yield on two steps 30%) after precipitation in EtOEt-light petroleum. Mp 113-114°C; ^{1}H NMR (400 MHz, DMSO-d_6): δ 9.09 (bs, 1H), 8.85 (bs, 1H), 7.45 (t, *J* = 7.9 Hz, 2H), 7.36 (d, *J* = 4.2 Hz, 4H), 7.33-7.21 (m, 4H), 4.60 (s, 4H). ^{13}C NMR (101 MHz, DMSO-d_6): δ 165.3, 164.7, 159.3, 152.9, 152.4, 138.3, 130.0, 128.7, 128.22, 128.03, 125.8, 122.2, 72.2, 65.5. ES-MS (methanol) m/z: 348.9 [M+H]$^+$, 370.8 [M+Na]$^+$, 386.8 [M+K]$^+$.

*Synthesis of 2-((benzyloxy)methyl)-N^5-cyclohexyl-[1,2,4]triazolo[1,5-a][1,3,5]triazine-5,7-diamine (**36**).* Compound **35** (104 mg, 0.3 mmol) and cyclohexylamine (103 µL, 0.9 mmol) in absolute ethanol (3-4 mL) were poured into a sealed tube and heated at 90 °C for 72 h. When the reaction was completed, the solvent was removed under reduced pressure, the residue was purified by flash chromatography (eluent: EtOAc-light petroleum 1:1) and then precipitated (EtOAc-light petroleum) to afford the desired compound **36** as a white solid (52 mg, yield 49%). Mp 96-98 °C. ^{1}H NMR (400 MHz, DMSO-d_6): δ 8.32-7.91 (m, 2H), 7.36-7.19 (m, 6H), 4.56 (s, 2H), 4.47 (s, 2H), 3.76-3.65 (m, 1H), 1.87-1.52 (m, 5H), 1.33-1.03 (m, 5H). ^{13}C NMR (101 MHz, DMSO-d_6): δ 178.2, 163.4, 159.7, 150.4, 138.4, 128.7, 128.2, 128.0, 72.1, 65.7, 49.7, 32.7, 25.8, 25.3. ES-MS (methanol) m/z: 354.2 [M+H]$^+$, 376.2 [M+Na]$^+$.

*Synthesis of (7-amino-5-(cyclohexylamino)-[1,2,4]triazolo[1,5-a][1,3,5]triazin-2-yl)methanol (**37**).* To a stirred suspension of compound **36** (71 mg, 0.2 mmol) and an equal weight of 10% Pd-C in dry methanol (10 mL), ammonium formate (126 mg, 2 mmol) was added in a single portion. The resulting reaction mixture was stirred under argon atmosphere at reflux for 3 h. Once completed, the catalyst was removed by filtration through a celite pad, which was then washed with methanol. The solvent was evaporated under reduced pressure and the crude product dissolved in EtOAc (50 mL) and washed with water (3 x 15 mL). Finally, the organic phase was dried over anhydrous sodium sulfate, the solvent evaporated under reduced pressure and the residue precipitated with EtOEt and light petroleum to afford 38 mg of the desired derivative **37** as a white solid (yield 72%). Mp 177-180 °C; ^{1}H NMR (400 MHz, DMSO-d_6): δ 8.39-7.83 (m, 2H), 7.37-7.17 (m, 1H), 5.36-5.29 (m, 1H), 4.53-4.39 (m, 2H), 3.77-3.66 (m, 1H), 1.95-1.52 (m, 5H), 1.39-1.03 (m, 5H). ^{13}C NMR (101 MHz, DMSO-d_6): δ 166.5, 160.6, 159.7, 150.4, 58.0, 49.7+49.0, 33.1+32.7, 25.7+25.3. ES-MS (methanol) m/z: 264.1 [M+H]$^+$, 286.1 [M+Na]$^+$, 302.0 [M+K]$^+$.

*Synthesis of (5,7-bis(cyclohexylamino)-[1,2,4]triazolo[1,5-a][1,3,5]triazin-2-yl)methanol (**38**).* Compound **38** was obtained applying the same procedure used to obtain compound **37**, using 87 mg of compound **34** (0.2 mmol). Flash chromatography eluent: DCM-MeOH 95:5. Yield 62% (43 mg); white solid; 165-167 °C (EtOEt-light petroleum). ^{1}H NMR (400 MHz): δ 8.42 + 8.19 (d, *J* = 8.4 Hz, 1H), 7.44 + 7.34 (d, *J* = 7.7 Hz, 1H), 5.39-5.28 (m, 1H), 4.44 (d, *J* = 4.6 Hz, 2H), 3.97-3.79 (m, 1H), 3.76-3.61 (m, 1H), 1.95-1.36 (m, 12H), 1.36-1.00 (m, 8H). ^{13}C NMR (101 MHz, DMSO-d_6): δ 166.3, 163.3, 160.4, 148.2, 58.0, 49.76, 49.68, 32.9+32.7, 32.3+32.0, 25.7+25.51, 25.38+25.33. ES-MS (methanol) m/z: 346.5 [M+H]$^+$, 368.4 [M+Na]$^+$.

*Synthesis of 7-amino-5-(cyclohexylamino)-[1,2,4]triazolo[1,5-a][1,3,5]triazine-2-carbaldehyde (**39**).*[8] A solution of alcohol **37** (263 mg, 1 mmol) in 15 mL of DCM at 0 °C was oxidised at room temperature with Dess-Martin reagent (636 mg, 1.5 mmol). After 3 h of stirring, the reaction mixture was diluted with DCM (20 mL) and washed with a 1:1 solution of saturated sodium thiosulfate and saturated sodium bicarbonate to destroy the excess of Dess-Martin periodinane (3x10 mL). The organic phase was then dried over anhydrous sodium sulfate, the solvents removed under reduced pressure and the residue purified by flash chromatography (eluent: EtOAc- MeOH 95:5). Yield 68% (0.178 g); white solid; mp 153-156 °C (EtOEt-light petroleum); ^{1}H NMR (500 MHz, DMSO-d_6): δ 9.91 (s, 1H), 8.68-8.22 (m, 2H), 7.63 + 7.51 (d, *J* = 8.0 Hz, 1H), 3.82-3.63 (m, 1H), 2.03-1.42 (m, 5H), 1.41-1.04 (m, 5H). ES-MS (methanol) m/z: 262.1 [M+H]$^+$, 284.0 [M+Na]$^+$.

*Synthesis of 5,7-bis(cyclohexylamino)-[1,2,4]triazolo[1,5-a][1,3,5]triazine-2-carbaldehyde (**40**).*[8] Compound **40** was obtained applying the same procedure used to obtain compound **39**, using 345 mg of compound **38** (1 mmol). Flash chromatography eluent: DCM-MeOH 95:5. Yield 73% (0.251 g); white solid; mp 133-135 °C (EtOEt-light petroleum); ^{1}H NMR (400 MHz, DMSO-d_6): δ 9.92 (s, 1H), 8.92 + 8.68 (d, *J* = 8.0 Hz, 1H), 7.74 + 7.66 (d, *J* = 7.8 Hz, 1H), 4.01-3.83 (m, 1H), 3.78-3.64 (m, 1H), 1.92-1.45 (m, 12H), 1.36-1.06 (m, 8H). ES-MS (methanol) m/z: 376.5 [M+Na]$^+$.

*Synthesis of 3-(7-amino-5-(cyclohexylamino)-[1,2,4]triazolo[1,5-a][1,3,5]triazin-2-yl)-2-cyanoacrylamide (**12**).*[9] To a solution of aldehyde **39** (104 mg, 0.4 mmol) in DCM (5 mL), DBU (0.72 mL, 4.8 mmol) and 2-cyanoacetamide (404 mg, 4.8 mmol) were added. The reaction was stirred at room temperature for 2 h. Then the organic phase was dried over anhydrous sodium sulphate, the solvent

was removed under reduced pressure and the residue was purified by flash column chromatography (eluent: DCM-MeOH 96:4) to give the desired products as a pale yellow solid. Yield 14% (18 mg); yellow solid; mp 218-221 °C (EtOEt-light petroleum); ^{1}H NMR (400 MHz, DMSO-d_6): δ 8.84-7.68 (m, 4H), 7.81 (s, 1H), 7.51 (d, *J* = 7.8 Hz, 1H), 3.77 (bs, 1H), 2.06-1.51 (m, 5H), 1.54-0.90 (m, 5H). ^{13}C NMR (68 MHz, DMSO-d_6): δ 162.3, 160.6, 159.5, 158.3, 150.1, 138.8, 115.0, 112.6, 49.5, 32.2, 25.3, 24.8. ES-MS (methanol) m/z: 328.1 $[M+H]^+$, 350.1 $[M+Na]^+$, 366.0 $[M+K]^+$. HRMS (ESI-TOF) m/z: $[M+H]^+$ Calc. for $C_{14}H_{18}N_9O$ 328.1634, found 328.1629; $[M+Na]^+$ Calc. for $C_{14}H_{17}N_9ONa$ 350.1454, Found 350.1450.

*Synthesis of 3-(5,7-bis(cyclohexylamino)-[1,2,4]triazolo[1,5-a][1,3,5]triazin-2-yl)-2-cyanoacrylamide (**13**).*[9] Compound **13** was obtained applying the same procedure used to obtain compound **12**, using 150 mg of compound **40** (0.4 mmol). Flash chromatography eluent: DCM-MeOH 99:1. Yield 8% (13 mg); pale yellow solid; mp 199-204 °C (EtOEt-light petroleum); ^{1}H NMR (400 MHz, DMSO-d_6): δ 8.65+8.44 (bd, *J* = 8.7 Hz, 1H), 8.06 (bs, 1H), 7.93 (bs, 1H), 7.80 (s, 1H), 7.64 (bd, *J* = 7.8 Hz, 1H), 4.47-3.57 (m, 2H), 2.07-1.42 (m, 12H), 1.41-0.93 (m, 8H). ^{13}C NMR (68 MHz, DMSO-d_6): δ 162.2, 160.4, 159.4, 158.1, 147.8, 138.7, 115.0, 112.5, 49.6, 49.5, 32.2, 31.7, 25.2, 25.0, 24.8. ES-MS (methanol) m/z: 410.3 $[M+H]^+$, 432.3 $[M+Na]^+$.

Synthesis of (cyanomethylene)triphenylphosphorane.[10] Triphenylphosphine (6.55 g, 25 mmol) and chloroacetonitrile (1.9 g, 25 mmol) were dissolved in ethyl acetate (5 mL) and the mixture was heated under reflux for 90 min. The resulting precipitate was filtered off and washed with diethyl ether to afford (cyanomethyl)triphenylphosphonium chloride as colorless crystals (1.15 g, 3.4 mmol), that were suspended in DCM (40 mL) and stirred while triethylamine (1.18 mL, 8.5 mmol) was added over 15 min. The mixture was stirred for further 30 min and then washed with water (3x10 mL), dried, and evaporated to give the ylide as a white solid. Yield 10% (0.753 g); mp 195-196 °C (EtOEt-light petroleum); ^{1}H NMR (400 MHz, DMSO-d_6): δ 7.74-7.56 (m, 15H), 1.73-1.71 (m, 1H). ES-MS (methanol) m/z: 302.1 $[M+H]^+$.

*Synthesis of 3-(7-amino-5-(cyclohexylamino)-[1,2,4]triazolo[1,5-a][1,3,5]triazin-2-yl)acrylonitrile derivatives (**14**,**15**).*[9] To a solution of aldehyde **39** (0.100 mg, 0.38 mmol) in DCM (10 mL) 0.458 g of (triphenylphosphoranylidine)acetonitrile (1.52 mmol) were added and the reaction mixture was stirred at room temperature. After 3 h the solvent was removed under reduced pressure and then it was adsorbed on silica and purified by flash chromatography to yield the two isomers of the acrylonitrile derivative.

Isomer Z (cis), compound **14**. Flash chromatography eluent: EtOAc-light petroleum 1:1 to 7:3. Yield 27% (30 mg); white solid; mp 197-200 °C (EtOEt-light petroleum). ^{1}H NMR (400 MHz; DMSO-d_6): δ 8.58-7.96 (m, 2H), 7.52-7.41 (m, 1H), 7.21 (d, *J* = 12.0 Hz, 1H), 6.17 (d, *J* = 12.0 Hz, 1H), 3.82-3.71 (m, 1H), 1.93-1.53 (m, 5H), 1.43-1.04 (m, 5H). ^{13}C NMR (68 MHz, DMSO-d_6): δ 160.1, 159.1, 158.8, 149.9, 137.5, 116.4, 102.6, 49.4, 32.4+32.3, 25.3+24.9. ES-MS (methanol) m/z: 285.1 $[M+H]^+$, 307.1 $[M+Na]^+$, 323.1 $[M+K]^+$.

Isomer E (trans), compound **15**. Flash chromatography eluent: EtOAc-light petroleum 1:1. Yield 27.5% (30 mg); white solid; mp 247-249 °C (EtOEt-light petroleum). ^{1}H NMR (400 MHz; DMSO-d_6): δ 8.52-8.05 (m, 2H), 7.57-7.42 (m, 2H), 6.62 (d, *J* = 16.2 Hz, 1H), 3.79-3.61 (m, 1H), 1.91-1.55 (m, 5H), 1.35-1.05 (m, 5H). ^{13}C NMR (68 MHz, DMSO-d_6): δ 160.2, 159.3, 158.9, 149.9, 140.01, 117.7, 104.1, 49.7+49.5, 32.5+32.2, 25.3+24.8. ES-MS (methanol) m/z: 285.1 $[M+H]^+$, 307.1 $[M+Na]^+$.

Chemical Reactivity of compound **12**

HPLC-MS methodology.[11] Hundred microliters of a methanol solution of compound **12** (25 mM), 100 µL of methanol solution of 2-mercaptoethanol (25 mM) and 100 µL of methanol solution of triethylamine (25 mM) were added to 700 µL of methanol and stirred for 1, 2 or 24 h. The reaction progress was followed by HPLC-MS (HPLC Finningan Surveyor with *Waters* 2996 PDA Detector, coupled to ESI-IT mass spectrometer Pump Plus; column SunFire™ C18, 3.5 µm, 4.6 mm x 50 mm), in a gradient from water-acetonitrile 90:10 to acetonitrile (100%), with both solvents containing 0.1% formic acid, over 25 minutes. Peaks corresponding to compound **12** and BME adduct were identified by their masses and the percentage in each sample was determined by measuring the area under the curve for these peaks in the full scan PDA trace. Compound **12** (MW = 327) showed a retention time of 18.0 min, while retention time for the S-alkylated derivative (MW = 405) presented a retention time of 16.7 min.

UV-visible spectrometry methodology.[9] Reactions of compound **12** with βME were monitored with a multimode plate reader Tecan Infinite® M1000, using Greiner UV Star® flat-bottom clear 96-well plates. Reactions were initiated by mixing 25 µL of compound **12** (1.7 mM in PBS/DMSO 70:30, pH 7.4) with 25 µL of 2-mercaptoethanol (0–200 mM in PBS/DMSO 70:30, pH 7.4, two-fold dilution series). Final solutions, containing 0.85 mM compound **12** and increasing concentrations of BME, were incubated for 10 min at room temperature before acquiring absorption spectra (250–500 nm). Formation of the thiol adduct was monitored by the disappearance of the absorbance peak (λ_{max}= 350 nm) relative to the no-BME control sample.

Biochemistry

Kinases activity assays.

KinaseGlo assay. Compounds were evaluated towards CK-1δ (Merck Millipore, recombinant human, amino acids 1-294, with N-terminal GST-tagged) and GSK-3β (Merck Millipore, recombinant human, full length, with N-terminal GST-tagged) with the KinaseGlo® luminescence assay (Promega) following procedures reported in literature.[12,13] In detail, luminescent assays were performed in black 96-well plates, using the following buffer: 50 mM HEPES (pH 7.5), 1 mM EDTA, 1 mM EGTA, and 15 mM magnesium acetate. Compound CR8 (IC_{50} = 0.4 µM) was used as positive control for CK-1δ and SB415286 (IC_{50} = 0.103 µM) for GSK-3β,[12,14] while DMSO/buffer solution was used as negative control. In a typical assay, 10 µL of inhibitor solution (dissolved in DMSO at 10 mM concentration and diluted in assay buffer to the desired concentration) and 10 µL (16 ng of CK-1δ or 20 ng of GSK-3β) of enzyme solution were added to the well, followed by 20 µL of assay buffer containing 0.1% casein substrate and 4 µM ATP for CK-1δ or 20 µL of assay buffer containing 50 µM of GS-2 substrate and 2 µM ATP for GSK-3β. The final DMSO concentration in the reaction mixture did not exceed 1-2%. After 60 minutes of incubation at 30 °C for CK-1δ and 30 minutes at the same temperature for GSK-3β, the enzymatic reactions were stopped with 40 µL of Kinase-Glo reagent (Promega). Luminescence signal (relative light unit, RLU) was recorded after 10 minutes at 25 °C using Tecan Infinite M100 or FLUOstar Optima multimode readers.

The activity is proportional to the difference of the total and consumed ATP. The inhibitory activities were calculated on the basis of maximal activities measured in the absence of inhibitor, following this equation:

Inhibition (%) = $(RLU_X - RLU_{CTRL-}) / (RLU_{CTRL+} - RLU_{CTRL-}) \cdot 100$

Where RLU stays for Relative Light Unit and in particular: RLU_X is the luminescence signal measured in the well of the test compound; RLU_{CTRL-} the luminescence measured in absence of inhibitor, RLU_{CTRL+} the luminescence of the well containing the reference compound at a concentration that ensure total enzyme inhibition (100 μM for both compounds). First, enzyme activity percentage was determined at 10 μM for each inhibitor with respect to DMSO; subsequently, subsequently for the most active compounds the IC_{50} values were determined. Data were analyzed using Excel and GraphPad Prism software (version 6.0); IC_{50} curve fits were determined using sigmoidal dose–response (variable slope) equations.

In GSK-3β reversibility studies, the evaluation of enzymatic activity was determined after different times of pre-incubation (0, 5, 10 min) of the enzyme with the inhibitor before adding substrates.[15] Data were analyzed using Excel.

ATP competition assays. Kinetic experiments varying both the ATP (from 1 to 50 μM) and the concentrations of inhibitors (compound **12** from 0.5 to 1 μM for CK-1δ and from 0.1 to 0.5 μM for GSK-3β; compound **4** from 5 to 10 μM for GSK-3β) were performed using the ADP-Glo Kinase Assay (Promega) in black 96-well plates. Tests were carried out applying the same procedure reported above for activity assays, but after incubation at 30 °C the enzymatic reactions were stopped with 40 μL of ADP-Glo™ Reagent, followed by Kinase Detection Reagent addition. Then, luminescence was recorded after 10 min at 25 °C using a FLUOstar Optima multimode reader. Data were analyzed using Excel.

CNS permeation prediction: PAMPA-BBB assay

Prediction of the brain penetration of active compounds was evaluated using a parallel artificial membrane permeability assay (PAMPA).[16] Ten drugs of known BBB permeability (2-6 mg of Caffeine, Enoxacine, Hydrocortisone, Desipramine, Ofloxacine, Piroxicam, Testosterone, 12-15 mg of Promazine and Verapamil and 23 mg of Atenolol dissolved in 1000 μL of ethanol) were included in each experiment to validate the analysis set. Compounds were dissolved in a 70/30 PBS pH=7.4 buffer/ethanol solution in a concentration that ensures adequate absorbance values in the UV-VIS light spectrum. 5 mL of these solutions were filtered with PDVF membrane filters (diameter 30 mm, pore size 0.45 μm). The acceptor indented 96-well microplate (MultiScreen 96-well Culture Tray clear, Merck Millipore) was filled with 180 μL of PBS/ethanol (70/30). The donor 96-well filtrate plate (Multiscreen® IP Sterile Plate PDVF membrane, pore size is 0.45 μM, Merck Millipore) was coated with 4 μL of porcine brain lipid (Spectra 2000) in dodecane (20 mg mL^{-1}) and after 5 minutes, 180 μL of each compound solution were added. Then the donor plate was carefully put on the acceptor plate to form a "sandwich", which was left undisturbed for 2.5 h at 25 °C. During this time the compounds diffused from the donor plate through the brain lipid membrane into the acceptor plate. After incubation, the donor plate was removed. The concentrations of compounds and commercial drugs were determined measuring the absorbance in the donor (before the incubation) and the acceptor wells (after the incubation) with UV plate reader Tecan Infinite M1000. Every sample was analyzed at two to five wavelengths, in 3 wells and in two independent runs. The permeability coefficient (*Pe*) of each drug, in centimeter per second, was calculated applying the following formula: [17]

$$Pe \quad \frac{Vd \quad Vr}{(Vd \quad Vr) \cdot S \cdot t} \quad \frac{100 \cdot Vd}{100 \cdot Vd - \%T(Vd \quad Vr)}$$

$$\%T = \frac{Vr \cdot Ar}{Ad \cdot Vd} 100$$

where Vd and Vr are the volume of the donor and the receptor solutions (0.18 cm^3), S is the membrane area (0.266 cm^2), t is the time of incubation (2.5 h = 9000 s), Ar is the absorbance of the receptor plate after the experiment and Ad_0 is the absorbance in the donor compartment before incubation. Results are given as the mean and the average of the two runs ± standard deviation (SD) is reported. Obtained results for quality control drugs were then correlated to permeability data found in literature. The linear correlation between experimental and literature permeability values was used for the classification of compounds in those able to cross the BBB by passive permeation (CNS+ which correlate with a bibliographic Pe>4) and those not (CNS- which correlate with a bibliographic Pe<2). Compounds correlating with reported Pe values from 2 to 4 10^{-6} cm s^{-1} are classified as CNS+/-.

Calculated physicochemical and ADME properties

The physicochemical and ADME (absorption, distribution, metabolism and excretion) properties of all the 1,2,4-triazolo[1,5-a][1,3,5]triazines analogues, such as, aqueous solubility (logS), lipophilicity (clogP), cytochrome P450 metabolism (2D6 and 2C9), human ether-à-go-go related gene (hERG) channel inhibition, blood–brain barrier (BBB) penetration, human intestinal absorption (HIA), P-glycoprotein binding (P-gp) and plasma protein binding (PPB90) were in-silico predicted through theoretical calculations performed using StarDrop software. [18] Compound PF-5236216(9), a selective CK1δ brain penetrant radiolabel, was chosen as reference in the evaluation phase of the calculated pharmacokinetic parameters. [19] ADME properties were also calculated for (R)-CR8 and SB415286, the positive controls used in the kinase activity assays, respectively for CK1δ and GSK3β proteins kinase.

GSK-3β-compound 12 co-crystallization

GSK-3β cloning and transfection in insect cells

The DNA fragment encoding for residues 35-386 of the human GSK-3β protein (Uniprot ID: P49841) was PCR amplified from the full-length cDNA template purchased by Genescript and using primers TACTTCCAATCCAAGGTGACAACAGTGGTGGCAAC, TATCCACCTTTACTGTCATGCTTGAATCCGAGCATGAGGAG. The cDNA was cloned in pFB-Bse vector (kindly provided by Dr. Opher Gileadi, SGC-Oxford) by Ligation Independent Cloning[20].

The resulting transfer vector pFB-Bse-[GSK-3β(35-386)] was transformed into EMBacY E.coli strain (kindly provided by Dr. Imre Berger, University of Bristol) for bacmid generation.

Spodoptera frugiperda SF9 insect cells (Expression Systems LLC, Davies - USA) at $0.5x10^6$ cells/mL were transfected with transfection mix (50μL of Bacmid DNA supplemented with ESF-921™ medium (Expression systems) and 10μL FuGene® reagent (Promega)) and incubated for 55/60 h at 27 °C in six-well plates. The P0 virus obtained was collected and amplified by infecting 5 mL of $1.6x10^6$ cells/mL for 4 days in adhesion in T25 culture flasks (Thermo Fisher) at 27 °C to generate P1 viral stock. The P2 viral stock was obtained upon infection of 50 mL P1 into $1x10^6$ cells/mL cultivated for 4 days in suspension in 250 mL flasks (Corning).

GSK-3β expression and purification

Trichoplusia ni High 5 (H5) insect cells (Expression Systems LLC, Davies - USA) were infected with the P2 viral stock with a multiplicity of infection (MOI) 2. The culture ($1,5x10^6$ cells/mL) was incubated in 1 L bottles (Vitlab) for 2 days at 27 °C, 180 rpm. The cells were harvested by centrifugation at 1000xg at 4 °C for 1 h. After a wash step in 10% glycerol PBS the pellet was stored at -80 °C until use.

The cells were resuspended in lysis buffer (20 mM Tris pH 8.0, 150 mM NaCl, 5% glycerol, 10 mM Imidazole, 1x cOmplete™ (Roche)). The resuspension was filtered with gauze and then homogenized (Emulsiflex - Avestin) to disrupt the cells. Ten μL of Benzonase and 5 mM $MgCl_2$ were added and the mixture was incubated at RT for 10 minutes. After the incubation the lysate was centrifuged at 30000xg for 1 h at 4 °C. The supernatant was loaded on NiNTA (Qiagen) resin and incubated under slow agitation for 1 h, at 4 °C. The flow through was collected upon mild centrifugation at 500xg for 15 minutes. The resin was subsequently washed with 20 CV of Resuspension buffer (20 mM Tris pH 8.0, 150 mM NaCl, 5% glycerol,10 mM Imidazole). The protein fractions were eluted in Elution buffer (20 mM Tris pH 8.0, 150 mM NaCl, 5% glycerol, 500 mM Imidazole) and further purified by cation exchange chromatography on HiTrap SP 5 mL column (GE Healthcare). The protein was purified by applying a salt gradient from 3% to 30% of NaCl in 20 CV with buffer A (20 mM HEPES pH 7.5, 1 mM DTT, 5% w/v Glycerol) and buffer B (buffer A + 1 M NaCl). The main elution peak, corresponding to the unphosphorylated GSK-3β(35-386) protein (data not shown) was collected and further purified. The 6His tag was removed by digestion with Tobacco Etch Virus (TEV) protease while dialyzing O/N at 4 °C in buffer 20 mM Tris pH 8.0, 10% Glycerol, 150 mM NaCl, 1 mM DTT. The cleaved protein was collected upon a passage on NiNTA beads (Qiagen) to remove TEV and uncleaved protein and the concentration was brought to 1.4 mg/mL (38.5 μM). The protein was stored in small aliquots at -80 °C for further use.

Thermal stability assay (TSA)

To test the effect of inhibitor binding on protein stability, the purified GSK-3β(35-386) protein was incubated for 3 h at 4°C with 3x molar excess of compound **12** in DMSO, and with DMSO alone as control (3.3% and 2.8% final concentrations), and TSA tests were run. Twenty-five µL reaction mixtures were prepared in white 96 well plate with the kinase at final concentration of 1.5 µM, 20 mM Tris pH 8.0, 10% Glycerol, 150 mM NaCl, 1 mM DTT, 5x Sypro Orange (Invitrogen). The plate was centrifuged at 200xg for 1 minute and immediately put into Real Time PCR instrument (CFX96 Touch, BioRad). A program was run having the following steps: 5' at 5 °C followed by 0.3 °C increment in 10" every minute, ranging from 5 °C to 90 °C. Apo and DMSO incubated GSK-3β(35-386) kinase (3.3% and 2.8% final concentrations of DMSO) were used as controls. The data were analysed with Excel for average and standard deviation calculation, and CFX Manager program for graphs.

Crystallization

GSK-3β(35-386) aliquots were concentrated to 4.4 mg/mL and used for crystallization trials. GSK3β(35-386)-compound **12** co-crystals were grown using the sitting drop vapor diffusion technique in 0.2M DL-Malic acid pH 7.0, 20% PEG 3350 as reservoir solution. The protein was previously incubated with 3x molar excess of compound **12** for 3 h at 4 °C. Crystallization drops were prepared from 0.5 μL of protein solution and 0.5 μL of reservoir, and incubated for 10 days at 20°C. Crystals were cryoprotected in 30% glycerol and frozen in liquid nitrogen prior to data collection.

Data collection, structure solution and refinement

X-ray diffraction data were collected at the XRD1 beamline of the synchrotron Elettra (Trieste, Italy), using monochromatic radiation of 1.00 Å and a Pilatus-2 M (Dectris). Data were indexed, integrated and scaled using XDS[21]. Data reduction statistics are reported in Table S1.

Table S1: Data reduction statistics.

	GSK-3β(35-386)+compound 12
Diffraction source	XRD1
Wavelength (Å)	1.00
Temperature (K)	100
Detector	Pilatus-2 M (Dectris)
Resolution range	47.27 - 2.30 (2.38 – 2.30)
Space group	$P\ 2_1\ 2_1\ 2_1$
a, b, c (Å)	86.803, 94.542, 106.579
Mosaicity (°)	0.21
Total number of reflections	145310 (14711)
Unique reflections	39567 (3843)
Redundancy	3.7 (3.8)
$<I/\sigma(I)>$	7.4 (1.5)
R_{pim}	0.084 (0.560)
$CC_{1/2}$	0.991 (0.570)

The structure was solved by Molecular Replacement using MolRep [22] and the structure 1Q5K as reference model [23]. Inhibitor and water molecules were removed from the model prior to phase calculation. The model was improved by iterative cycles of manual fitting using Coot [24] and refined using REFMAC5 [25]. During refinement, 5% of the data were used for calculation of the R-free value. Refinement statistics are reported in Table S2. Coordinates and structure factors have been deposited in the Protein Data Bank with accession number 6H0U.

Table S2: Refinement statistics.

	GSK-3β(35-386) + compound 12
Resolution (Å)	47.27 – 2.30
Number of reflections	37543
R_{work} / R_{free} (%)	19.2 / 24.0
Number of atoms	5722
Protein	5380
Ions/Other	76
Water	266
R.m.s. deviations	
Bond lengths (Å)	0.009
Bond angles (°)	1.386
Ramachandran plot (%)	
Favored	91.8
Allowed	7.5
Disallowed	0.3
PDB code	6H0U

***In vitro* assays on neurodegeneration models**

The neuroprotective effects of compound **12** were evaluated in PC12 cells following induction of cell death by two different dopamine neurotoxins: MPP+ (1-methyl-4-phenylpyridinium) or 6-OHDA (6-hydroxydopamine).

Cell culture. Rat pheochromocytoma cell line (PC12) was obtained from American Type Culture Collection (ATCC) and grown in RPMI 1640 medium supplemented with heat-inactivated 10 % horse serum (HS), 5 % fetal bovine serum (FBS) and 1 % penicillin and streptomycin. Cells were grown in 10 cm^2 tissue culture dishes and cultured to a confluence of 80–90 % and then subcultured with 0.25 % trypsin. Cells were maintained in a humidified atmosphere of 5 % carbon dioxide (CO_2) at 37 °C. The cell culture medium was replaced every 2 days. All the experiments were conducted at least three times.

Cell treatments. PC12 cells were seeded in 96-well plates at 8×10^4 cells in a final volume of 100 µL/well and incubated in a humidified atmosphere of 5 % carbon dioxide (CO_2) at 37 °C. Twenty-four h after plating, cells were used for treatments. Cells were incubated for 24 h in the presence of MPP+ at different concentrations ranging from 100 µM to 1.5 mM and incubated for 5 h with gradually increased concentrations of 6-OHDA (50-300 µM). For both of toxins, the dose that produces a significant neurotoxic effect was determined and used in the following neuroprotection experiments. For neuroprotection experiments, cells were treated for 24 h with MPP+ in the presence of different concentrations of compound **12** (0.1-10 µM). In parallel, cells were treated with MPP+ with LiCl (1-10 mM). At the end of the cell treatments, cells were processed in various ways. For the experiments with 6-OHDA, cells were pretreated with gradually increased concentrations of compound **12** (0.1-10 µM), LiCl (1-10 mM) for 2 h and then treated with 100 µM 6-OHDA for another 5 h. To investigate Wnt/β-catenin signaling pathway, PC12 cells were seeded in 6-well plates at a density of 5 10^5 for 24 h. Cells were pretreated with gradually increased concentrations of compound **12** (0.1-10 µM), LiCl (1-10 mM) for 2 h and then treated with 100 µM 6-OHDA for another 2 h.

Cell viability assays. *CellTiter-Glo luminescent assay:* The CellTiter-Glo® Luminescent Cell Viability Assay (Promega) is a homogeneous method to determine the number of viable cells in culture based on quantitation of the ATP present, which signals the presence of metabolically active cells. The addition of solution consisting of two reagents results in cell lysis and generation of a luminescent signal proportional to the amount of ATP present. The plates were equilibrated at room temperature for approximately 30 minutes. 100 µL of reagents were added to 100 µL of medium containing cells and incubated at room temperature for 10 minutes to stabilize luminescent signal. The luminescence is recorded with a luminometer.

MTT assay: The MTT (3-[4,5-dimethylthiazol-2-yl]-2,5 diphenyl tetrazolium bromide) assay is based on the conversion of MTT into formazan crystals by living cells, which determines mitochondrial activity. Cells were grown in a 96-well tissue culture plate and incubated with 10µl of 5mg/ml MTT solution for approximately 4 h in a humidified incubator. After this incubation period, a water-insoluble formazan dye is formed. After solubilization, with 10 µL of DMSO 100%, the formazan dye is quantified using a scanning multi-well spectrophotometer (ELISA reader). The measured absorbance at a wavelength of 570 nm with 655 nm as a reference wavelength is directly correlates to the number of viable cells.

Western Blotting. Cells were washed with cold PBS and homogenized 5 minutes with ice-cold lysis buffer (10 mM Hepes, 10 mM KCl, 0.1 mM EDTA, 1 mM DTT, 0.5% Nonidet, 0.5 mM PMSF) containing protease inhibitor cocktail. Tubes are centrifuged at 12.000 g at 4 °C for 15 minutes. BCA protein assay kit was used to measure protein concentration. 25 µg of protein samples were boiled for 5 min with loading buffer and separated onto 4-15 % Mini-PROTEAN TGX Precast Protein Gel. Proteins were transferred onto nitrocellulose membranes. Membranes were subsequently blocked for 1 h at room temperature in blocking buffer (5 % skim milk, 0.05 % Tween 20 and Tris-buffered saline (TBS)). Then, the membranes were incubated overnight at 4 °C on an orbital shaker with primary antibodies: rabbit polyclonal anti-β-catenin (1:500 dilution) and mouse monoclonal anti-GAPDH (1:2000). After washed three

times with TBST (15 min each), membranes were incubated with secondary antibodies: peroxcateninidase-labeled goat anti-rabbit IgG (1:5000), goat anti mouse IgG/IgM HRP (1:5000) at room temperature for 1 h and washed with TBST for three times. The bands were visualized using enhanced chemiluminescences (ECL) method. Membranes probed for GAPDH used as an internal control. The protein bands were quantified using image analysis software (ImageJ, V1.42, National Institute of Health, Bethesda, MD) and protein levels were expressed as percent (%) of control.

Data Analysis and Statistic. Data, representative of three independent experiments, were expressed as means ± (S.E.M.). One-way anova analysis of variance (ANOVA) followed by Newman-Keuls test were used to compare differences between means in more than two groups. The level of significance was set at P<0.1. All the statistical analyses were performed with GraphPad Prism Software.

Docking Studies

GSK-3β. A standard docking procedure was applied to generate the bound pose of compound **4** and the non-covalently bound pose of compound **12** at the binding site of GSK-3β (PDB: 1Q5K). This specific crystal structure was selected in light of the suitable results obtained in previous exploratory docking studies.[26] Hydrogen atoms were added. Polar hydrogen atoms and the positions of asparagine and glutamine side chain amidic groups were optimized and assigned the lowest energy conformation. After optimization, histidines were automatically assigned the tautomerization state that improved the hydrogen-bonding pattern. Finally, the original ligand was deleted. All the residues with at least one side chain non-hydrogen atom in the range of 3.5 Å from the co-crystallized ligand were considered part of the pocket. The binding site was represented by pre-calculated 0.5 Å spacing potential grid maps, representing van der Waals potentials for hydrogens and heavy atoms, electrostatics, hydrophobicity, and hydrogen bonding, respectively. The van der Waals interactions were described by a smoother form of the Lennard Jones potential, capping the repulsive contribution to 4 kcal/mol. Each ligand was assigned the MMFF force field atom types and charges.[27] The docking engine used was the Biased Probability Monte Carlo (BPMC) stochastic optimizer as implemented in ICM.[28] Given the number of rotatable bonds in the ligand, the basic number of BPMC steps to be carried out was calculated by an adaptive algorithm (thoroughness 3.0). The binding energy was assessed with the ICM empirical scoring function.[29] For each ligand, the best scoring pose was selected as representative of the ligand bound conformation.

The covalently bound pose of compound **12** was obtained by means of the covalent docking procedure as implemented in ICM3.8, identifying Cys199 as the activated nucleophile residue.

CK-1δ. Inhibitors were built and their partial charges calculated after semi-empirical (PM6) energy minimization using the MOE2015.[30,31] The crystallographic structure selected to perform docking studies was the human CK-1δ in complex with the inhibitor PF4800567 (PDB ID: 4HNF). All water molecules present in the pdb file were retained and the protein was subjected to the structure preparation tool of MOE 2015.[31] Finally, protonate 3D tool was used to assign the protomeric state.[31] To identify the more appropriate protocol for the selected complexes we performed a self-docking benchmark using DockBench 1.01,[32] which compared the performance of 17 different posing/scoring protocols. The active site was defined using a radius of 10 Å from the centre of mass of the co-crystallized ligand. Each ligand was docked 20 times, using GOLD (PLP and Goldscore were used as scoring functions for 4HNF)[33] and the virtual screening tool of DockBench, adopting the parameters used in the benchmark study. Finally, the obtained conformations with 4HNF from the docking were rescored with PLP.

Results and Discussion

Synthesis

The 1,2,4-triazolo[1,5-*a*][1,3,5]triazines of this work were basically obtained following the procedure reported by Caulkett et al. with some modifications.[2] The synthesis of compounds **1-5** is depicted in scheme S1. It started reacting the commercial available 2,4,6-trichloro[1,3,5]triazine (**16**) with phenol under reflux for 5 h. The resulting 2,4,6-triphenoxy[1,3,5]triazine (**17**) was treated with hydrazine monohydrate to afford the hydrazinyl derivative **18**, which was successively formylated with formic acid to give the intermediate **19**. The latter synthesis derives from the optimization of the procedure described by Bakhite et al., where the hydrazinyl derivative **18** was reacted in formic acid under reflux for 6 h (yield <10%).[34] We decided to perform the reaction in milder conditions (room temperature), with restrained excess of formic acid (10 equivalents) and in presence of an organic solvent as toluene,[33] and these expedients allowed us to obtain the product **19** with an average yield of 69%. Derivative **19** underwent intramolecular cyclization to afford the 1,2,4-triazolo[1,5-*a*][1,3,5]triazine **20** in dehydrative conditions (phosphorous anhydride and hexamethyldisiloxane in xylene).[3] Compounds **1** and **4**, presenting the same substituents at both 7- and 5- positions of the TT scaffold, were obtained reacting directly compound **20** with a large excess of methanolic ammonia or cyclohexylamine, while monosubstitution at the 7 position of compound **20** was conducted in presence of a less amount of the required amine, at lower temperatures and for shorter time, affording compounds **21** and **22**. The second substitution at the 5 position of compounds **21-22** required 90 °C and 3 days of reaction with the appropriated amine, affording compounds **2**,**3** and **5**.[36]

The nucleophilic displacement of the phenoxy group at the 5 position with aniline did not occur due to the lower reactivity of aniline. Therefore, we decided to apply another procedure reported in scheme S2 which starts from the 7-amino-5-methylsulfanyl[1,2,4]triazolo[1,5-*a*][1,3,5]triazine (**24**), obtained by thermal reaction of 3-amino-1,2,4-triazole (**23**) with dimethyl *N*-cyanodithioiminocarbonate. Reactivity of 5-methylsulfanyl group was enhanced oxidizing it to the sulfoxide, affording compound **25**.[2,4] This successfully allowed the introduction of the aminophenyl group on the TT scaffold, leading to derivative **6**.

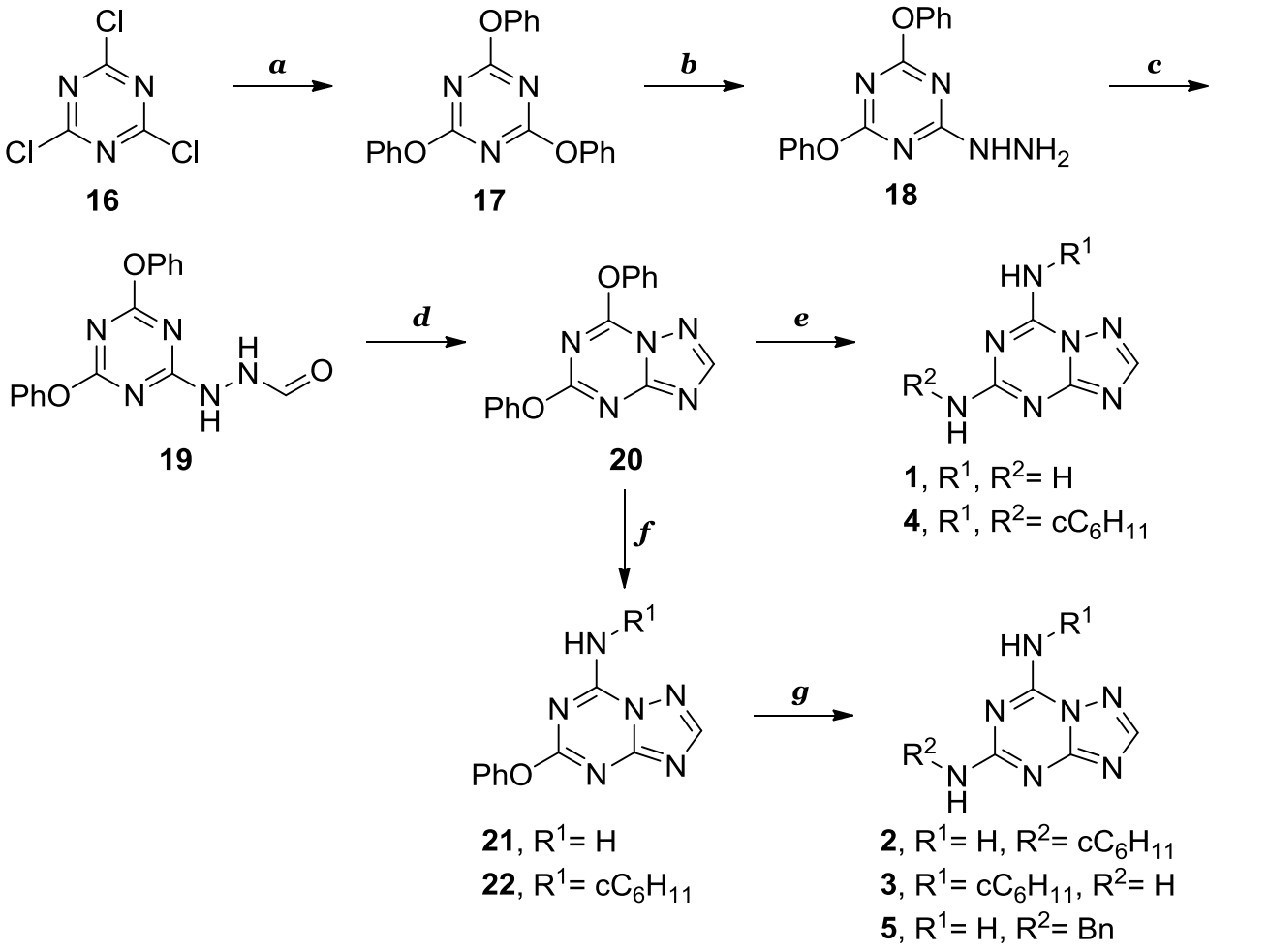

Scheme S1. ***a:*** phenol, reflux, 5 h; ***b:*** hydrazine monohydrate in THF, DCM, rt, 12 h; ***c:*** formic acid, toluene, rt, 4 h; ***d:*** i) P_2O_5, HMDSO, xylene, from rt to 90°C, 1.5 h, 90°C 1h; ii) compound **19**, reflux, 2-3 h; ***e:*** ammonia 7N in methanol (**1**) or cyclohexylamine (**4**), methanol (**1**) or ethanol (**4**), 75 (**1**) or 95 (**4**) °C, 12 h; ***f:*** ammonia 7N in methanol (**21**) or cyclohexylamine (**22**), methanol (**21**) or ethanol (**22**), rt (**21**) or 50°C (**22**), 3h; ***g:*** R_2-NH_2, ethanol, 90°C, sealed tube, 72 h.

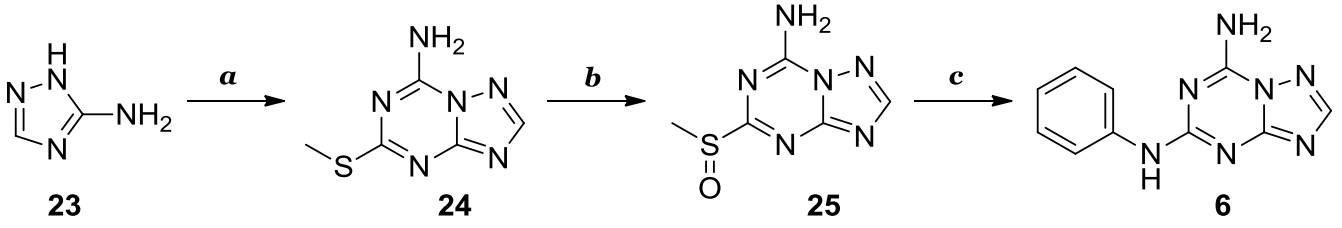

Scheme S2. ***a:*** i) dimethyl-*N*-cyanodithioiminocarbonate (neat), Ar, 170°C, 1 h; ii) DCM-methanol, reflux, 1 h; ***b:*** *m*-PCBA, DCM, rt, 12 h; ***c:*** aniline, acetonitrile, sealed tube, 80°C, 48 h.

The 3-cyano-N'-(4,6-diphenoxy-1,3,5-triazin-2-yl)benzohydrazide (**29**) is obtained differently from compound **19**, in fact, as depicted in scheme S3, it implies the reaction of the desired hydrazide (i.e. 3-cyanobenzohydrazide **28**) with the triphenoxy-triazine **17** in presence of DBU.[5] The 2-substituted 5,7-diphenoxy-[1,2,4]triazolo[1,5-*a*][1,3,5]triazine derivative, obtained by intramolecular cyclization under dehydrative conditions, was immediately converted into the 7-amino derivative **29** with methanolic ammonia at room temperature.[4] The further substitution at the 5 position, which required heating the mixture of compound **29** and desired amines in a sealed tube, gave compounds **10-11**.[36] The amido derivatives **8-9** were obtained after conversion of the nitriles via acid-catalysed hydration using a trifluoroacetic/sulfuric acids mixture.[6] The 3-cyanobenzohydrazide **28** was obtained from the corresponding carboxylic acid (**26**), which was subsequently reacted with ethanol to obtain the ester (**27**) and then with hydrazine to give the desired compound (Scheme S3A).

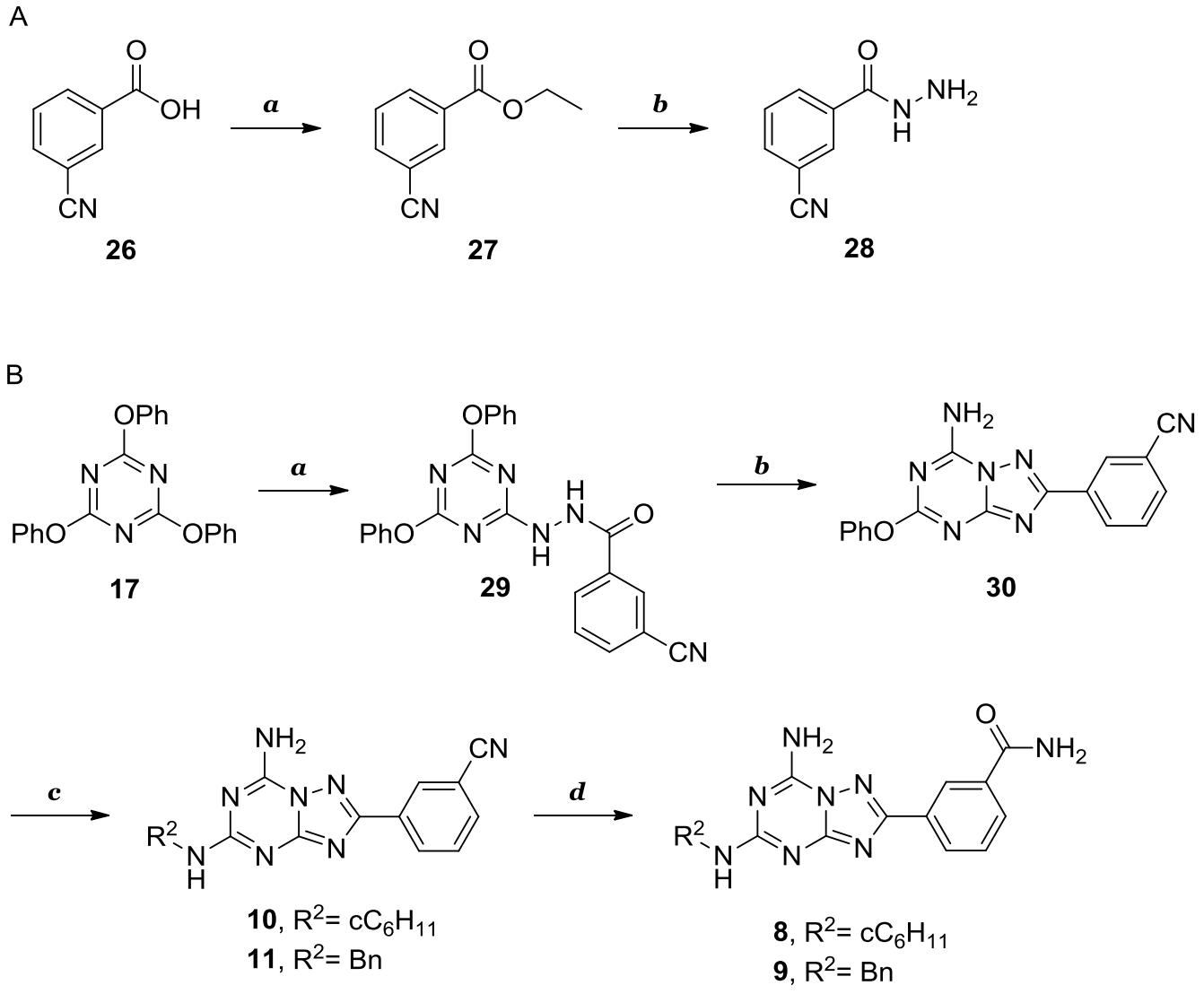

Scheme S3. A *a:* H_2SO_4, ethanol, reflux, 12 h; ***b:*** $NH_2NH_2{\cdot}H_2O$, ethanol, reflux, 48 h; **B *a:*** compound **28**, DBU, dry THF, rt, 12 h; ***b:*** i) P_2O_5, HMDSO, xylene, from rt to 90 °C, 1.5 h, 90 °C 1h; ii) compound **29**, reflux, 2-3 h; iii) ammonia 7N in methanol, methanol, rt, 3 h; ***c:*** R_2-NH_2, ethanol, 90 °C, sealed tube, 72 h; ***d:*** TFA-H_2SO_4 (4:1), 70 °C, 3 h.

Finally, compounds **12-15** were obtained as reported in scheme S4. 2-Hydrazinyl-4,6-diphenoxy-1,3,5-triazine (**18**) was treated with the chloride of 2-(benzyloxy)acetic acid, obtained by Williamson reaction between chloroacetic acid and benzyl alcohol (**31**) (Scheme S4A).[7] As for compound **30**, cyclization of hydrazinyl compound **33** gave the 5,7-diphenoxytriazolo-triazine which was directly reacted with excess of cyclohexylamine to afford the 5,7-dicyclohexylamino derivative **34** or with ammonia at room temperature to afford the 7-amino derivative **35**. On the other hand, compound **36** was obtained by reaction of derivative **35** with cyclohexylamine at 90-100 °C (Scheme S4A).

In order to insert the Micheal-acceptor warhead at the 2 position, deprotection of hydroxyl groups fo compounds **34** and **36** was performed with palladium on carbon as catalyst and heated ammonium formate as hydrogen source, delivering the alcohol derivatives **37-38**, which were in turn oxidized to aldehydes (**39-40**) with Dess-Martin periodinane.[8] The cyanoacrilamido derivatives **12-13** were obtained by Knoevenagel condensation between aldehydes and cyanoacetamide, in presence of DBU, while cis- and trans cyanoacrilates **14** and **15** derived from Wittig reaction of **39** and (triphenylphosphoranylidine)acetonitrile in a 50:50 ratio (Scheme S4C).[9] (Triphenylphosphoranylidine)acetonitrile was freshly made by treatment between triphenylphosphine and chloroacetonitrile.[10]

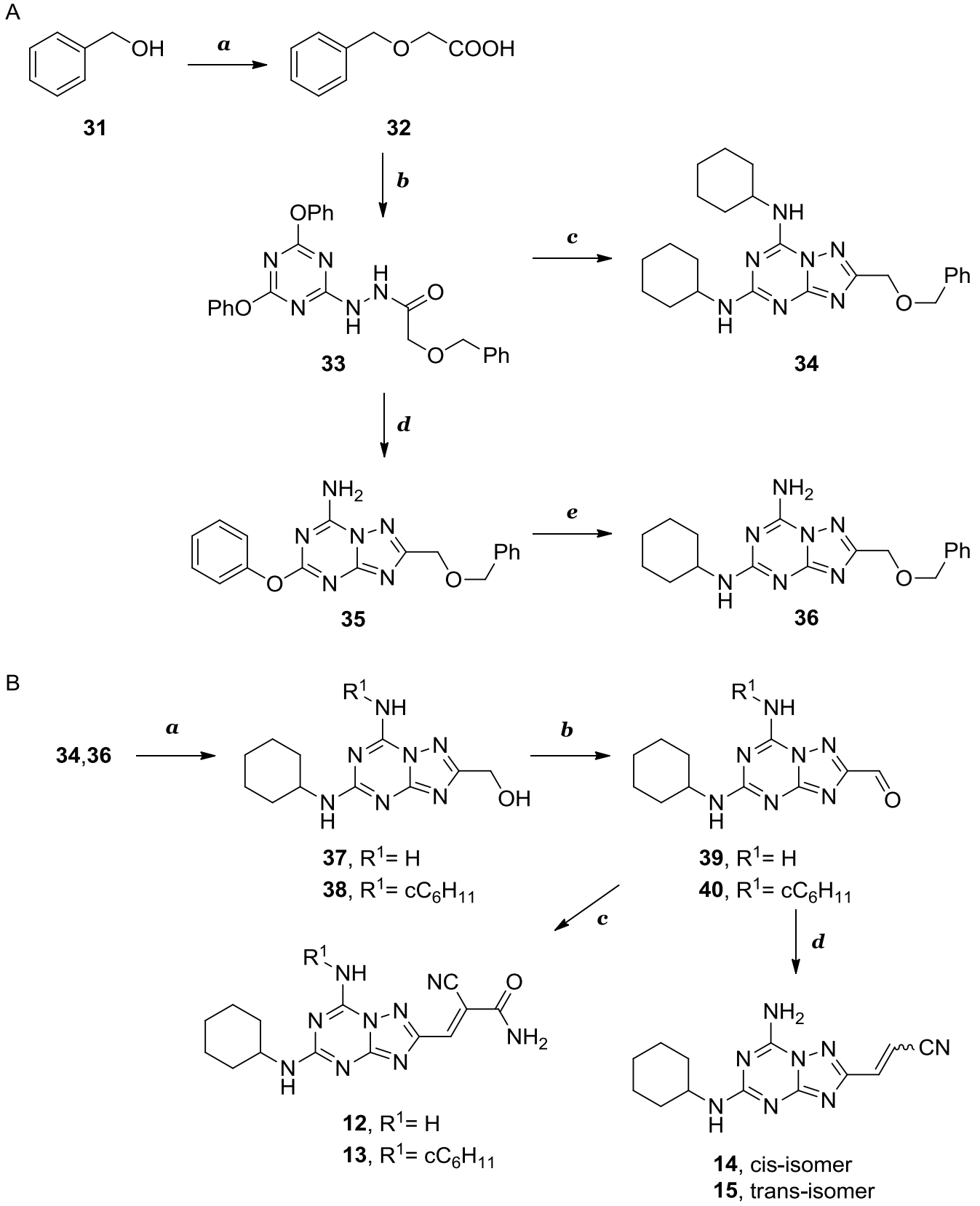

Scheme S4. A ***a:*** i) NaH, dry toluene, rt for 1 h; ii) chloroacetic acid, rt for 1 h, 80 °C for 2 h; ***b:*** i) oxalyl chloride, DCM, reflux, 4 h; ii) compound **18**, TEA, DCM, rt, 12 h; ***c:*** i) P_2O_5, HMDSO, xylene, from rt to 90 °C, 1.5 h, 90 °C 1h; ii) compound **33**, reflux, 2-3 h; iii) cyclohexylamine, ethanol, 95 °C, 24 h; ***d:*** i) P_2O_5, HMDSO, xylene, from rt to 90 °C, 1.5 h, 90 °C 1 h; ii) compound **33**, reflux, 2-3 h; iii) ammonia 7N in methanol, methanol, rt, 3 h; ***e:*** cyclohexylamine, ethanol, 90 °C, sealed tube, 72 h; **C** ***a:*** $HCOONH_4$, Pd/C, MeOH, reflux, 3 h; ***b***: Dess-Martin periodinane, DCM, rt, 3 h; ***c***: cyanoacetamide, DBU, DCM, rt, 2 h; ***d***: (triphenylphosphoranylidine)acetonitrile, DCM, rt, 3 h.

SUPPORTING INFORMATION

Structure-activity relationship analysis

Data about a preliminary series of triazolo-triazines (compounds **1-6**) were reported in Table 1. These compounds were synthesized with the aim of elucidate the role of the substitutions at the 5 and 7 position of the TT scaffold on their affinity towards GSK-3β. In particular we decided to maintain the 2-position free (R=H) and to modify the 7- (R^1= -H, cyclohexyl) and 5- (R^2= -H, cyclohexyl, phenyl, benzyl) positions. A certain activity towards GSK-3β was found only with the 5,7-disubstituted derivative **4** [IC_{50}(GSK-3β)= 3.1 μM], thus rendering it the scaffold to work on to further improve the affinity towards GSK-3β, but all compounds resulted inactive towards CK-1δ. A suggestion to obtain affinity against CK-1δ came from D4476 (**8**) which bears an aminophenyl moiety and displays an IC_{50} value of 0.3 μM towards CK-1δ.[37] Thus, we tried to validate the efficacy of the amido group by introducing the 3-amidophenyl moiety at the 2 position of the TT ring in compounds **8** and **9**. The choice of the 3-substituted phenyl ring is due to results previously obtained, that showed that *meta* substitution on the phenyl ring with groups able to make hydrogen bonding is better than *para* substitution (data not shown). As supposed, **8** and **9** showed good IC_{50} values towards CK-1δ [**8**, IC_{50}(CK-1δ)= 4.28 μM; **9**, IC_{50}(CK-1δ)= 2.59 μM] (Table 1), while the corresponding cyano derivatives are inactive at a concentration of 40 μM. At GSK-3β, these compounds showed a percentage of enzyme activity more than 90% at a concentration of 10 μM. Aiming to enhance the inhibitory activity of TTs and hypothesizing a similar pose between ATP and compounds **4**, **8** and **9** in the ATP binding pocket of GSK-3β, we supposed that a focused substitution at the 2-position of the TT nucleus could target the non-catalytic cysteine 199, hence offering the opportunity to obtain a covalent inhibition of GSK-3β, which in general lead to improved selectivity and potency against the target. The 2-cyanoacrylamide moiety is an example of a group useful for this scope and it contains the amido group favourable to gain interactions also at CK-1δ ATP binding cleft.[9] Then, taking into account all these observation, we decided to synthetize new [1,2,4]triazolo[1,5-*a*][1,3,5]triazine derivatives bearing at the 2-position the 2-cyanoacrylamide moiety, that should confer potency against both GSK-3β, through a covalent bond with Cys-199, and CK-1δ. Concerning the other positions, we maintained the double substitution with the cyclohexyl group (**13**), as present in compound **4**, and we decided to synthetize also the not-substituted derivative in position 7 (**12**), since the substitution at this position seems to affect negatively the affinity against CK-1δ [**4**, IC_{50}(CK-1δ)= >40 μM *vs* **9**, IC_{50}(CK-1δ)= 2.59 μM]. Then, to further investigate the role of the amido moiety we decided to synthetize also the corresponding acrylonitrile (**14** and **15**, cis and trans isomers) derivatives. As depicted in Table 2, the introduction of the cyanoacrylamide moiety at the 2-position of TT scaffold led to a substantial improvement of affinity towards both GSK-3β and CK-1δ, improving the IC_{50} values up to the sub-micromolar range [**12**, IC_{50}(GSK-3β)= 0.17 μM; IC_{50}(CK-1δ)= 0.68 μM]. The well-balanced GSK-3β/CK-1δ inhibitory activities allowed us to consider **12** as a dual inhibitor, thus confirming the validity of the rationale of the work. Notably, regarding the GSK-3β inhibitory profile, the cyanoacrilamide warhead introduced in the TT scaffold converted the inactive compound **2** [IC_{50}(GSK-3β)> 10 μM] into a GSK-3β inhibitor with an acceptable potency [**12**, IC_{50}(GSK-3β)= 0.17 μM], while the same modification on the promising **4** scaffold [IC_{50}(GSK-3β)= 3.1 μM] resulted detrimental in terms of inhibitory activity [**13**, IC_{50}(GSK-3β)> 10 μM]. The replacement of the electrophilic warhead of compound **12** with the acrylonitrile moiety led to more than 30-fold less potent derivatives (**14** and **15**), which resulted inactive also towards CK-1δ, highlighting the importance of the amido group in gaining polar interactions within the ATP binding site of both kinases.

Docking studies

Docking studies at the binding site of GSK-3β allowed to gain insight in effective interactions that led compound **12** to inhibit this kinase with an IC_{50} of 0.17 μM. This value likely resulted from a complex inhibition mechanism, including reversible competition with ATP and covalent interaction with GSK-3β through a thia-Michael reaction. As depicted in panel A of figure 1, compound **12**, being an adenine-like derivative, lies in the Hinge region, reproducing the typical binding fingerprints of protein kinases ATP-competitive inhibitors establishing two H-bonds, one between primary amino group at the 7-position and carbonyl of Asp133 and the other between secondary amino group at the 5-position and Val135. Moreover, compound **12** was able to establish a hydrogen bond interaction also between its carbonyl of the amido group at the 2-position and amino group of the lateral chain of Lys85. Subsequently a covalent docking study was carried out in which a thia-Michael reaction occurred by nucleophilic attack of GSK-3β Cys199 residue on the reactive cyanoacrilamide warhead at the 2-position of the TT scaffold (Figure S1). We can assume that non-covalent interactions of the molecule with the binding pocket of GSK-3β (Asp133, Val135, Lys85) are critical for the optimal orientation of the electrophile moiety toward a specific protein nucleophile residue (driving group), thus increasing the speed and selectivity of the covalent bond, and are ultimately responsible for the high potency of derivative **12**. Instead, the different binding pose of compound **4** (Panel B, Figure S1) could provide an explanation for the inactivity of the corresponding di-substituted derivative **13**. In particular, the two cyclohexyl groups lie in the hydrophobic region II, the triazolo part of the ring interacts with the Hinge residue Val135, while the 2 position of the TT is oriented towards Asp133 of the Hinge region, so in the opposite site respect to Cys199.

Concerning CK-1δ, a molecular docking investigation on compound **12** showed that it interacts both with the Hinge region and the phosphate-binding region of the ATP-binding cavity (Figure 1). In fact, derivative **12** makes two stabilizing interactions with the Hinge region: the first between its amino group at the 7-position and the backbone carbonyl group of Glu83, the second between its nitrogen at 5-position and backbone amino group of residue Leu85. Other hydrogen-bonding interactions have been detected between the carbonyl and amino group of the cyanoacrilamide moiety at the 2-position and the amino group of Lys38 and the carbonyl group of Glu52, respectively. Moreover, hydrophobic interactions contribute to stabilize compound in complex with CK-1δ, the two heteroaromatic cores and the amino group at the 2-position are involved in these kind of interactions. It is worth noticing how the orientation of compound **12** in the ATP-binding pocket of GSK-3β (Figure 1, S1) and CK-1δ (Figure 1) is highly similar in both kinases.

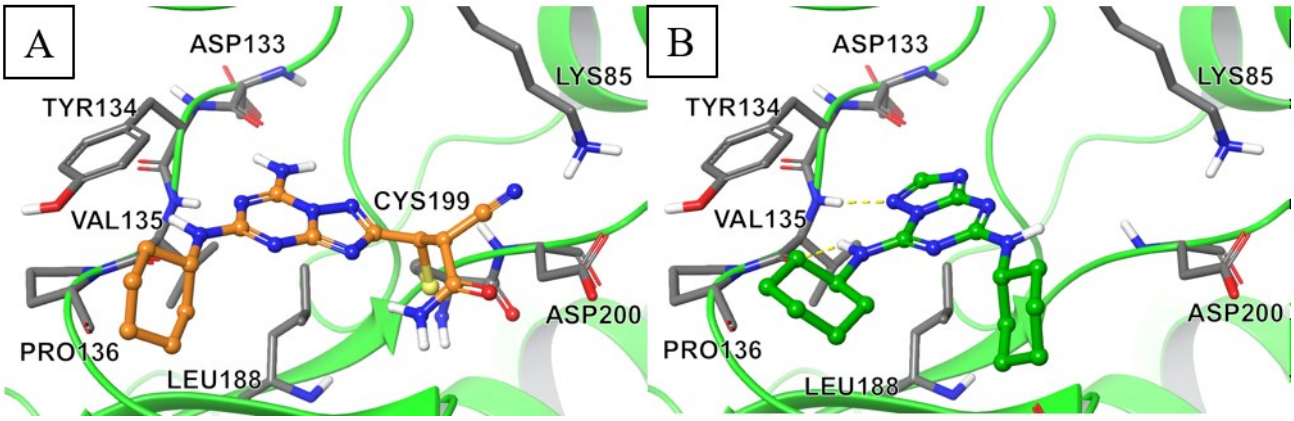

Figure S1. A) Covalently bound conformation of compound **12** docked at the binding site of GSK-3β (PDB code: 1Q5K). The ligand is reported in orange x-sticks. B) Bound conformation of compound **4** at the binding site of GSK-3β (PDB code: 1Q5K) as predicted by ligand docking simulations. The ligand is reported in green x-sticks. The key residues of the binding pocket are reported in light grey x-sticks and labelled explicitly. Hydrogen bond interactions are highlighted by dotted lines.

Prediction of CNS permeation

One of the main obstacles for the treatment of central nervous system (CNS) diseases is the drug's penetration into the blood-brain barrier (BBB) at therapeutic concentrations.[38] The majority of CNS drugs enter the brain by transcellular passive diffusion, due to the tight junction structure and limited transport pathways.[39] In early drug discovery stage, evaluation of ADME (Absorption, Distribution, Metabolism, Excretion) properties is of crucial importance to reduce the attrition rate in development process. PAMPA-BBB is a high throughput technique developed to predict passive permeability through BBB, based on the ability of a compound to cross an artificial membrane impregnated with a porcine brain lipid.[17,40] In particular, only compounds **12** and **15**, exhibiting promising IC_{50} values towards the two kinases, and compound **4** were assayed. In addition to synthesised compounds, ten commercial drugs have been evaluated for their *in vitro* permeability (*Pe*) (Table S3), thus, data were compared to the literature values in order to establish the limits corresponding to compounds ability to permeate BBB. In literature, the value of $4 \cdot 10^{-6}$ cm s^{-1} represents the lower limit to categorize a compound permeable to BBB and $2 \cdot 10^{-6}$ cm s^{-1} the upper limit to establish derivatives not able to cross BBB.

Table S3. Permeability in the PAMPA-BBB assay for 10 drugs and the newly synthetized compounds **4**,**12** and **15** with their predictive penetration in the CNS.

Compound	Bibl.[a]	*Pe* (10^{-6} cm s^{-1}) [b]	Prediction[c]
Atenolol	0.8	0.54 ± 0.70	
Caffeine	1.3	0.10 ± 0.21	
Desipramine	12	11.45 ± 1.48	
Enoxacin	0.9	0.10 ± 0.78	
Hydrocortisone	1.9	0.37 ± 0.01	
Ofloxacine	0.8	0.83 ± 0.57	
Piroxicam	2.5	0.1 ± 0.01	
Promazine	8.8	11.85 ± 1.24	
Testosterone	17	16.84 ± 2.89	
Verapamil	16	15.69 ± 3.89	
4		22.65 ± 2.04	CNS +
12		1.34 ± 0.23	CNS -/+
15		2.35 ± 0.52	CNS -/+

[a] Reference 17 [b] Data are the mean ± SD of 2 independent experiments. [c] Calculated limits: CNS + > 3.42, CNS - < 1.29.

Thus, according to curve in figure S2, we were able to classify compounds as CNS permeable (CNS+) when they present a permeability > 3.42 10^{-6} cm s^{-1} and CNS not-permeable (CNS-) when they present a permeability < 1.29 10^{-6} cm s^{-1}. Values between these two limits are in the zone of uncertainty and therefore for these compounds an univocal prediction cannot be given (CNS-/+).

Following this classification, we cannot consider compounds **12** and **15** clearly able to cross the BBB by passive permeation, while GSK-3β reference compound **4** gave a positive response. In fact, the double cyclohexylamino substitution present in compound **4** confers it a higher lipophilic character than compounds **12** and **15**, which instead present a more polar free amino group at the 7 position.

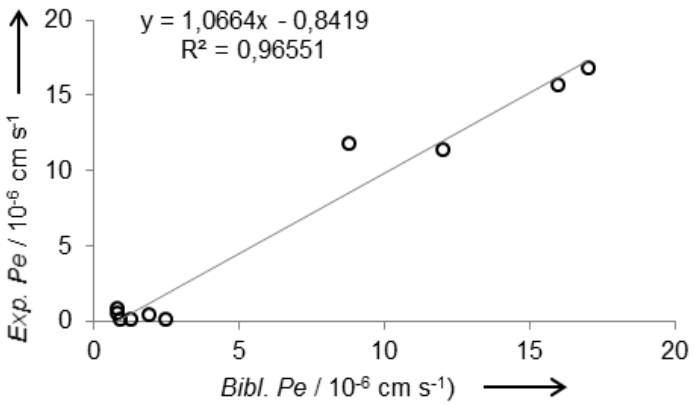

Figure S2. Linear correlation between experimental PAMPA-BBB and literature reported permeability of commercial drugs.

Chemical reactivity of compound 12 and 15 with thiols

We supposed that the GSK-3β inhibitory activity of compound **12** and **15** is enhanced by covalent interaction of the Michael-acceptor group at the 2 position of the triazolo-triazine nucleus with the thiol unit of Cys199, located in the GSK-3β ATP binding site. So it was therefore necessary to characterize the reactivity of this compound in front of thiol groups. To this end, we have analysed by HPLC-MS the reaction of compound **12** and **15** with the model thiol β-mercaptoethanol (BME) in presence of triethylamine (TEA) in a 1:1:1 ratio (**12**:BME:TEA) (Figure S3, S4).

Concerning compound **12**, the reaction afforded 42% of the S-alkylated product after 1 h, which increased to 53% after 2 h. Despite the reactivity showed in the first h, the total S-alkylation of compound **12** did not occur and the percentage remained nearly constant even after 24 h (47%) (Figure S3). A potential explanation for these results could be the reversible nature of the Michael-reaction between the cyanoacrylamide warhead and nucleophiles, as previously described in literature. In fact, the presence of two electron-withdrawing groups (EWGs) attached to the α-carbon of the Michael-acceptor group increases the susceptibility of the β-carbon to nucleophilic attack by thiols, but also increase the carbon acidity of the cyanoacrylamide adduct, thus enhancing the elimination rate and rendering the reaction reversible.[9] Instead, the same experiment on compound **15** showed a slower propensity of the cyanoacrylate to form a covalent interaction with BME thiol. In fact, only 4.1% of adduct was formed after 1 hour of reaction (versus 42% of adduct formed at the same time in the case of compound **12**) that increased at 20.4% after 1 day (Figure S4).
Finally, derivative **12** reaction with BME was monitored also by UV-VIS spectrophotometry. In particular, a 0.85 mM solution of compound **12** in PBS/DMSO 70:30 (pH 7.4) was treated with increasing concentrations of BME (from 0 to 100 mM) and monitored by UV-VIS absorption spectroscopy. As depicted in Figure S5, we can observe a stepwise decrease in the UV-VIS absorption band of the cyanoacrylamide moiety of compound **12** (λmax= 350 nm, highlighted in orange) after addition of increasing amounts of BME.

Calculated physicochemical and ADME properties

Table S4 shows the prediction of some general physicochemical and ADME parameters in which compound **12** showed quite good results in terms of metabolism (low pKi against CYP2C9 and medium affinity against CYP2D6) and cardiotoxicity (low affinity for hERG channels). In addition, software predicted that compound **12** is not a substrate of efflux protein P-gp, which increases the chance that compound permeate the BBB without be excluded back to plasma. On the contrary, our results in PAMPA-BBB and the low calculated logP value, indicate that strong efforts should be done in order to improve the pharmacokinetic properties of this compound, increasing the chance to reach the SNC.

Table S4 Calculated physicochemical and ADME properties for 1,2,4-triazolo[1,5-*a*][1,3,5]triazines **4**, **12** and **15**, brain penetrant CK-1δ radioligand PF-5236216 (9), CK-1δ positive control for biochemical assay (R)-CR8 and GSK-3β positive control for biochemical assay SB415286.

Compounds	logS[a]	logP[b]	2C9 pK_i[c]	hERG pIC_{50}[d]	HIA category[e]	P-gp category[f]	2D6 affinity category[g]	PPB90 category[h]
4	2.25	3.74	4.62	6.21	+	yes	high	low
12	2.64	0.99	4.50	4.41	+	no	medium	low
15	2.72	1.84	4.39	5.37	+	no	medium	low
PF-5236216 (9)	1.63	2.09	5.41	4.93	+	no	medium	low
(R)-CR8	1.18	3.31	5.91	6.26	+	yes	medium	high
SB415286	1.83	2.10	5.24	3.97	+	no	low	high

[a] Aqueous solubility (logS, μM), preferably >1. [b] Logarithm of partition coefficient between n-octanol and water (clogP), preferably 0 < clogP < 3.6. [c] CYP2C9 cytochrome metabolism (CYP2C9 affinity, μM), preferably ≤6. [d] hERG channel inhibition (pIC_{50}), preferably ≤5. [e] Human intestinal absorption (HIA): (+) indicates absorption ≥ 30% and (−) indicates absorption < 30%. [f] P-Glycoprotein binding (P-gp): "yes" indicates a substrate and "no" indicates a

non-substrate. [g] CYP2D6 cytochrome metabolism (CYP2D6 affinity, μM), “low” indicates pKi < 5, “medium” indicates 5 < pKi < 6, “high” indicates 6 < pKi < 7, “very high” indicates pKi > 7. [h] Plasma protein binding (PPB90): “low” indicates <90% of compound bound to plasma proteins, “high” indicates ≥90% of compound bound to plasma proteins. All properties were calculated using StarDrop™, version 6.2 (Optibrium Ltd, 7221 Cambridge Research Park, Beach Drive, Cambridge CB25 9TL, UK).

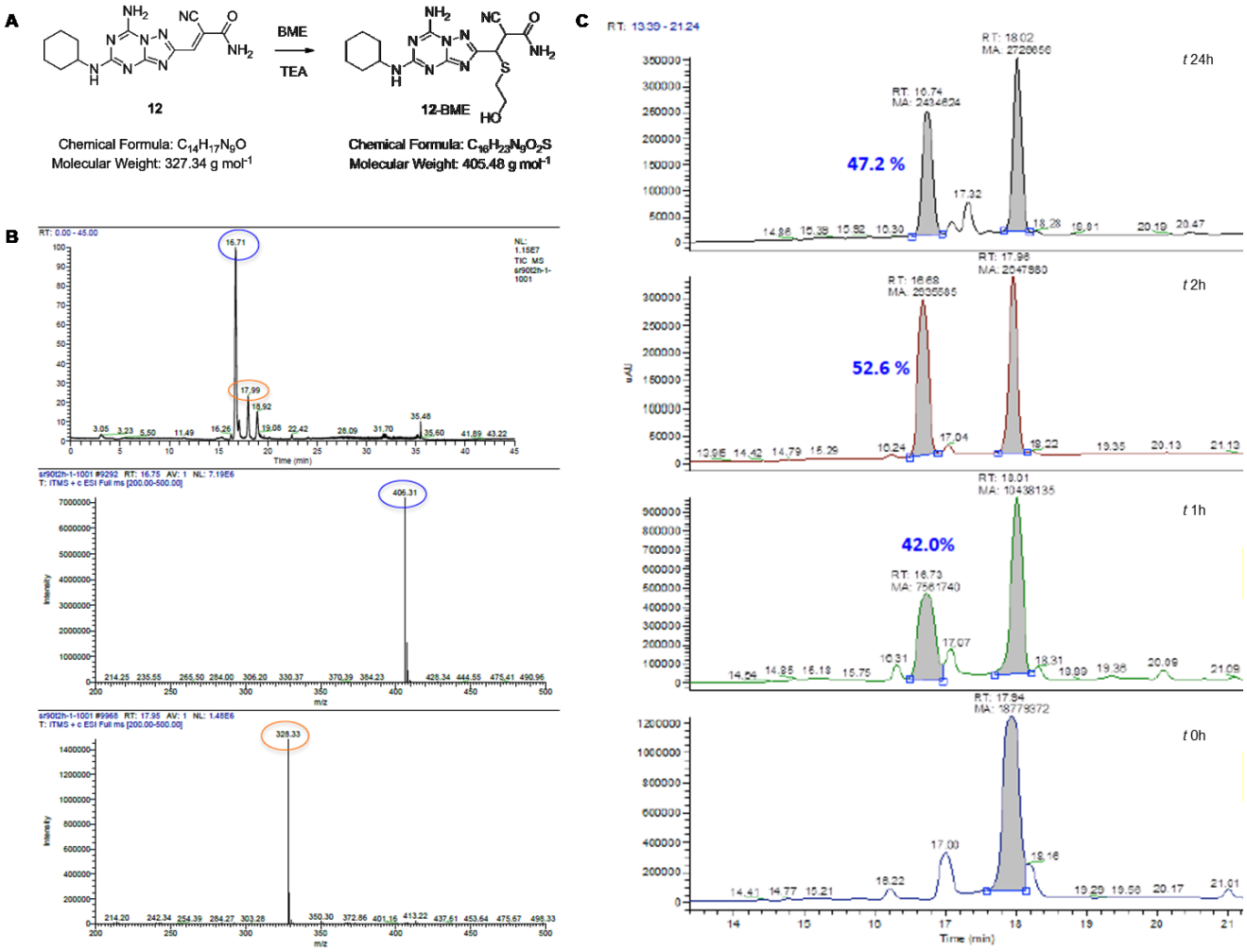

Figure S3. A. Thio-Michael reaction between compound **12** (internal code SR90) and BME; B. up: TIC chromatogram of compound **12**, middle: full MS spectrum at 16.75' corresponding to **12**-BME compound, down: full MS spectrum at 17.95' corresponding to compound **12**; C. Percentage of **12**-BME adduct registered after different times (0,1, 2 and 24h) of incubation of compound **12** with BME and TEA determined by HPLC-MS (see Figure S1).

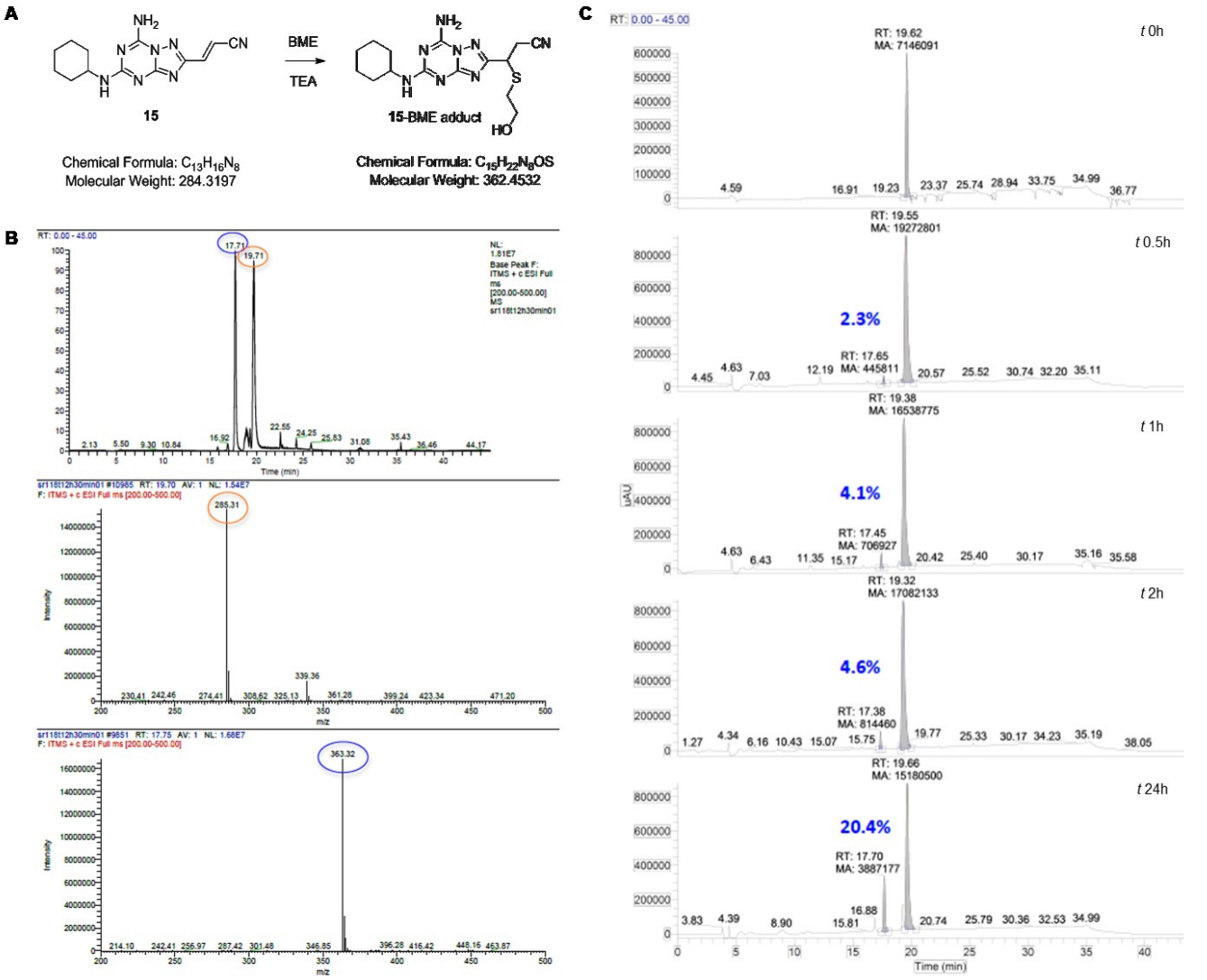

Figure S4. A. Thio-Michael reaction between compound **15** (internal code SR118T) and BME; B. up: TIC chromatogram of compound **15**, middle: full MS spectrum at 19.71' corresponding to compound **15**-BME compound, down: full MS spectrum at 17.71' corresponding to **15**-BME compound; C. Percentage of **15**-BME adduct registered after different times (0,0.5,1, 2 and 24h) of incubation of compound **15** with BME and TEA determined by HPLC-MS (see Figure S1).

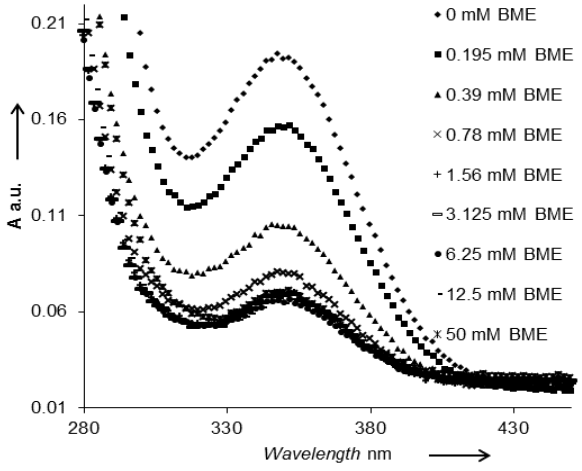

Figure S5. UV-VIS spectra of compound **12** (0.85 mM) with increasing concentrations of BME (0-50 mM) in PBS/DMSO 70:30.

Kinase Inhibition mechanism

To experimentally confirm compound **12** binding mechanism, substrate competition experiments were performed on both kinases varying ATP and compound **12** concentrations, while the concentration of peptide substrates was kept constant (Figure S6). Regarding CK-1δ, as depicted in figure S6A, the intercept of the plot in the vertical axis (1/*V*) does not change, meaning that compound **12** acts as a competitive inhibitor of ATP binding towards CK-1δ. On the other hand, double-reciprocal plotting of experimental data on GSK-3β (figure S6B), showed a mixed ATP-competitive/non-ATP-competitive behavior of compound **12**, in accordance to rationale underlying the design of this compound, which includes a covalent but reversible interaction with GSK-3β.

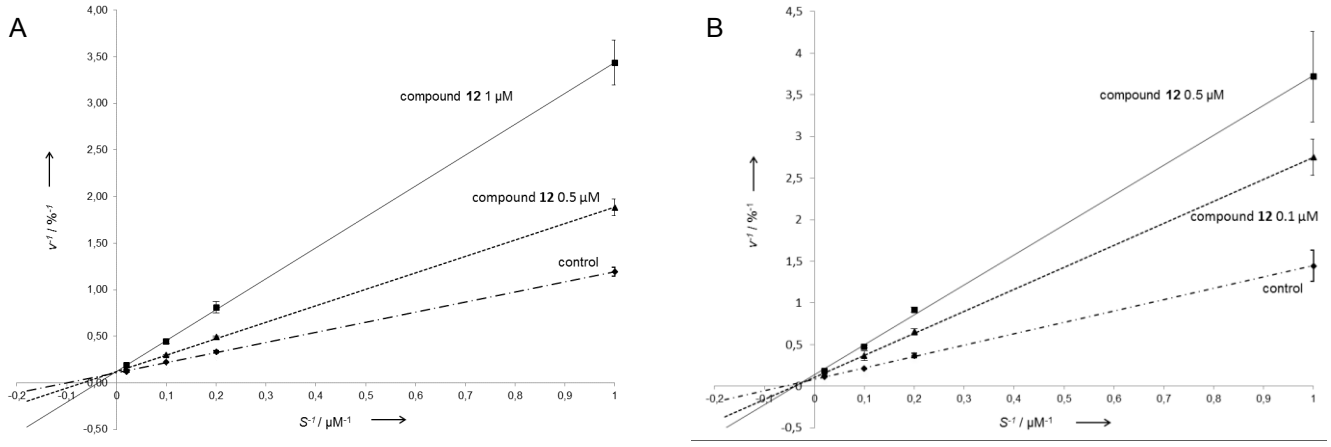

Figure S6. ATP competition curve of compound **12** at CK-1δ (panel A) and GSK-3β (panel B). v: % enzyme activity; S: [ATP].

On the contrary, compound **4**, when evaluated using the same competition experiment on GSK-3β, displayed the typical ATP competitive behavior (Figure S7).

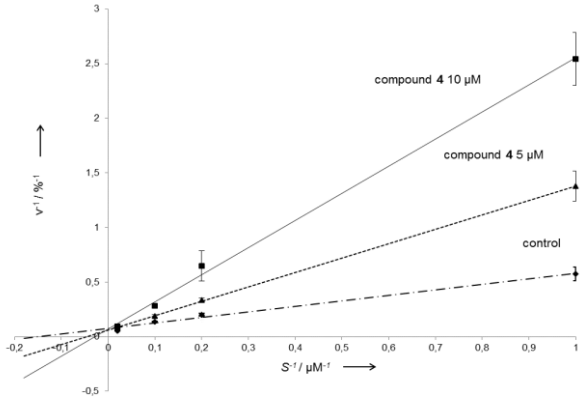

Figure S7. ATP competition curve of compound **4** at GSK-3β. v: % enzyme activity; S: [ATP].

Moreover, in order to study the binding reversibility of derivative **12** in respect to GSK-3β, kinase activity was determined after different times of incubation with the inhibitor. Hence, GSK-3β was pre-incubated for zero, five and ten minutes with compound **12** at concentrations near to its IC_{50} value, and then enzymatic activity was evaluated. The results (Table S4, Figure S8) showed that the percentage of inhibition slightly increased with the inhibitor exposure time, confirming that a covalent but not fully irreversible interaction between compound **12** and GSK-3β took place.

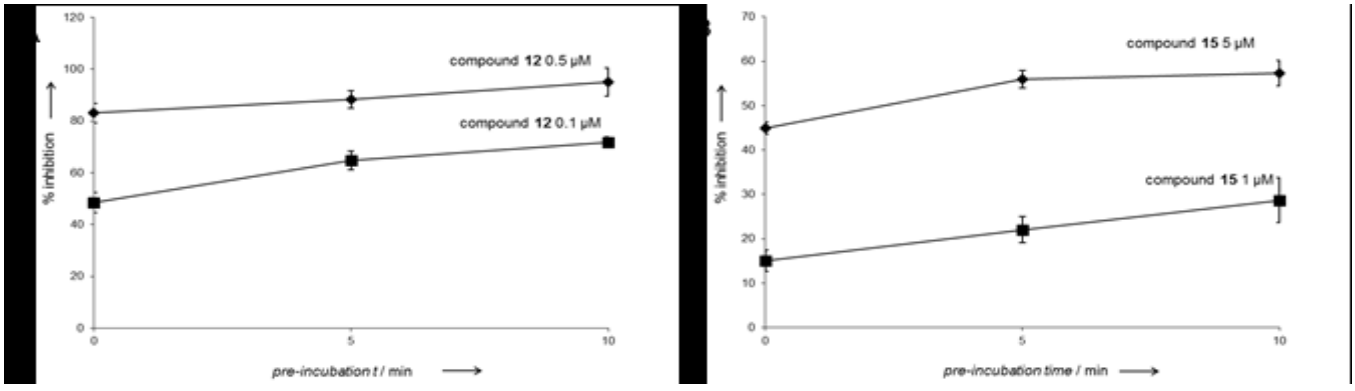

Figure S8. Pre-incubation time dependent GSK-3β inhibition of compound **12** (panel A) and compound **15** (panel B).

Table S5. GSK-3β activity inhibition of compounds **12** and **15** at different times of pre-incubation.

t min	% inhibition GSK-3β			
	[**12**] = 0.5 μM	[**12**] = 0.1 μM	[**15**] = 5 μM	[**15**] = 1 μM
0	83.07 ± 3.71	48.54 ± 3.91	44.91 ± 1.36	15.06 ± 2.35
5	88.23 ± 3.40	64.74 ± 3.73	55.93 ± 1.92	22.05 ± 2.89
10	95.04 ± 5.36	71.80 ± 2.10	57.23 ± 2.86	28.68 ± 5.01

Thermal stability assay

TSA is widely used in drug discovery to detect potential hit compounds from HTS libraries that have good affinity with the target protein. This technique provides a fluorescence readout measurement of thermally-induced protein melting. The increasing of protein melting temperature (T_m) indicates folding stabilization and may give an information of inhibitor's action towards the protein. Data obtained with this technique demonstrated to be consistent with enzymatic or radioactive assays, isothermal titration calorimetry or other assays [41]. For GSK-3β, this test was performed prior to crystallization trials to determine the effect of compound **12** onto kinase folding stability. [42] *Apo*-kinase and DMSO-incubated protein were used as controls to determine the T_m of *apo*-GSK-3β and the effect on protein stability of DMSO solvent, respectively.

Table S6: Melting temperatures of the *apo*-kinase without incubation, after incubation with DMSO, and GSK3β incubated with compound **12**

	T_m	st.dev.
Apo-GSK3β 35-386	39.15	±0.64
GSK3β 35-386β+ 2,8% DMSO	39.75	±0.21
GSK3β 35-386β+ compound **12**	46.35	±0.21

The increasing of the T_m for the bound protein demonstrated that binding of compound **12** stabilises the GSK3β folding. As reported in Table S5 the effect of DMSO was irrelevant compared to the seven-degrees increase of the melting temperature caused by compound **12** binding. The results of this test suggest the formation of a strong bond GSK-3β-compound **12**.

Crystal structure of GSK3β-compound 12

In order to remove flexible regions that would hamper crystallization attempts, a GSK--3β construct trimmed at the N- and C- region was used for crystallization, considering the flexibility observed in previous crystallographic studies.[43-45]

In the crystals structure, GSK-3β forms a dimeric assembly with two molecules in the asymmetric unit as previously described in literature.[43-45]The N- and C-terminal ends of the construct (residues 35 and 384-386) were partially disordered, a clear electron density was visible only for residues 36-383. In addition, surface residues were less ordered compared to the overall structure and electron density of surface Arg side chains was poor. A residual electron density was observed in each ATP binding pocket and refinement cycles confirmed the fitting of a compound **12** molecule in the active site (Figure 3 of the main text). Refinement tests were carried on with different conformations of unbound compound **12** and with the covalently bound form, but only the latter could fit the residual electron density, confirming the formation of a covalent bond between compound **12** and Cys199 of the kinase (Figure S10). In the asymmetric unit, a malonate ion, three glycerol molecules, two chloride ions, a sodium ion, and 266 water molecules are visible. According to literature,[43] GSK3β has two phosphorylation sites, Ser9 and Tyr216. In the construct used for crystallization the inhibitory phosphorylation site (Ser9) was not present. The electron density shows that no phosphate group is present on the side chain of residue 216, proving that the kinase in this crystal structure is unphosphorylated. Two Ramachandran outliers (Arg 220 and Tyr 221) are present in the final structure, despite a good fitting in the electron density map. The presence of Ramachandran outliers for these two residues in many of the previously determined GSK-3β structures [23,43-45] suggests a conserved strained conformation for residues 220-221.

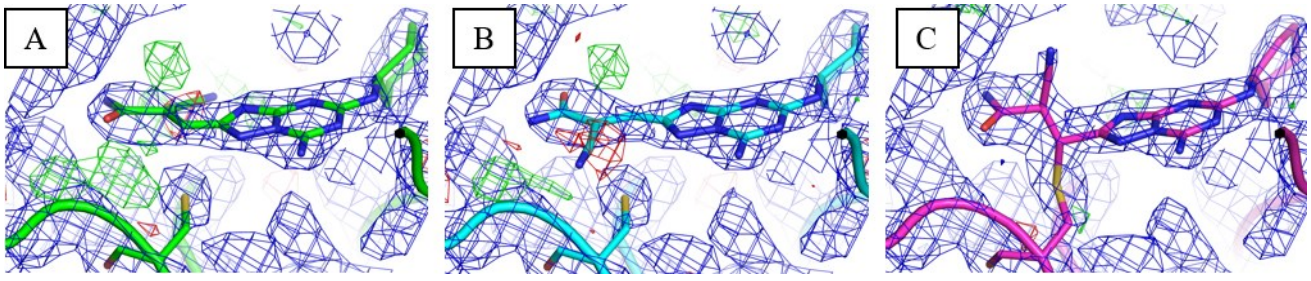

Figure S9: Results of the refinement tests using different compound **12** non-covalently bound conformers (A and B) and the compound 12-Cys199 bound conformation used in the final refinement (C). Electron density maps are depicted in blue (σ level: 1.0), difference electron density maps are depicted in green (σ level: 2.5) and red (σ level: -2.5).

Finally, the Michael reaction leads to the formation of two new stereocenters on the compound-**12**/Cys-199 adduct. Analysing the crystal structure, it is interesting to note that thia-Michael addition occurred in an enantio- and diastero-selective way, in fact, only the anti-(R,R) product was obtained.

IC_{50} of Compound 12 towards GSK- 3β(35-386)

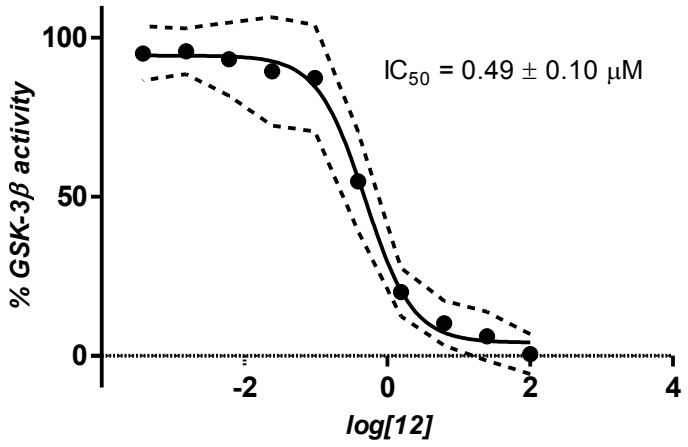

Figure S10. .Activity of purified GSK3β(35-386) protein at different concentrations of compound **12** (n=3).

Selectivity

Compound **12** was screened at 10 μM using the KINOMEScan™ approach on few other family related kinases in order to preliminary assess its selectivity. Data are reported in table S3.

Table S7. Results of binding interactions between compound **12** and the target kinases.

Target	% Ctrl[a] at [**12**] = 10 μM
CDK2	100
CDK5	100
CSNK1A1	74
CSNK1G1	76
CSNK1G2	81
CSNK1G3	86
CSNK1E	98
CSNK2A1	87

[a] calculated as ((test compound signal-positive control signal)/(negative control signal-positive control signal))x100 where negative control is DMSO (100% Ctrl) and positive control is a control compound (0% Ctrl).

In vitro neuroprotection studies

Since an abnormal increase in GSK-3β activity leads to an activation of the microglia followed by an increase in inflammation and neuronal death and,[46] similarly, CK-1δ contributes to exacerbate neurodegenerative disease progression, we decided to study in *in vitro* models the neuroprotective potential of GSK-3β/CK-1δ inhibition by compound **12**.[40]These first evaluations were assessed in Parkinson's disease (PD) *in vitro* models, in presence of different neurotoxins, such as 4-phenyl-1-methyl-1,2,3,6-tetrahydropyridine (MPTP) or 6-hydroxydopamine (6-OHDA).[45] Both MPP^+, the toxic metabolite of MTPT, and 6-OHDA, hydroxylated analogue of dopamine, are thought to induce dopaminergic toxicity, and consequent parkinsonism by intra- and extracellular oxidation, hydrogen peroxide formation, and direct inhibition of the mitochondrial respiratory chain.[46] In the MPTP or 6-OHDA injury models, cell viability was measured in the presence of these neurotoxins, with or without treatment with lithium (as reference compound) and derivative **12**, using rat PC12 pheochromocytoma cells, an immortalized cell line with neuronal phenotypes. In pilot experiments, compound **12** was proved not to be cytotoxic in this cell line up to a 10 μM concentration (Figure 4A). On the contrary, in the same assay, 6-OHDA produced a significant and concentration-dependent neurotoxic effect in PC12 cell line (Figure 4B). The dose of 100 μM, which caused a 50% of cell death, was chosen for the subsequent neuroprotection studies. Similarly, it was found that both compound **12** (Figure 4C) and lithium chloride (Figure 4D) prevent 6-OHDA-induced cell death in a concentration dependent manner. Two different assays were used to evaluate compound **12** in MPTP-model: The CellTiter-Glo® assay (Figure S12A-B) and 3-(4,5-dimethythiazol-2-yl)-2,5-diphenyl tetrazolium bromide (MTT) methodology (Figure S11C-D).

In both assays, cells were pre-treated with increasing concentrations of compound **12** (0.1, 1, 10 μM) for 2 h and then incubated with 1.5 mM of MPP^+ for 24 h. As we can observe, cell survival is diminished after treatment with MPP+ (second column of histograms); however, cells treated with the same dose of MPP^+ and derivative **12** showed a dose-dependent increase in cell viability. These

results are comparable to those obtained after treatment with lithium chloride (1, 5, 10 mM), a well-established neuroprotective agent, whose mechanisms of action also include GSK-3β inhibition.[49]

Recent studies reported compelling evidences for a linkage between Wnt/β-catenin signalling and inflammatory events during PD progression.[48] In particular, β-catenin pathway is considered a pro-survival signalling cascade, since stabilized β-catenin regulates the expression of genes responsible of dopamine neurons survival/protection. It is widely recognized that kinase upregulation, including GSK-3β, leads to β-catenin degradation and increased neurons vulnerability, degeneration and death.[50] Therefore, first of all influence of 6-OHDA on GSK-3β activity was analysed (Figure 5A). GSK-3β is less active when phosphorylated at the 9-Ser residue, thus ratio between 9-Ser-GSK-3β and GSK-3β (not phosphorylated at 9-Ser) was kept as marker for kinase activation status in the cells. Results showed that 6-OHDA increases the activity of GSK-3β, while **12** and LiCl counteract this effect (Figure 5A).

At this point, the effect in β-catenin expression of compound **12** in 6-OHDA-PD-model was examined. From the results reported in figure 5B, we can infer that derivative **12**, albeit weakly in comparison to lithium, promotes β-catenin stabilization, thus restoring its neuroprotective potential in a PD-model.

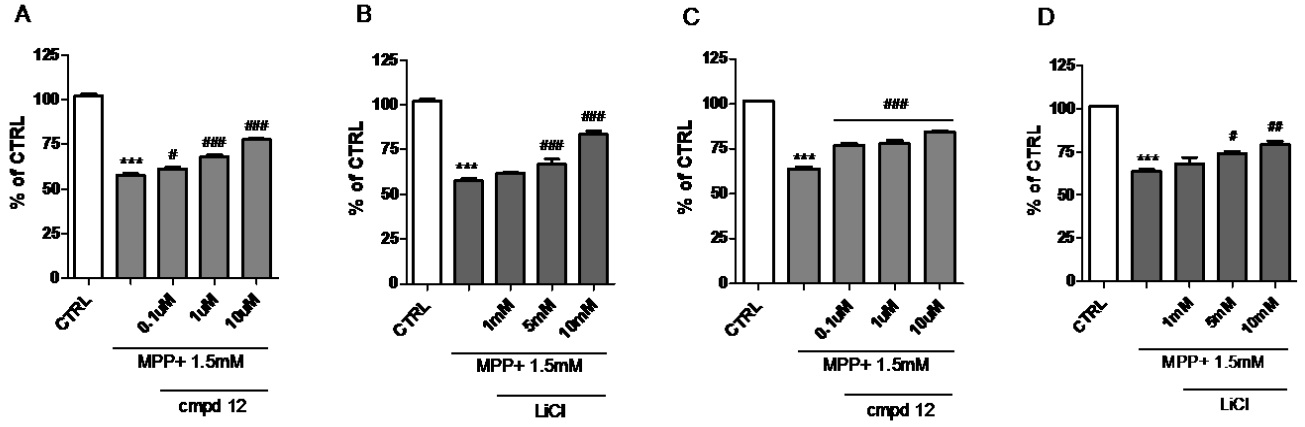

Figure S11. Compound **12** induced neuroprotection against MPP+. PC12 were pre-treated with increasing concentrations of compound **12** (0.1, 1, 10 μM) and LiCL (1, 5, 10 mM) for 2 h and then incubated with 1.5 mM of MPP^+ for 24 h. Effects of different treatments on cell viability were measured by using The CellTiter-Glo® assay (A-B) and 3-(4,5-dimethythiazol-2-yl)-2,5-diphenyl tetrazolium bromide (MTT) methodology (C-D). Data represent mean ± s.e.m. (n=3). ***p<0.001 vs CTRL, #p<0.1, ##p<0.01, ###p<0.001 vs MPP+ One-way Anova followed by Newman-Keuls test.

Spectra of tested compounds (1-6, 8-15)

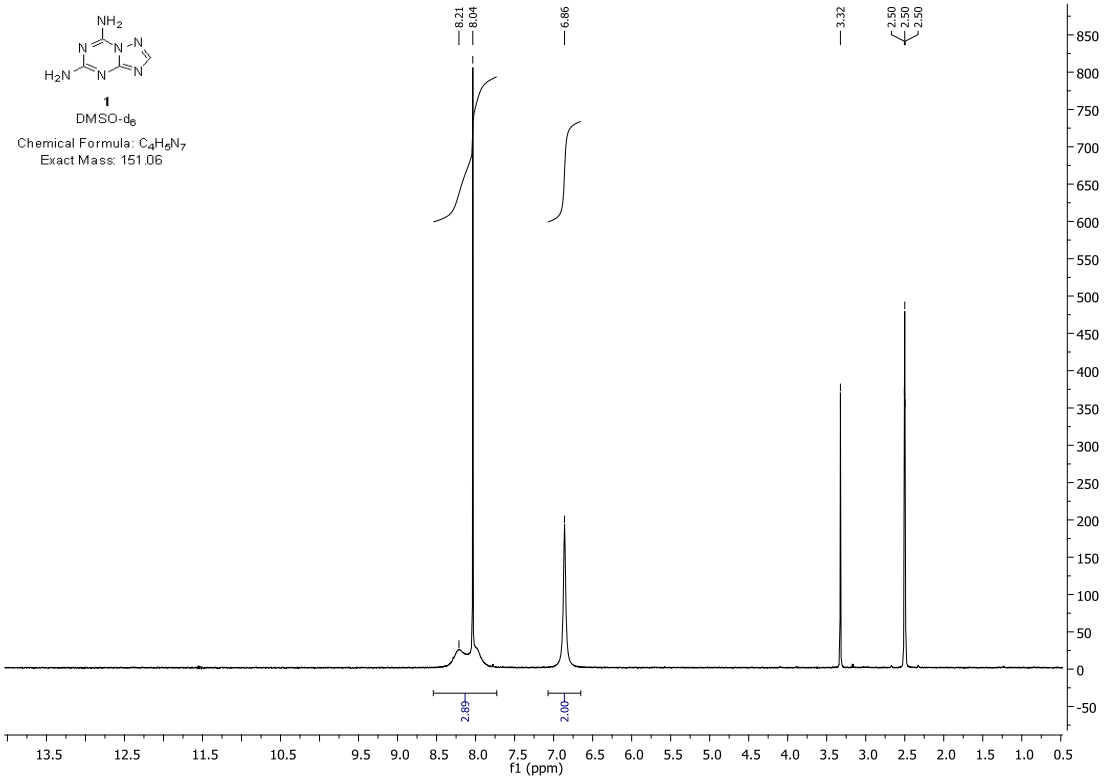

Figure S12. ^{1}H-NMR spectrum of compound **1**.

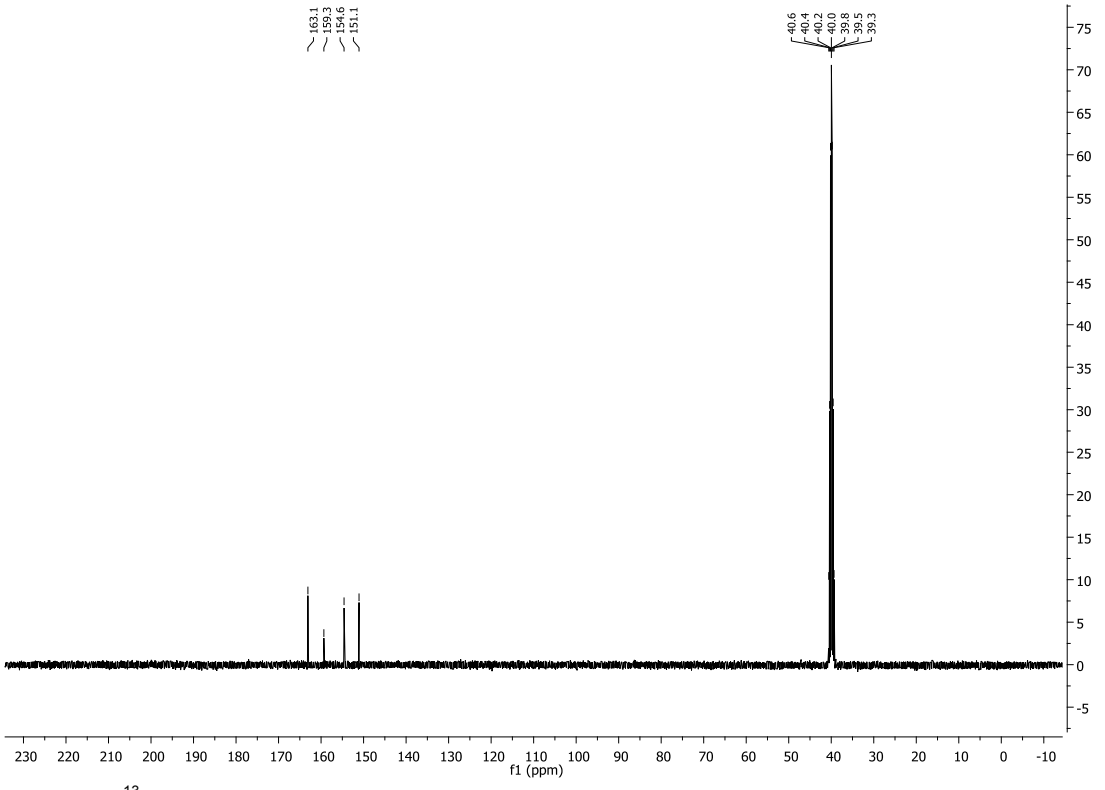

Figure S13. ^{13}C-NMR spectrum of compound **1**.

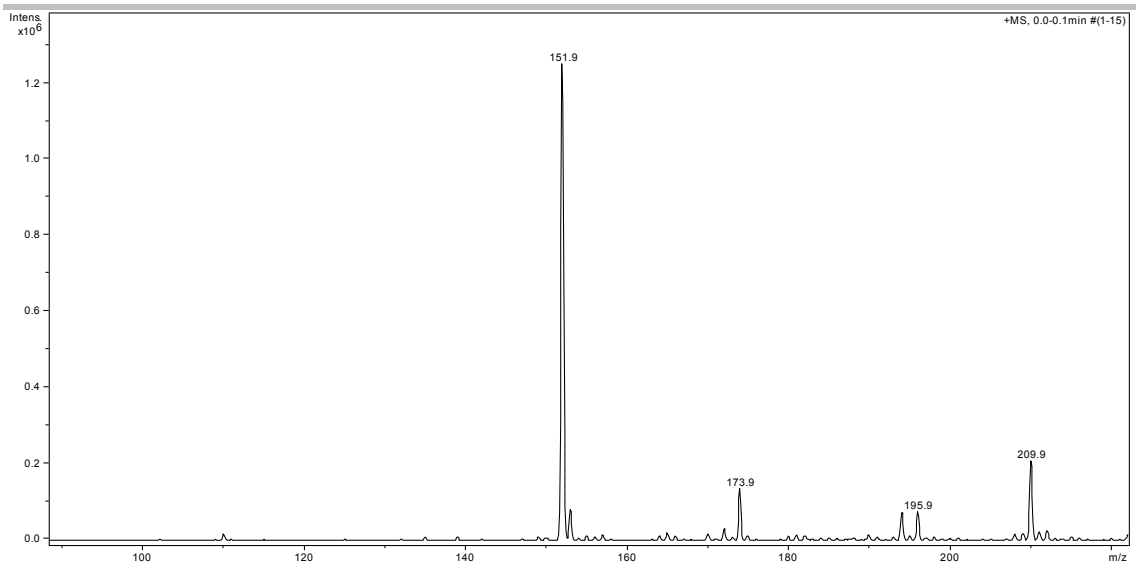

Figure S14. ESI-IT-MS spectrum of compound **1**.

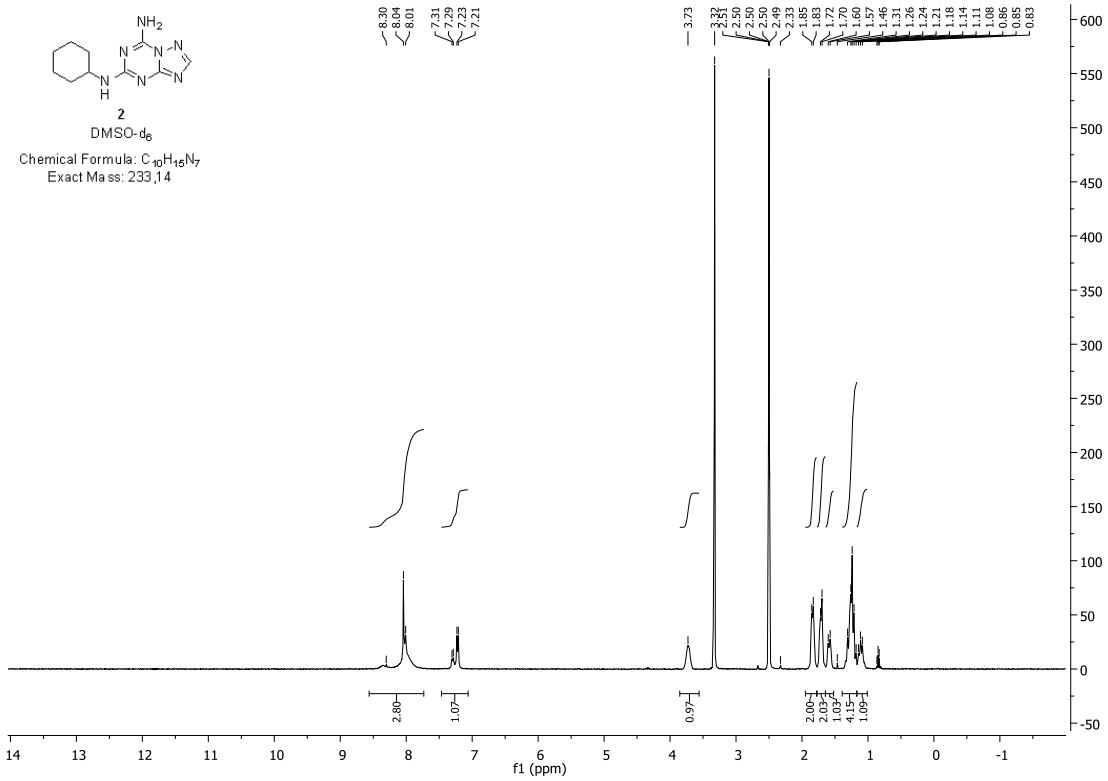

Figure S15. ^{1}H-NMR spectrum of compound **2**.

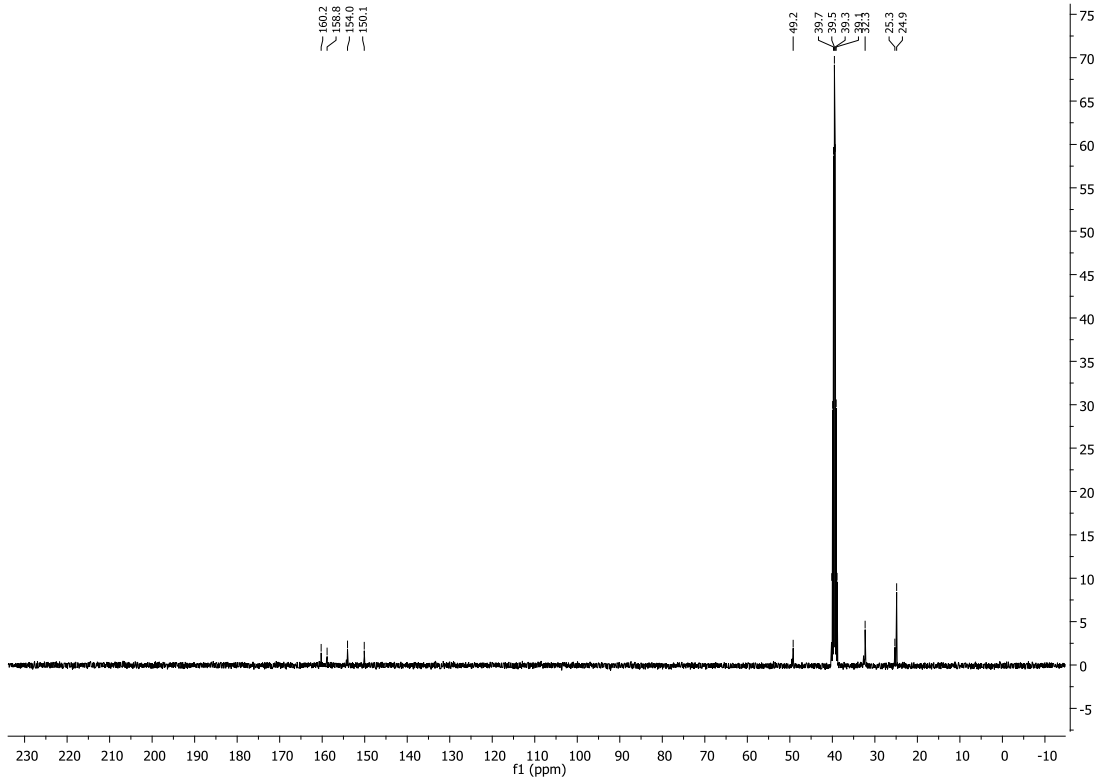

Figure S16. ^{13}C-NMR spectrum of compound **2**.

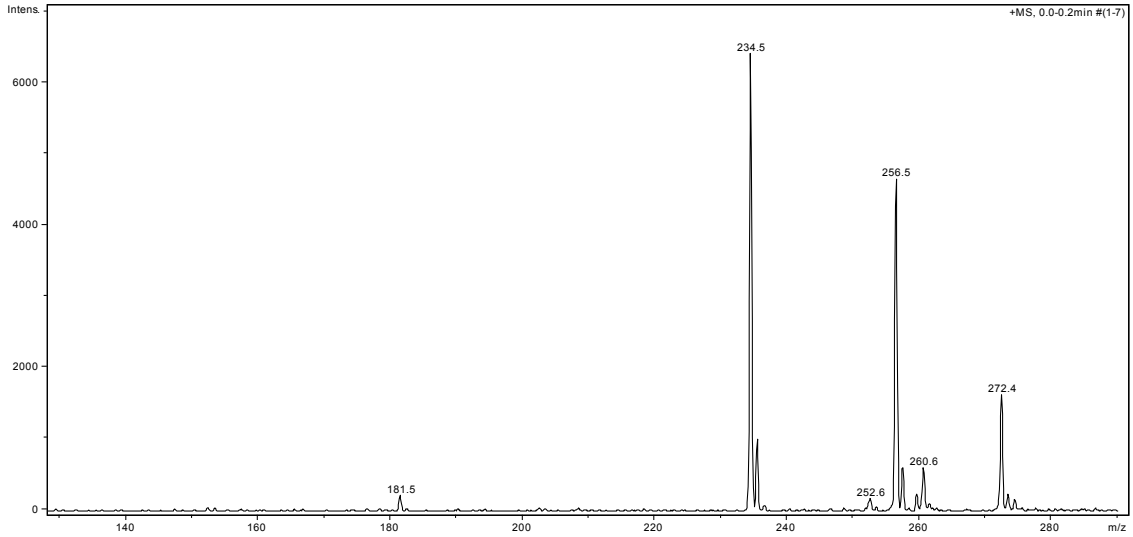

Figure S17. ESI-IT-MS spectrum of compound **2**.

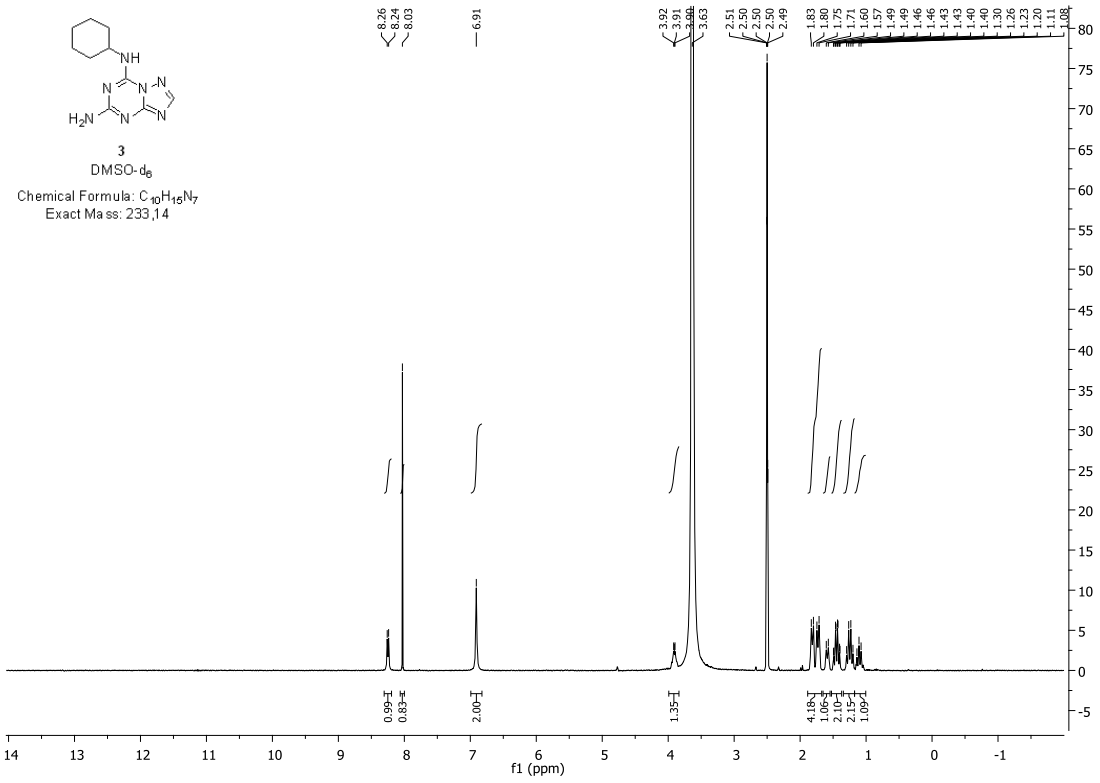

Figure S18. ^{1}H-NMR spectrum of compound **3**.

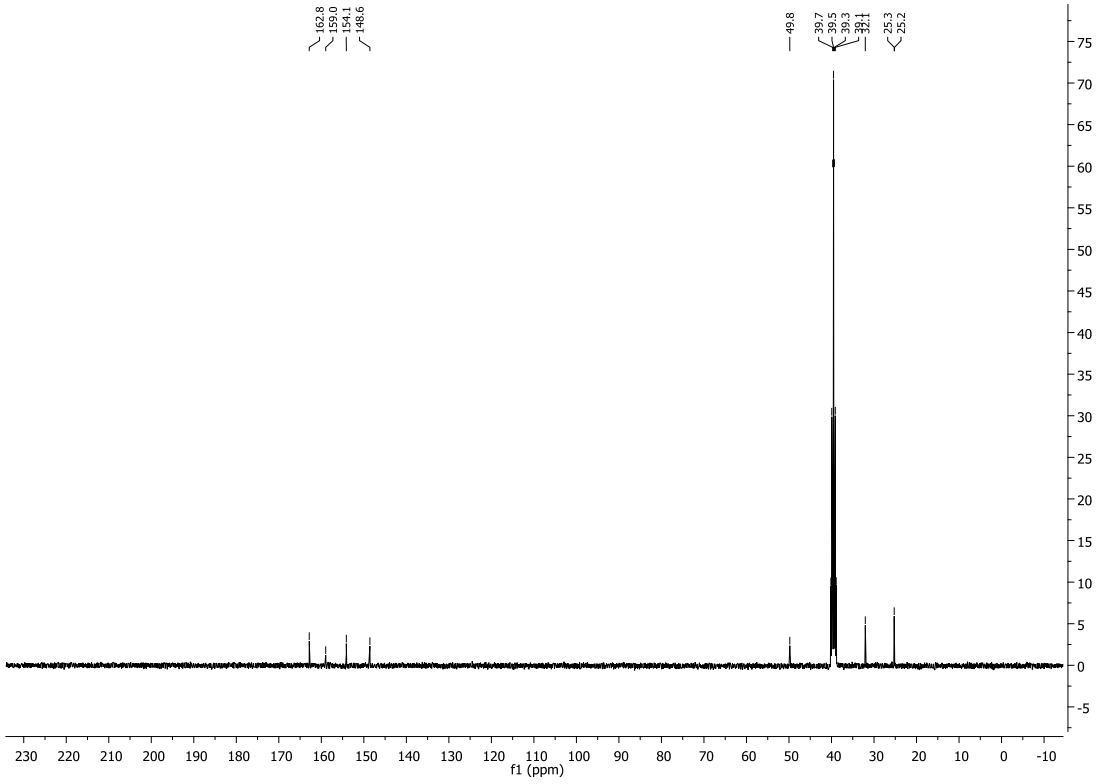

Figure S19. ^{13}C-NMR spectrum of compound **3**.

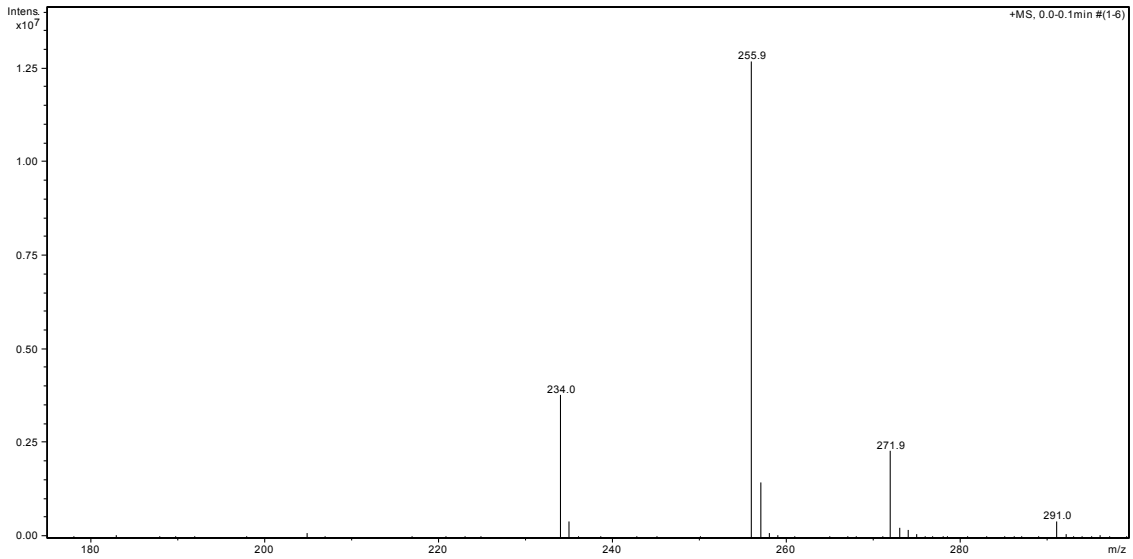

Figure S20. ESI-IT-MS spectrum of compound **3**.

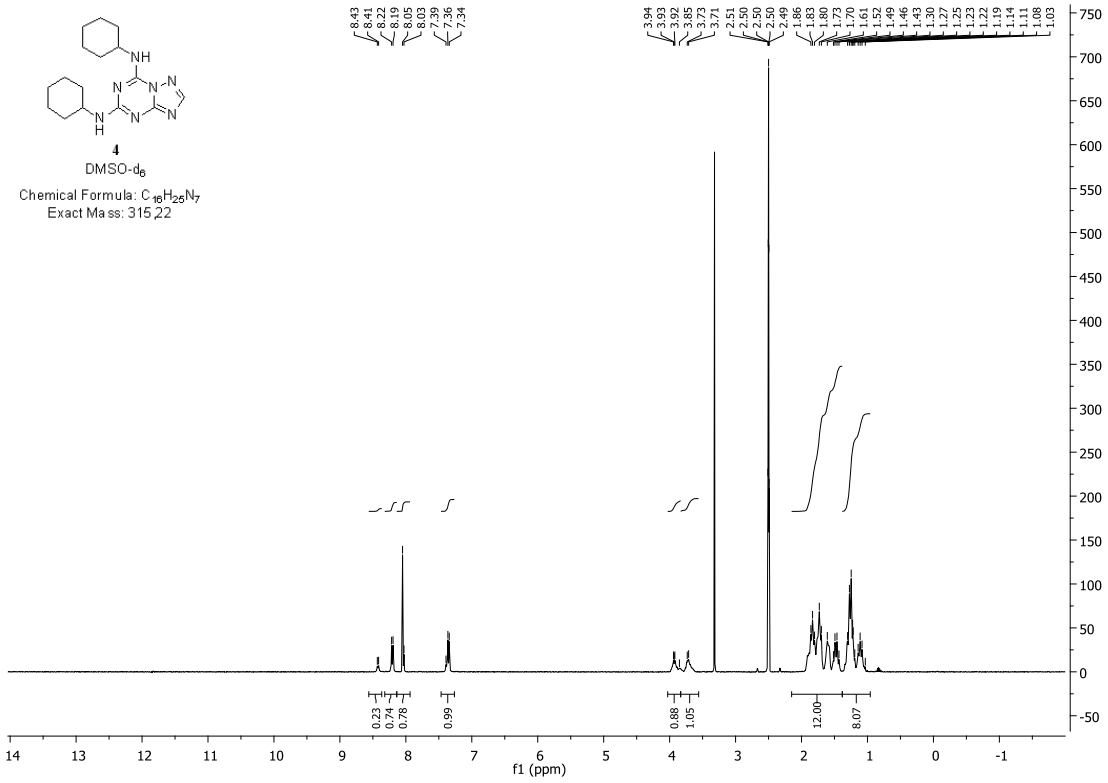

Figure S21. ^{1}H-NMR spectrum of compound **4**.

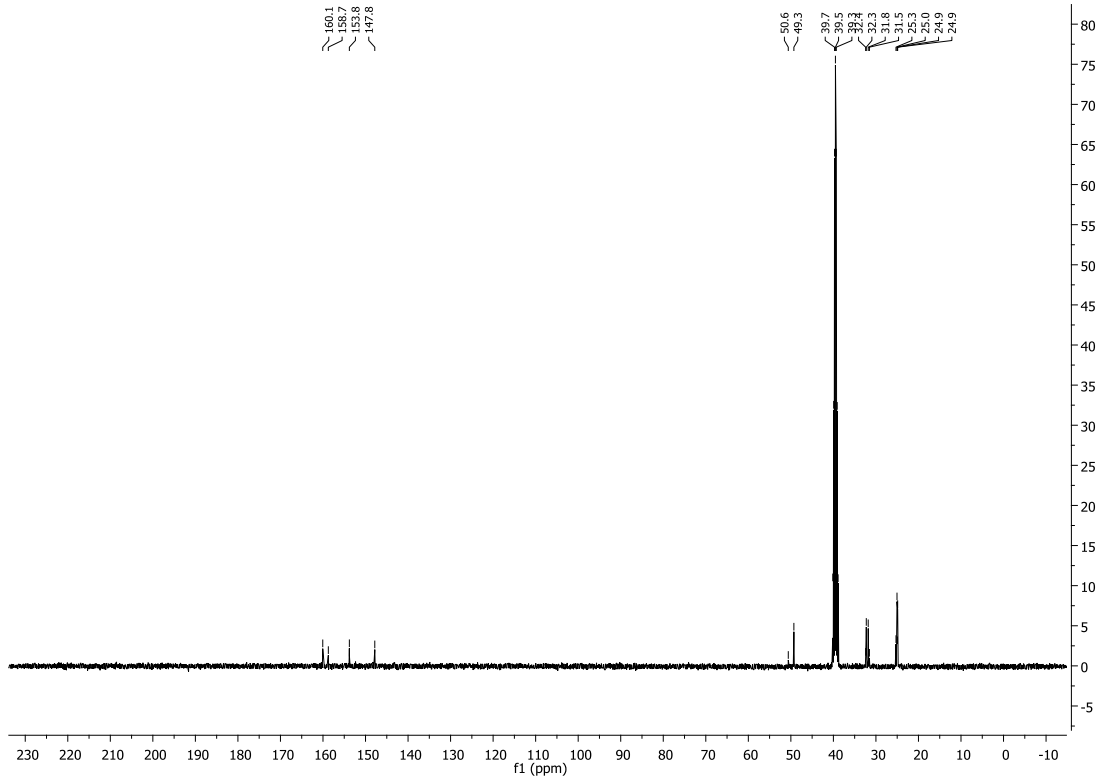

Figure S22. ^{13}C-NMR spectrum of compound **4**.

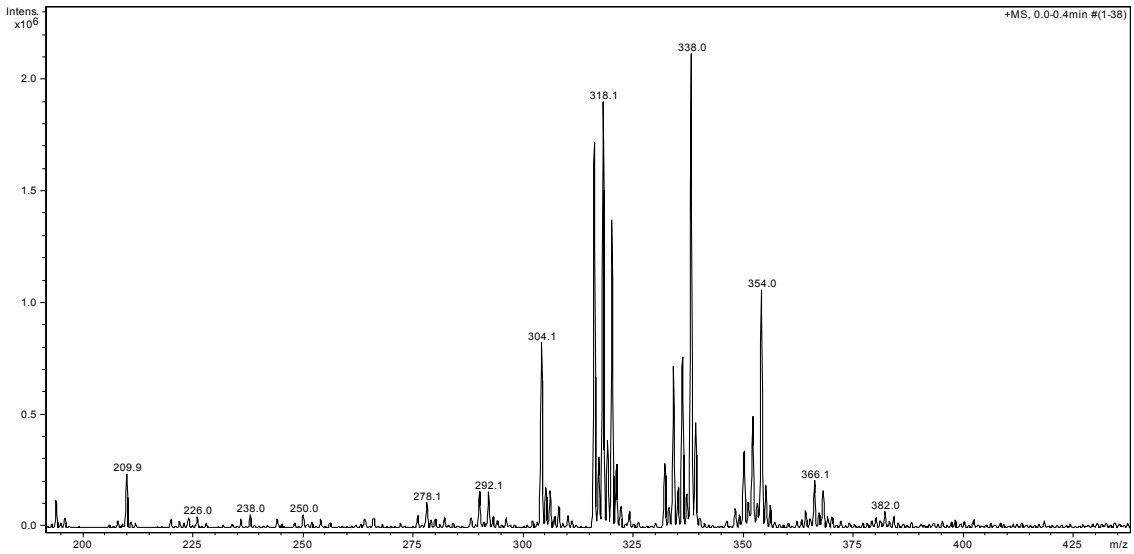

Figure S23. ESI-IT-MS spectrum of compound **4**.

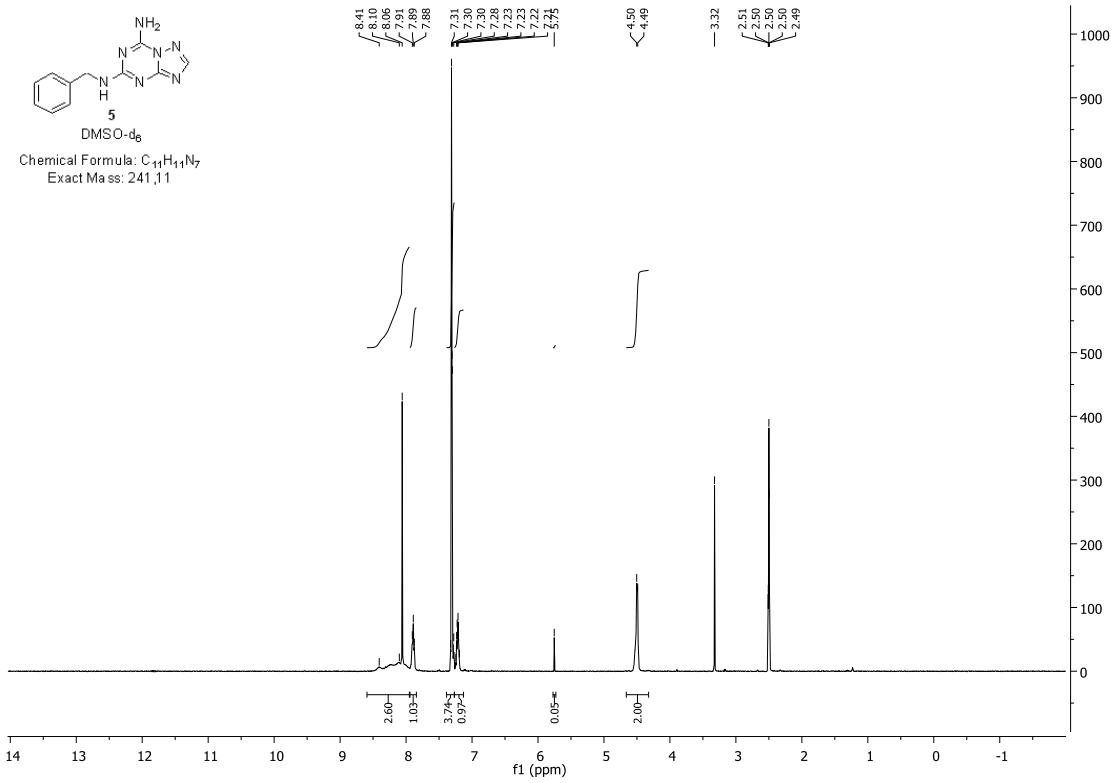

Figure S24. ^{1}H-NMR spectrum of compound **5**.

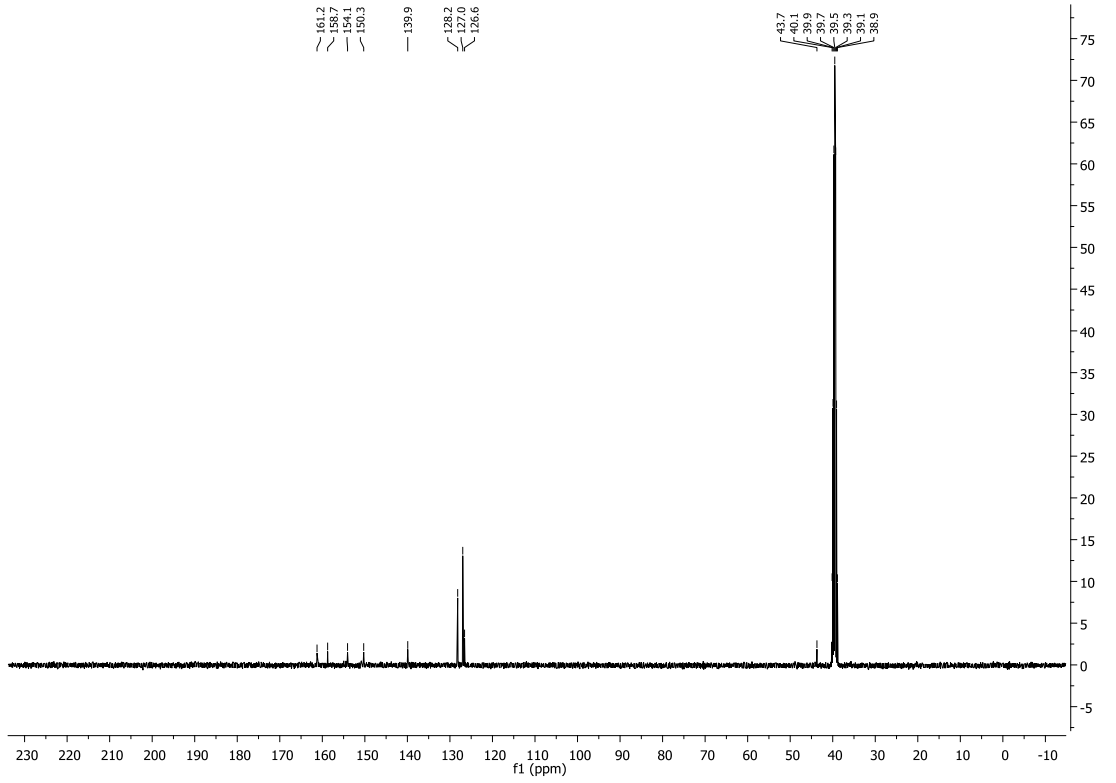

Figure S25. ^{13}C-NMR spectrum of compound **5**.

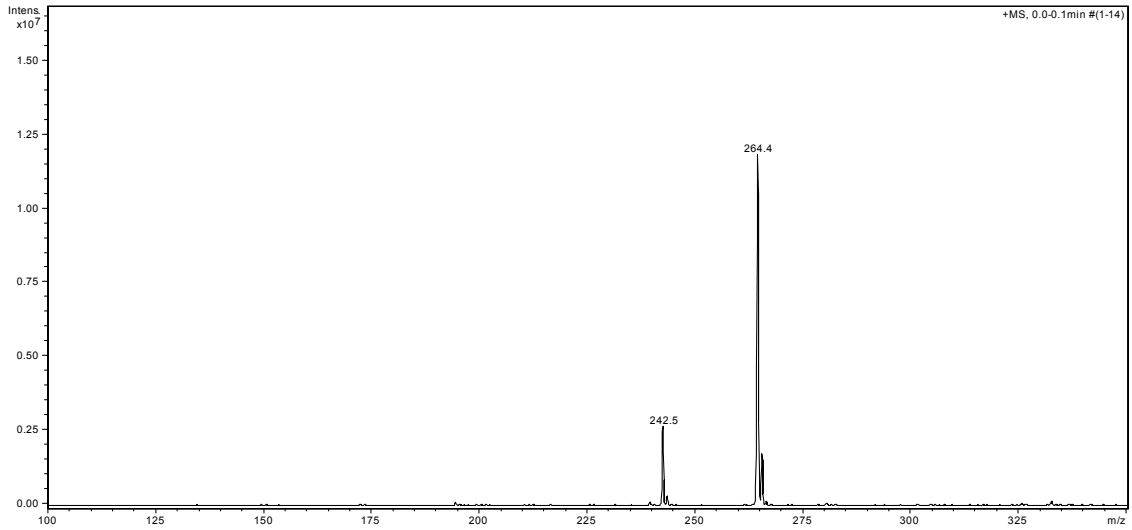

Figure S26. ESI-IT-MS spectrum of compound **5**.

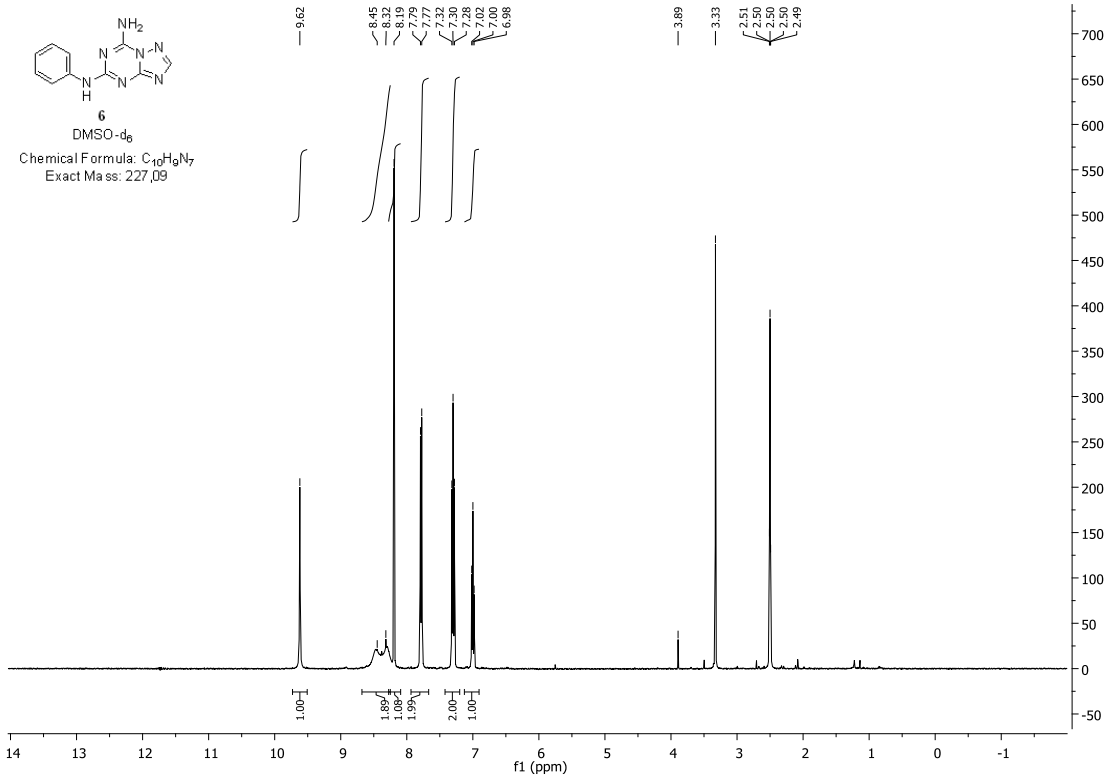

Figure S27. ^{1}H-NMR spectrum of compound **6**.

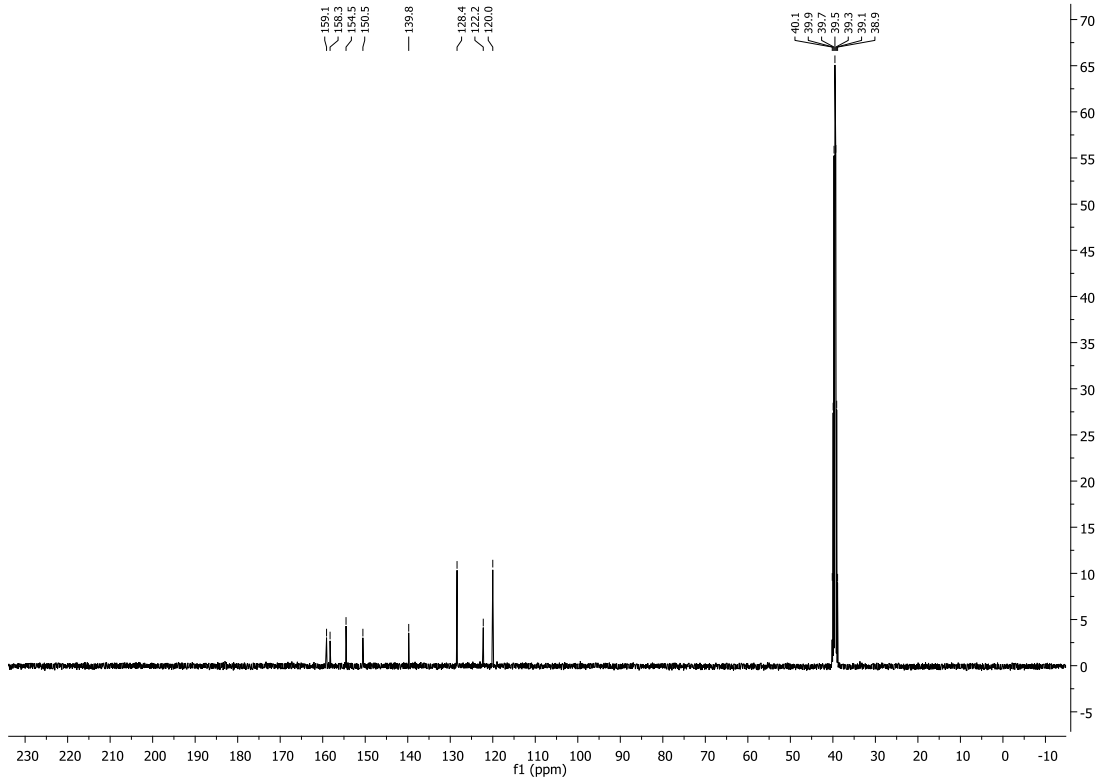

Figure S28. ^{13}C-NMR spectrum of compound **6**.

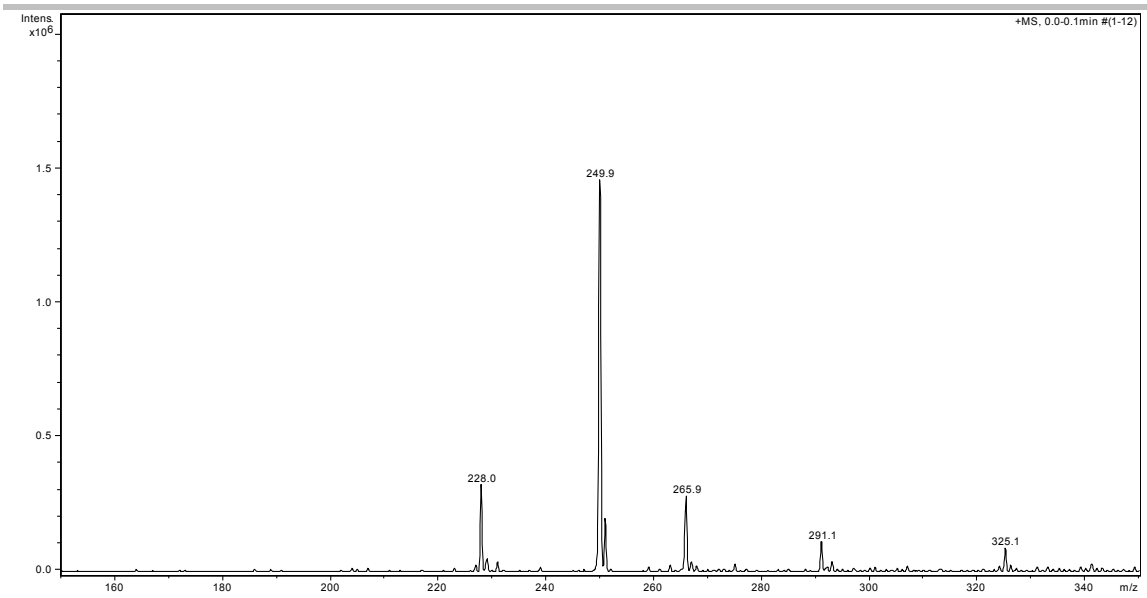

Figure S29. ESI-IT-MS spectrum of compound **6**.

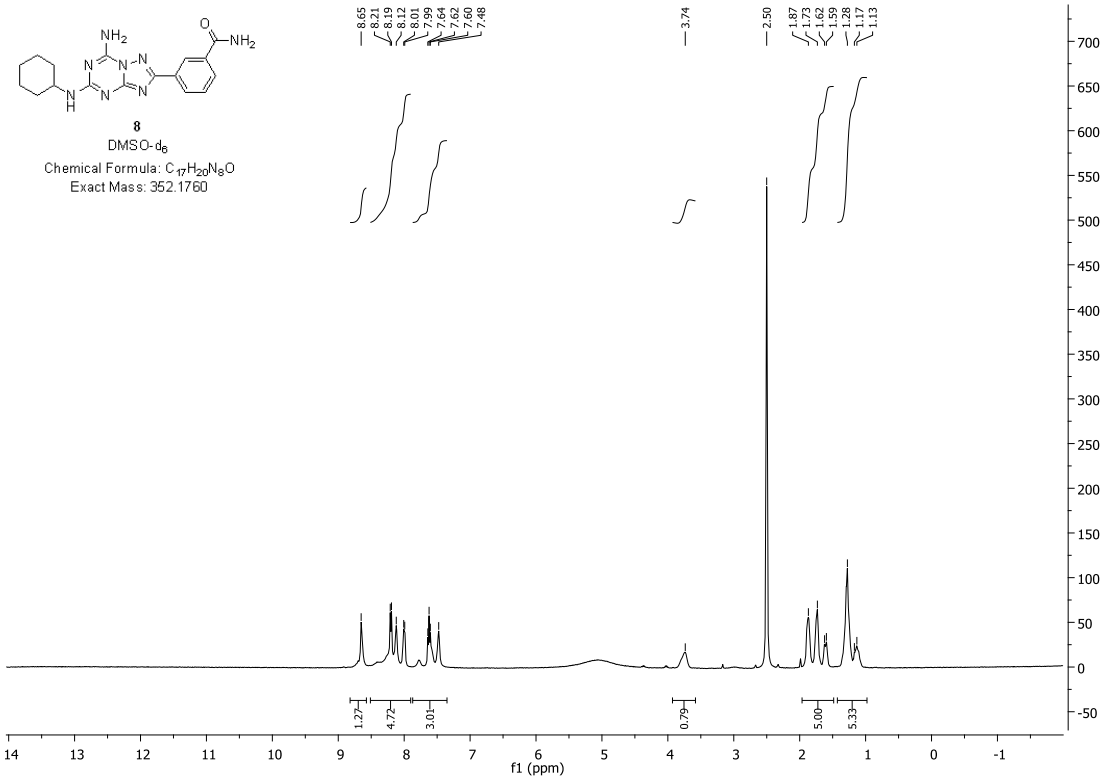

Figure S30. ^{1}H-NMR spectrum of compound **8**.

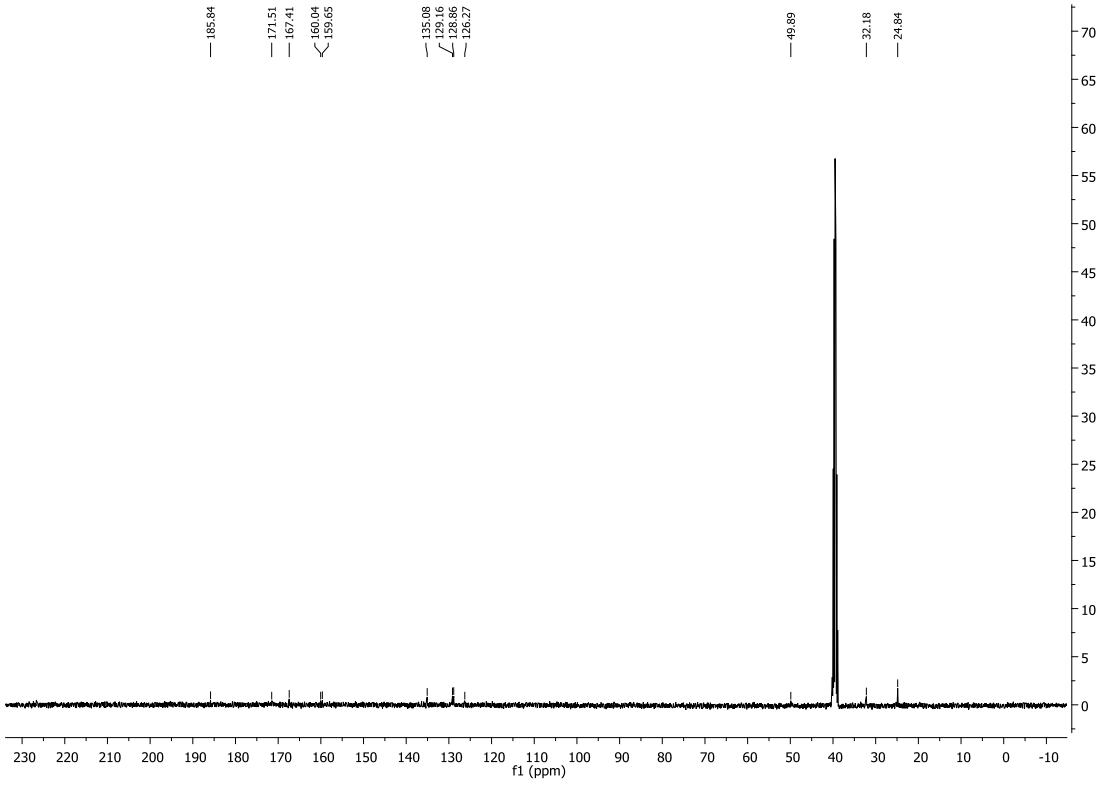

Figure S31. ^{13}C-NMR spectrum of compound **8**.

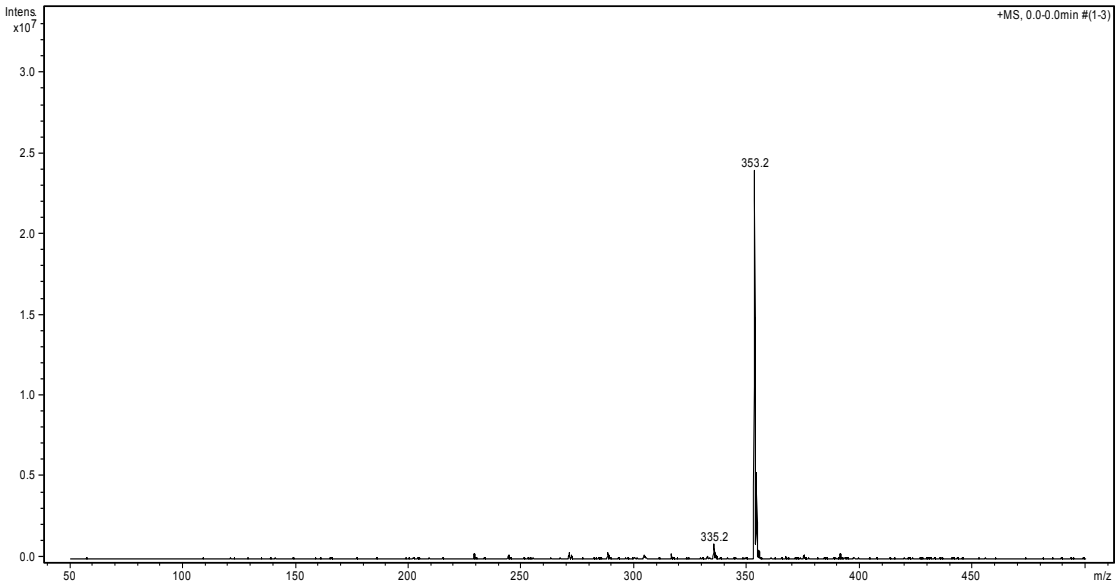

Figure S32. ESI-IT-MS spectrum of compound **8**.

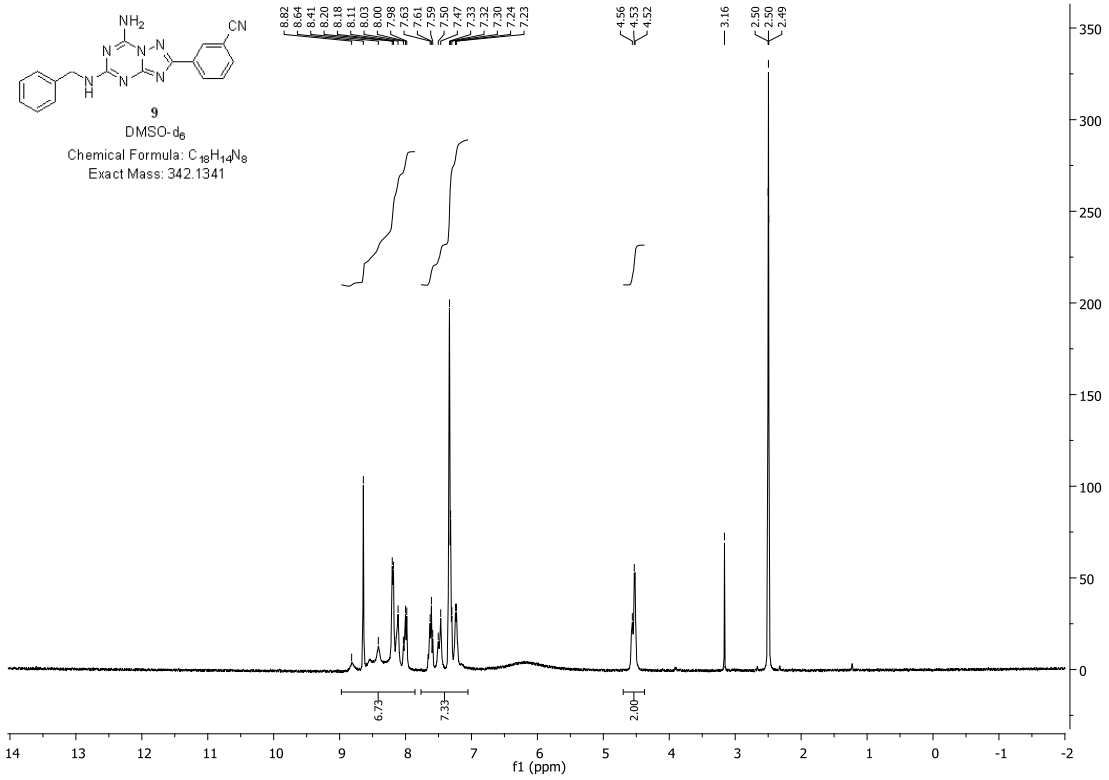

Figure S33. ^{1}H-NMR spectrum of compound **9**.

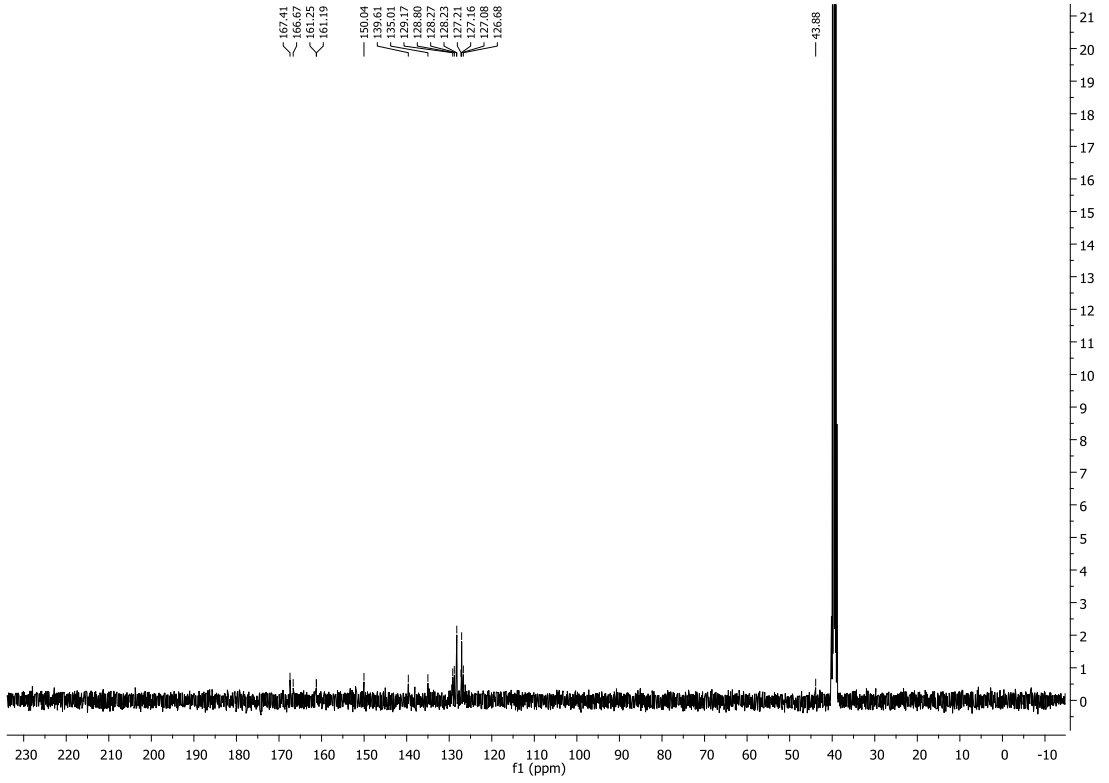

Figure S34. ^{13}C-NMR spectrum of compound **9**.

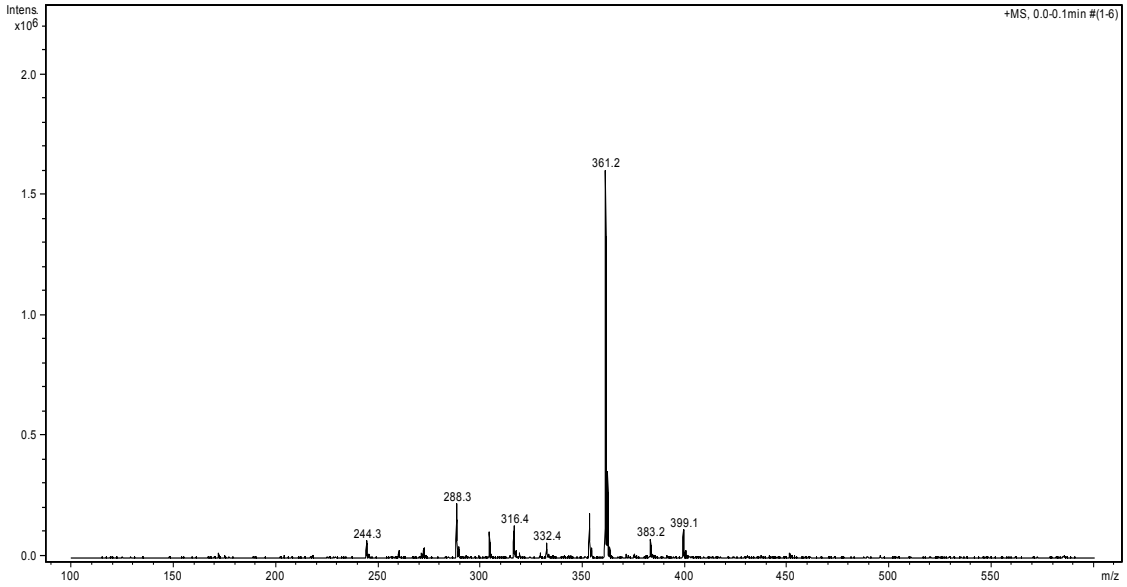

Figure S35. ESI-IT-MS spectrum of compound **9**.

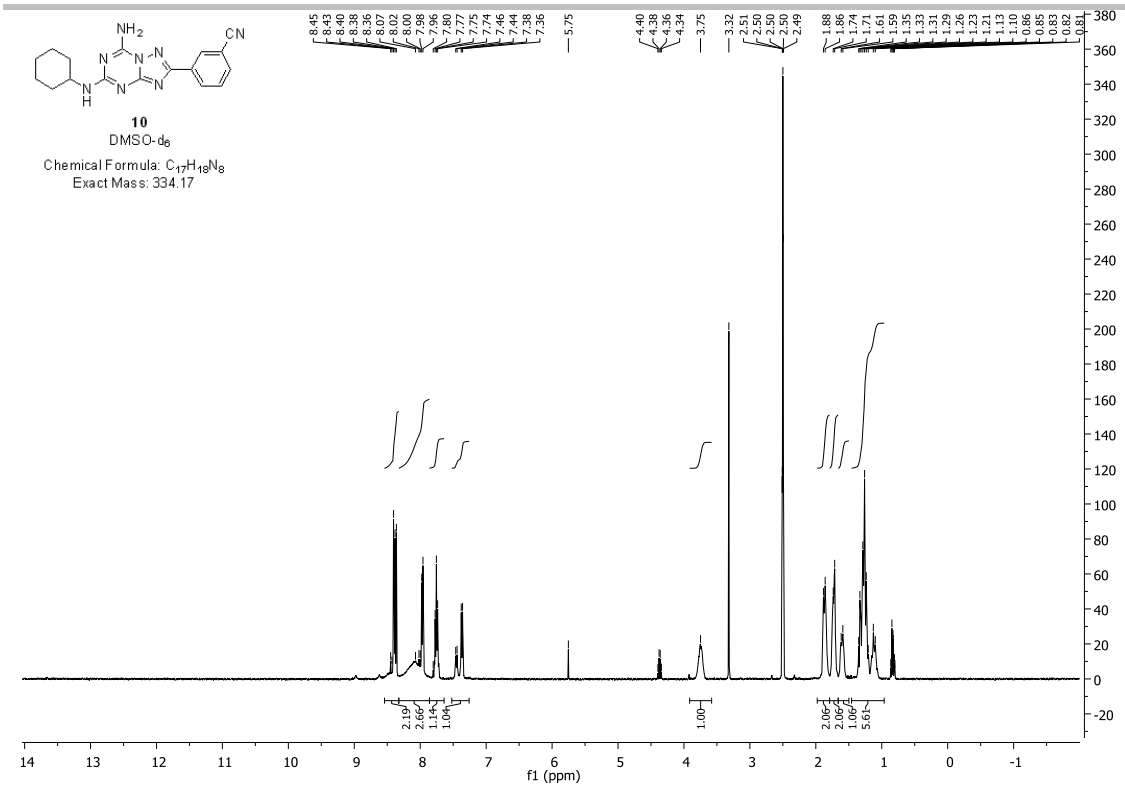

Figure S36. ^{1}H-NMR spectrum of compound **10**.

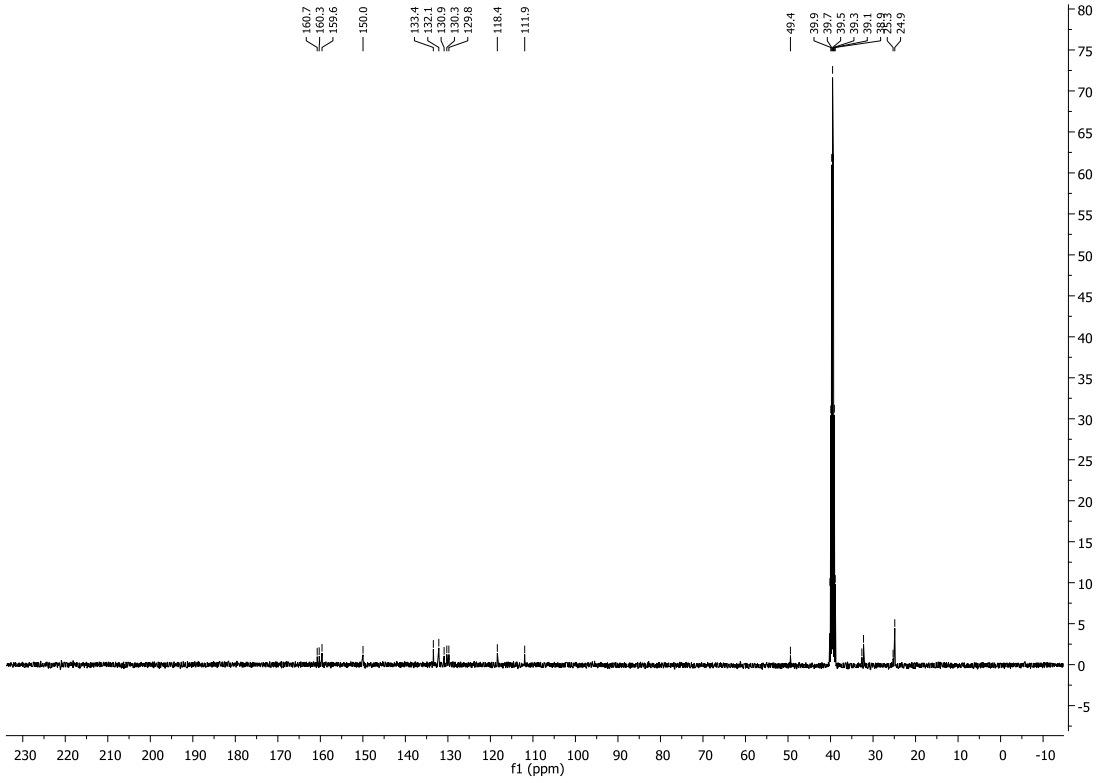

Figure S37. ^{13}C-NMR spectrum of compound **10**.

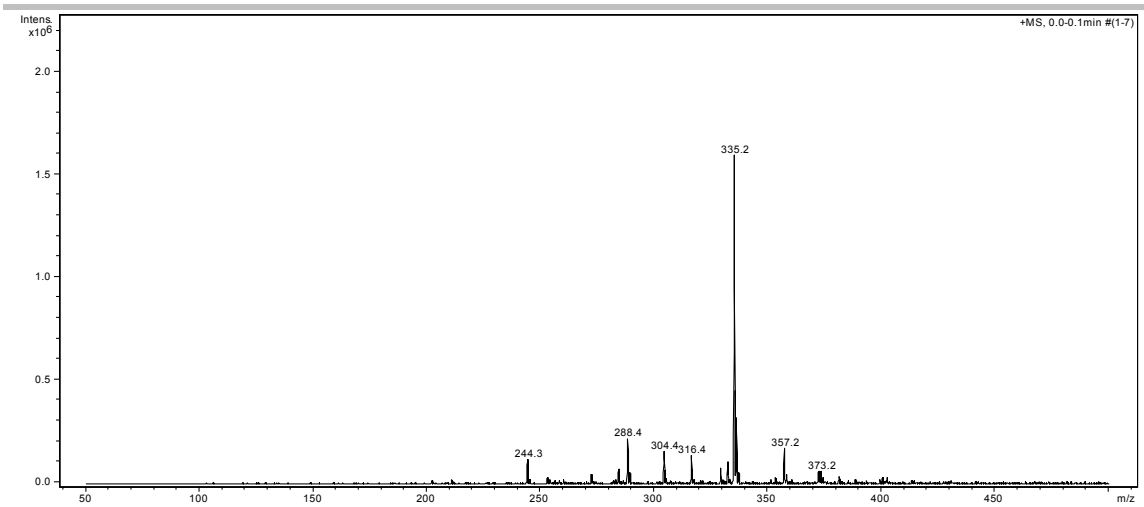

Figure S38. ESI-IT-MS spectrum of compound **10**.

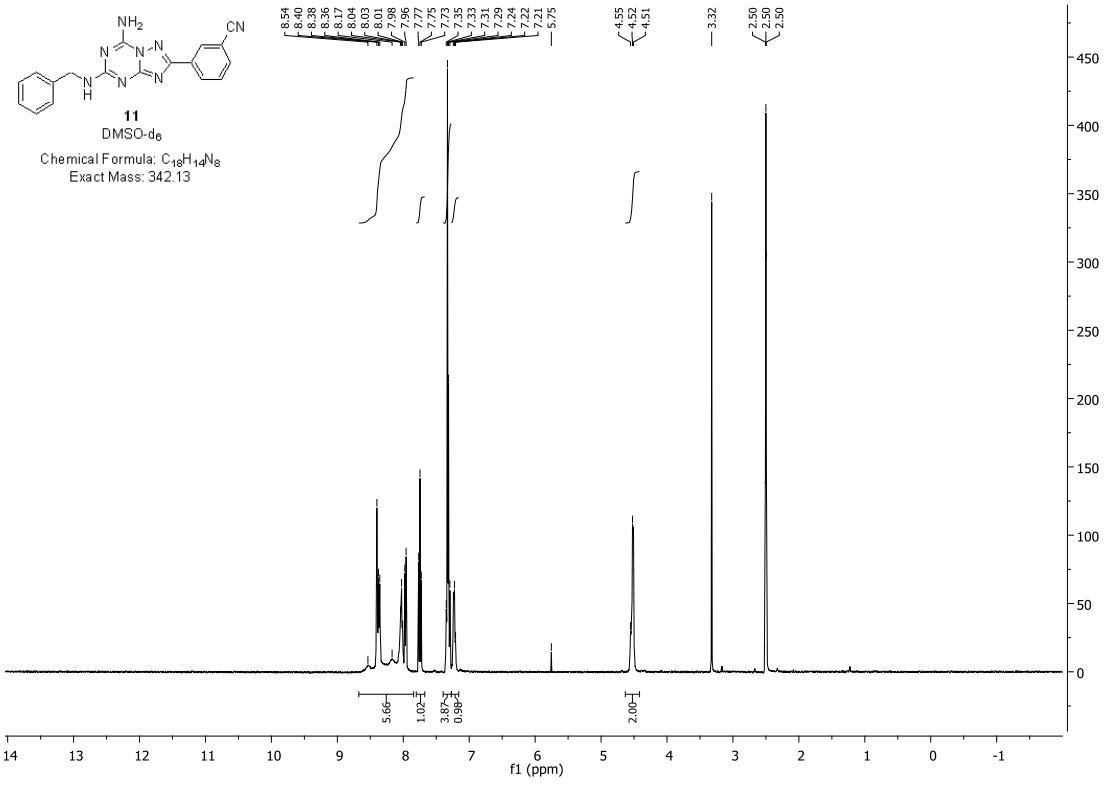

Figure S39. ^{1}H-NMR spectrum of compound **11**.

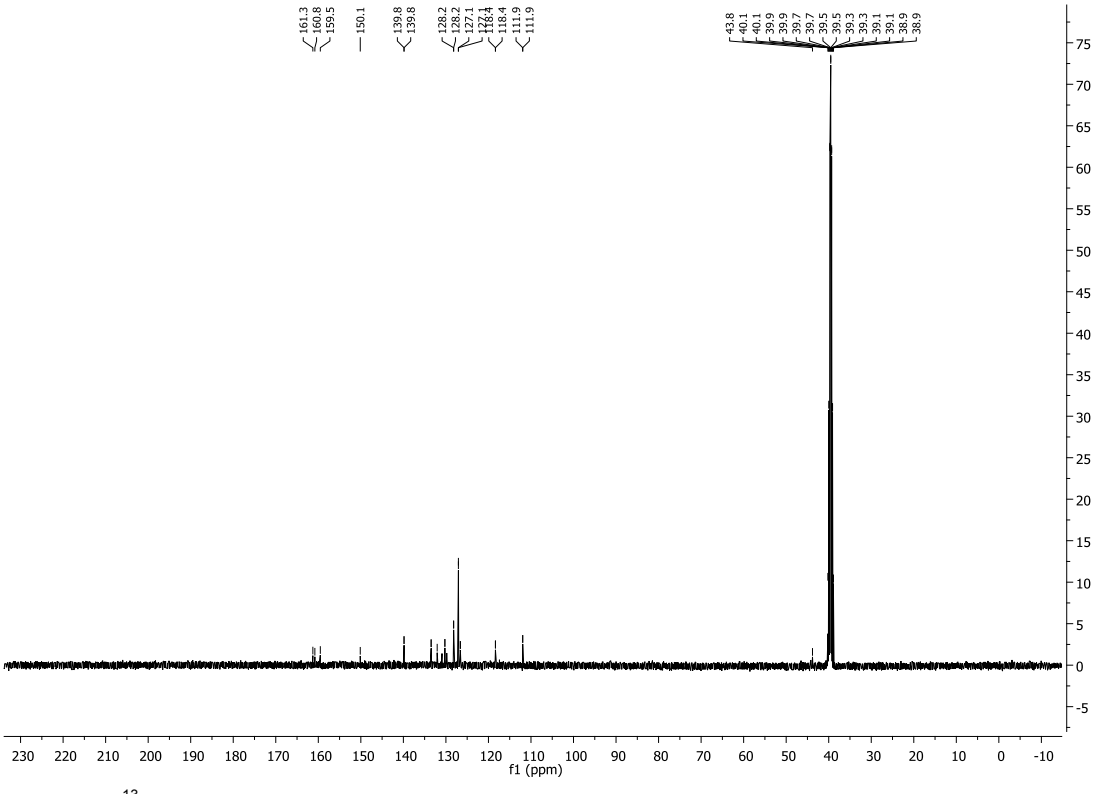

Figure S40. ^{13}C-NMR spectrum of compound **11**.

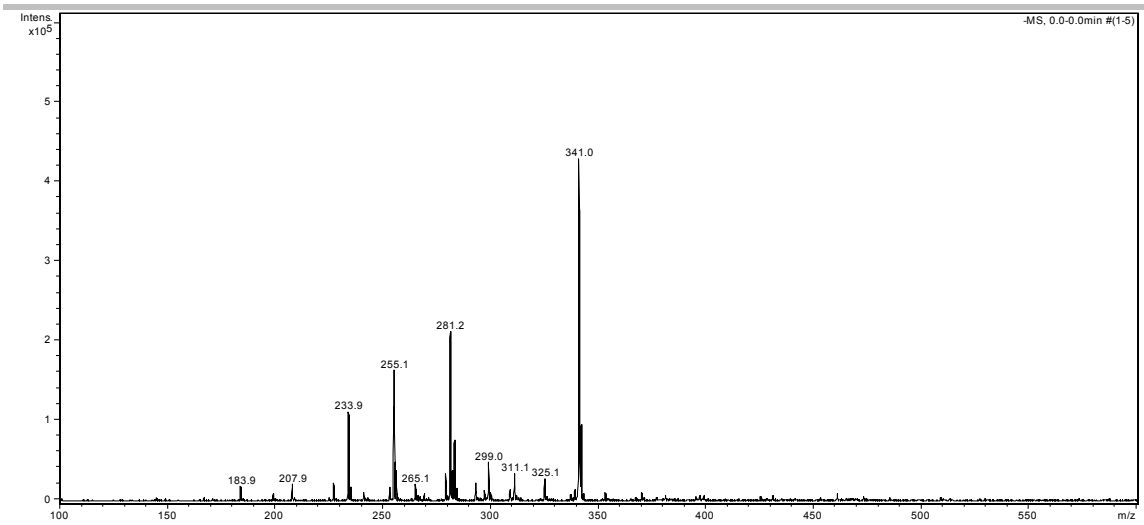

Figure S41. ESI-IT-MS spectrum of compound **11**.

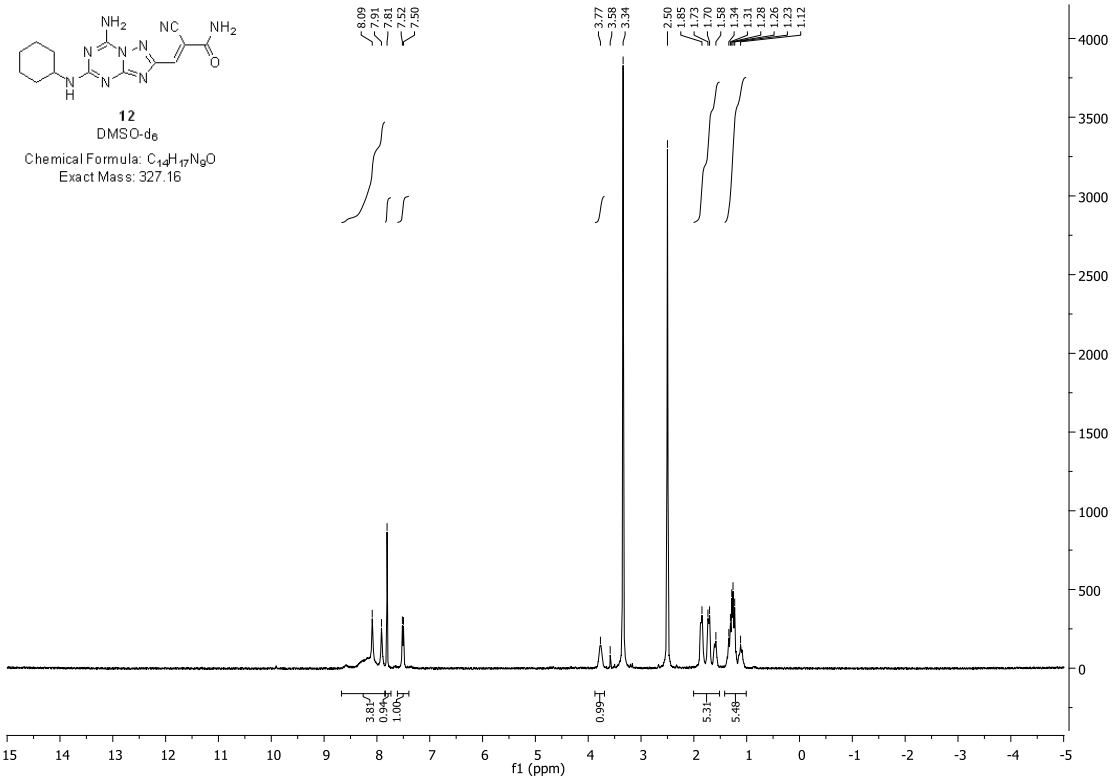

Figure S42. ^{1}H-NMR spectrum of compound **12**.

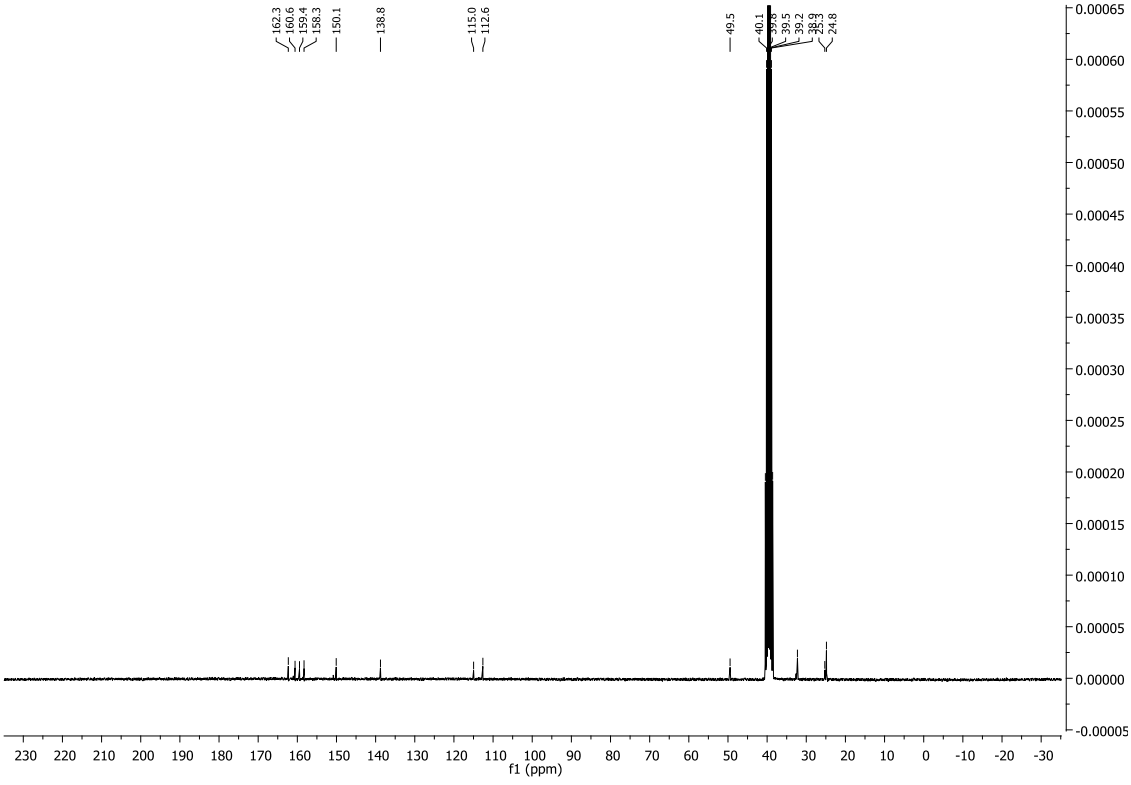

Figure S43. ^{13}C-NMR spectrum of compound **12**.

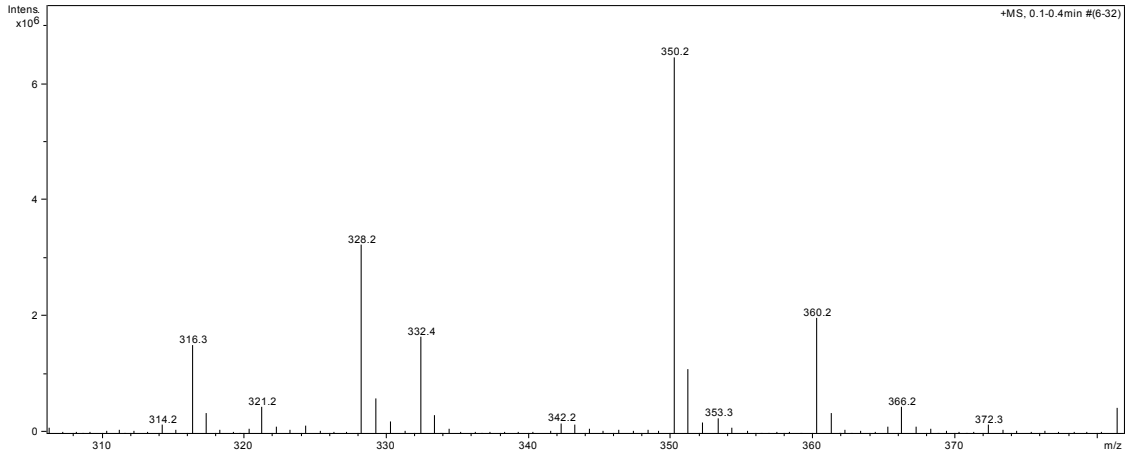

Figure S44. ESI-IT-MS spectrum of compound **12**.

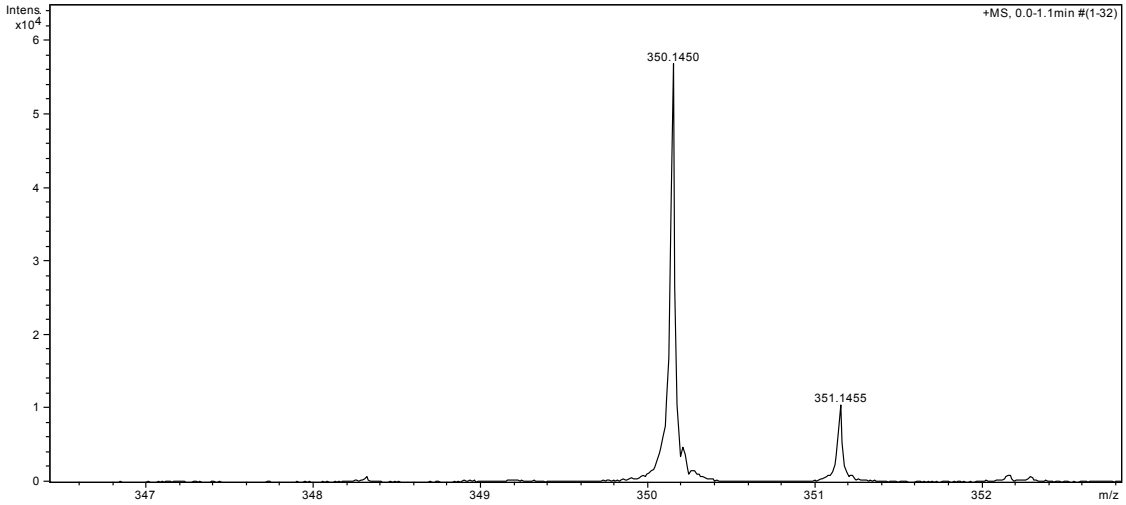

Figure S45. ESI-TOF-MS spectrum of compound **12**.

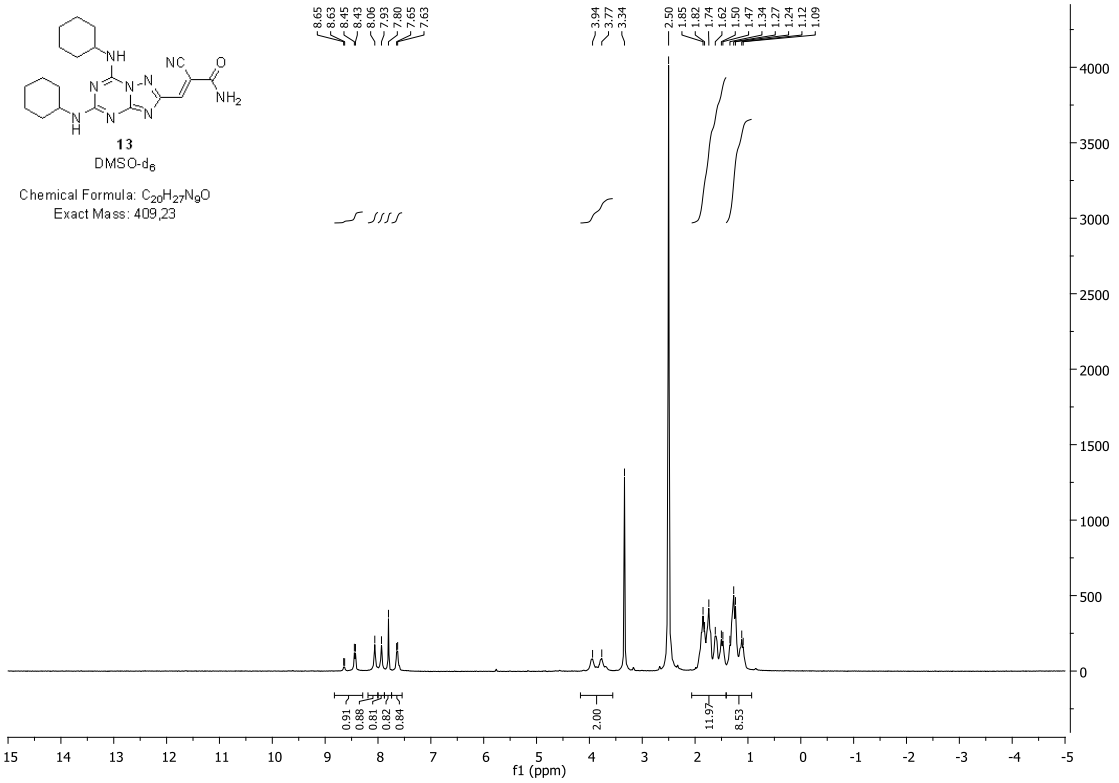

Figure S46. ^{1}H-NMR spectrum of compound **13**.

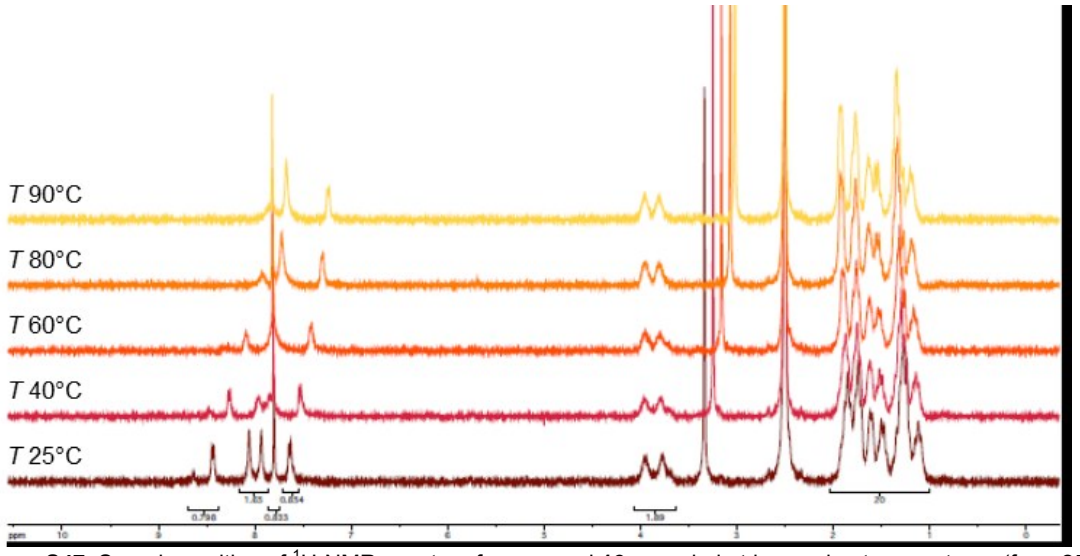

Figure S47. Superimposition of ^{1}H-NMR spectra of compound **13** recorded at increasing temperatures (from 25 °C to 90 °C).

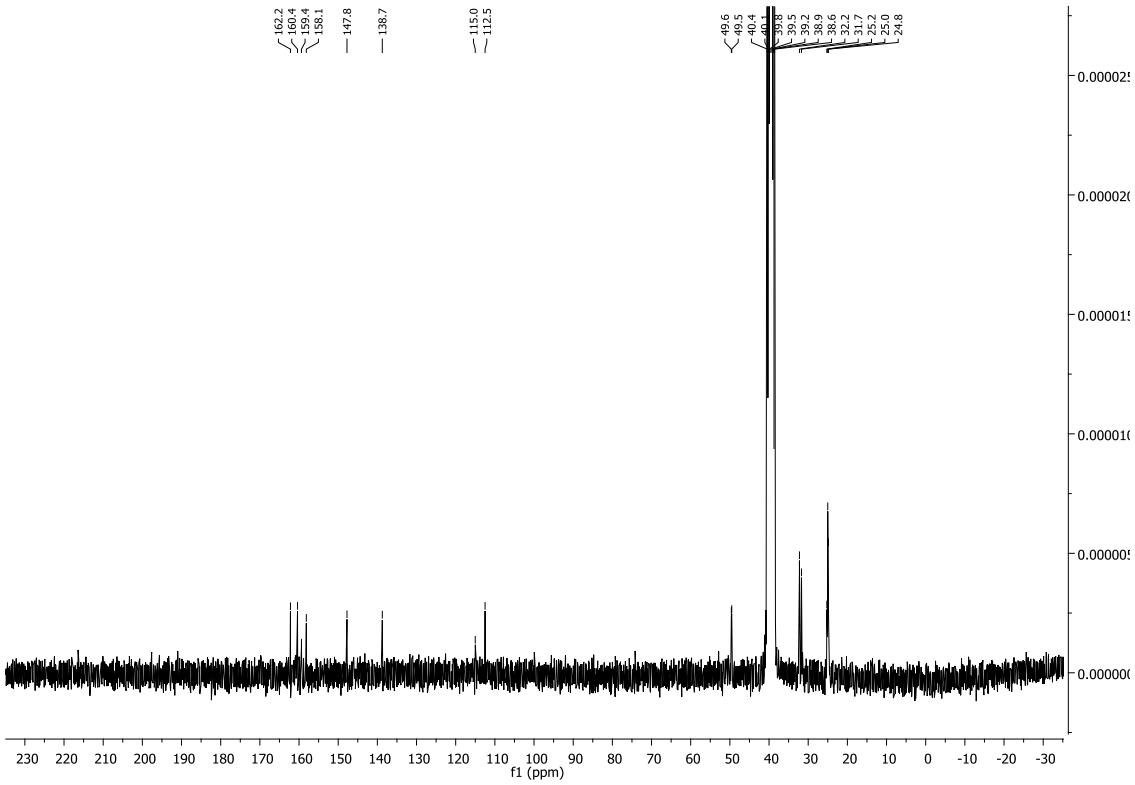

Figure S48. ^{13}C-NMR spectrum of compound **13**.

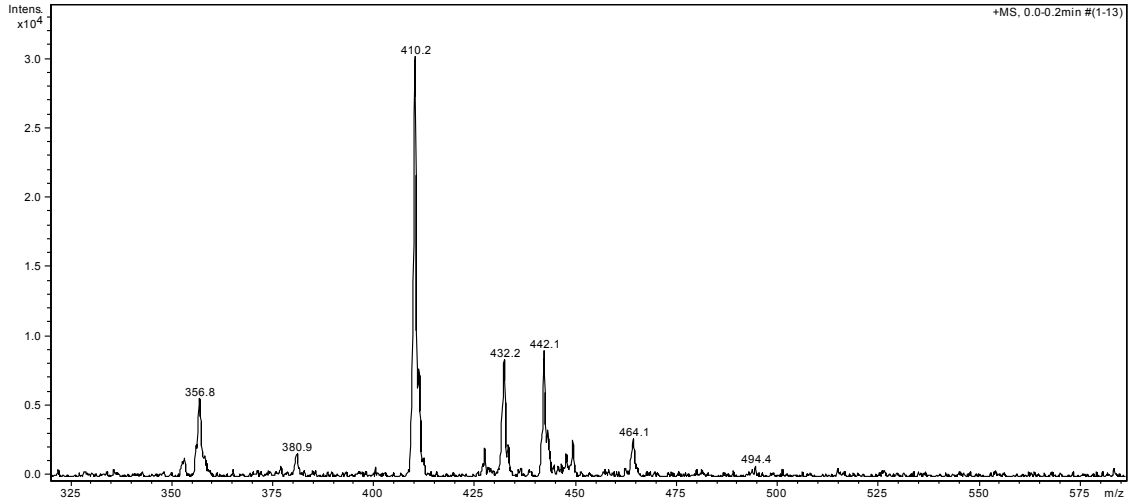

Figure S49. ESI-IT-MS spectrum of compound **13**.

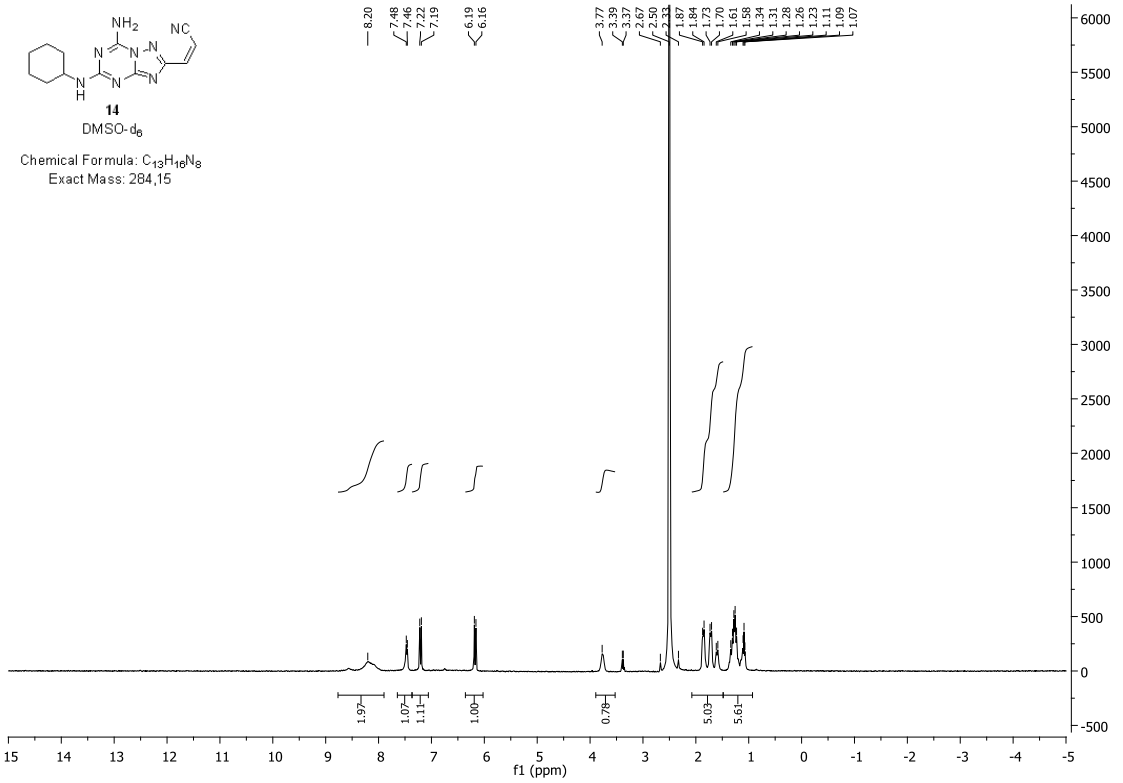

Figure S50. ^{1}H-NMR spectrum of compound **14**.

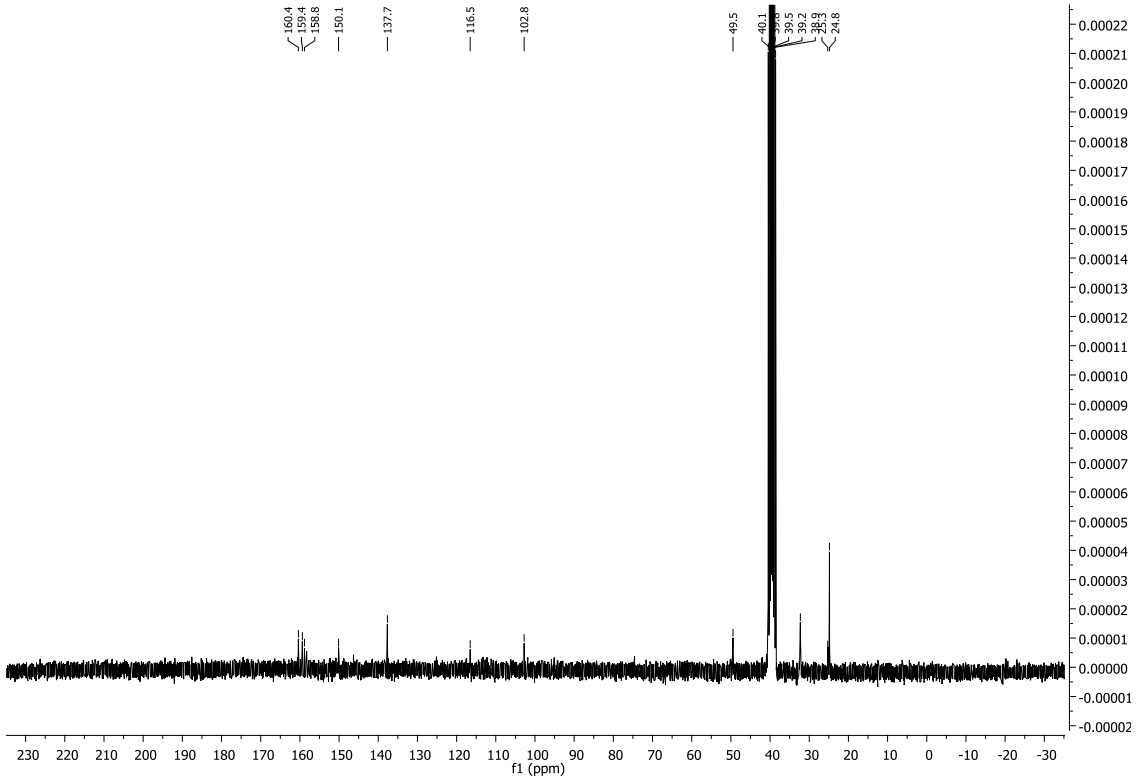

Figure S51. ^{13}C-NMR spectrum of compound **14**.

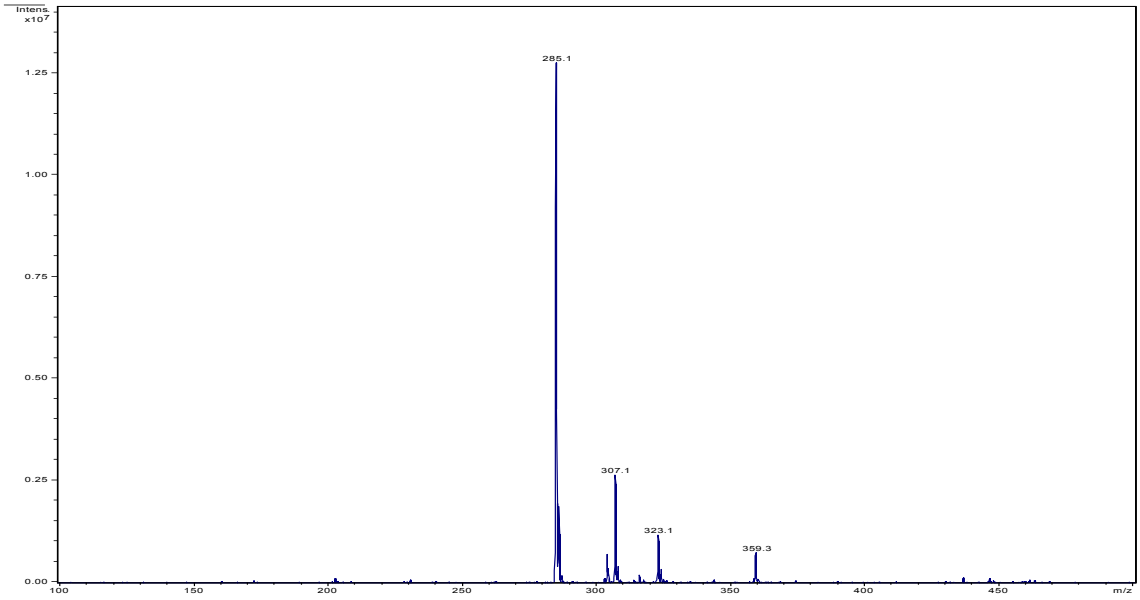

Figure S52. ESI-MS spectrum of compound **14**.

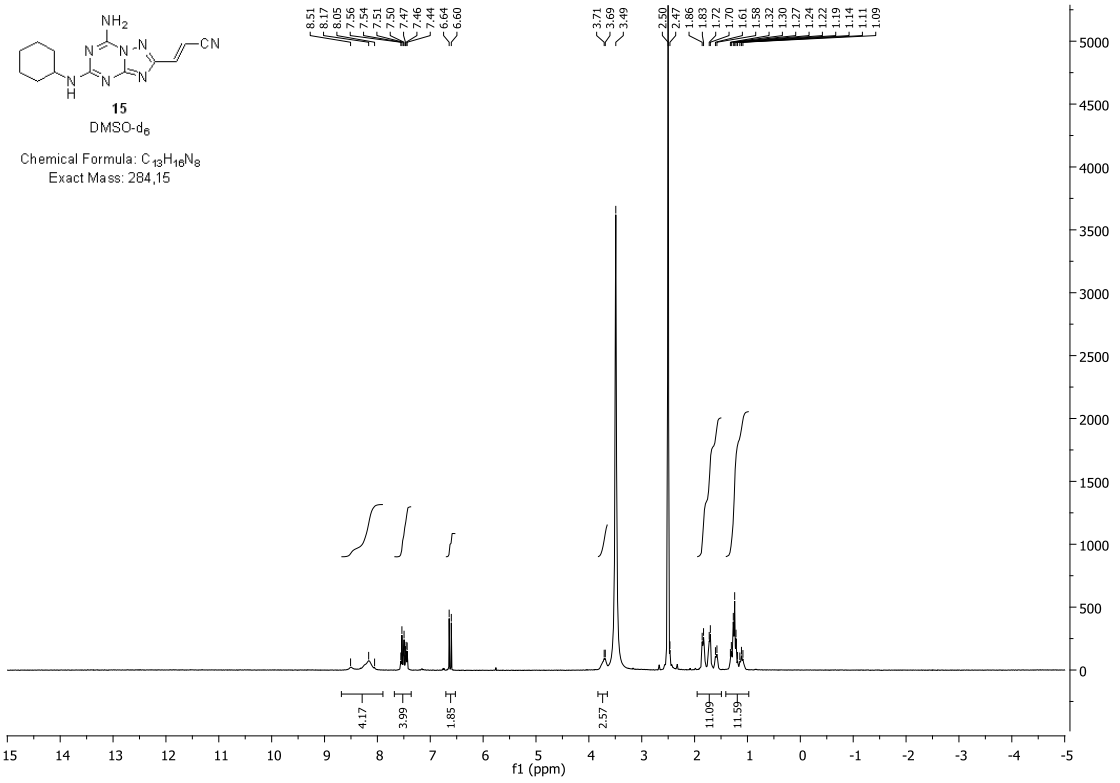

Figure S53. ^{1}H-NMR spectrum of compound **15**.

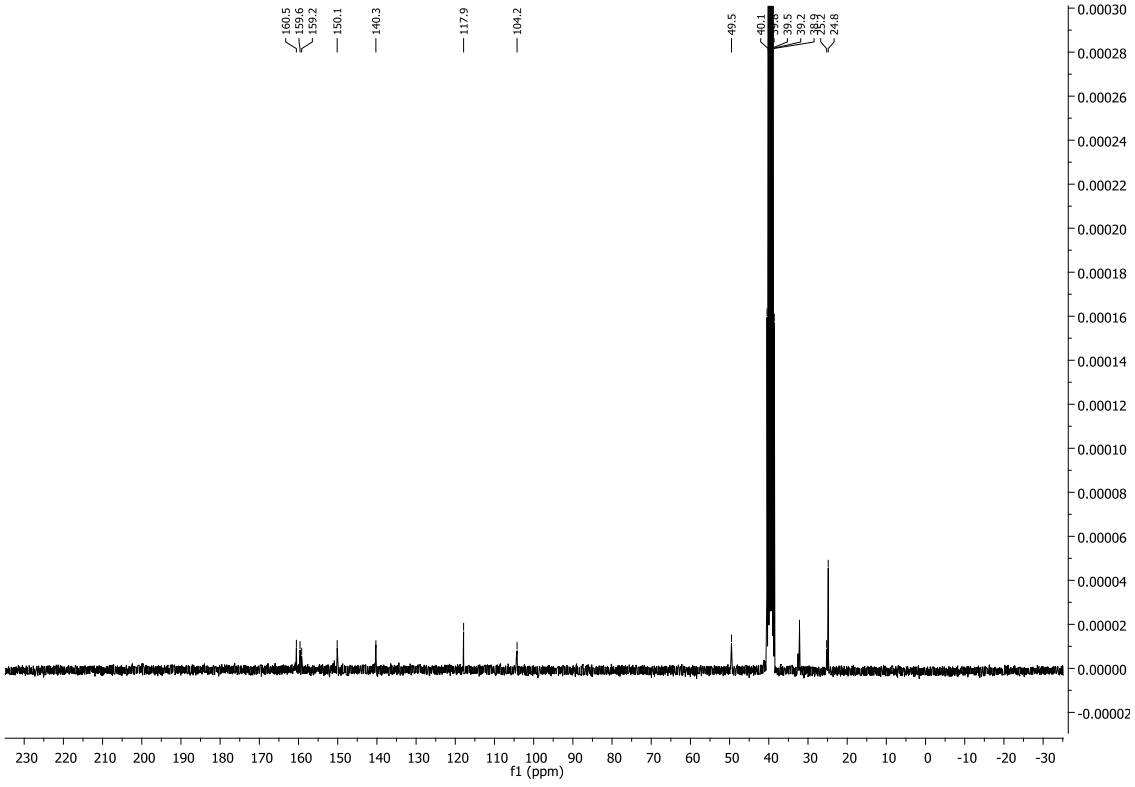

Figure S54. ^{13}C-NMR spectrum of compound **15**.

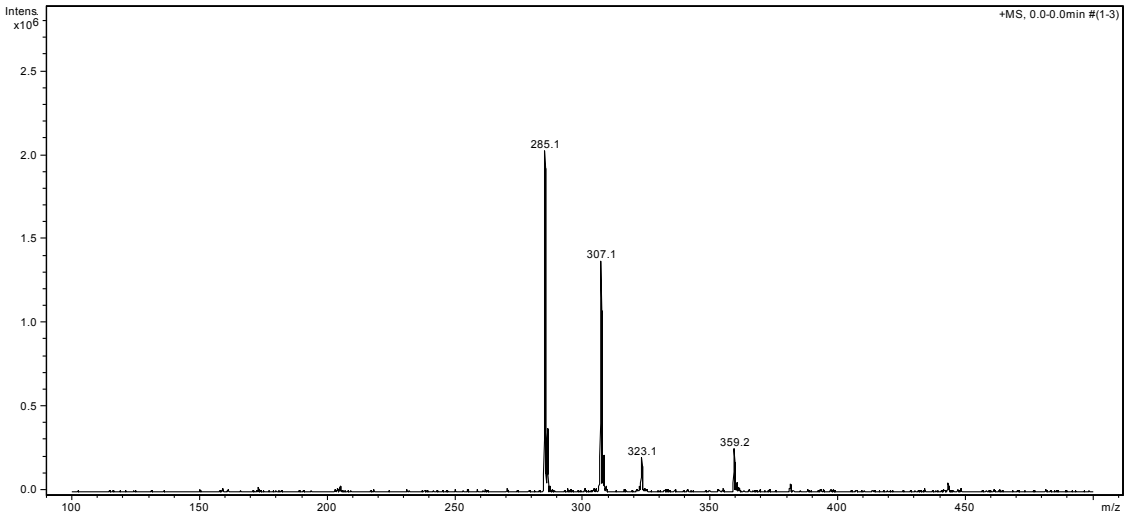

Figure S55. ESI-MS spectrum of compound **15**.

References

[1] F.C. Schaefer, J.T. Thurston, J.R. Dudley, *J. Am. Chem. Soc.* **1951**, *73*, 2990.

[2] P.W.R. Caulkett, G. Jones, M. McPartlin, N.D. Renshaw, S.K. Stewart, B. Wright, *J. Chem. Soc. [Perkin 1]* **1995**, *7*, 801.

[3] J. Hutton (Imperial Chemical Industries), US5326869, **1994**.

[4] P.W.R. Caulkett, G. Jones, M. Collis, S. Pouche (Imperial Chemical Industries), EP0459702 A1, **1991**.

[5] H. Tsumoki, J. Shimada, H. Imma, A. Nakamura, H. Nokaka, S. Shiozaki, S. Ichikawa, T. Kanda, Y. Kuwana, M. Ichimura, F. Suzuki (Kyowa Hakko Kogyo Co Ltd), EP0976753 A1, **1998**.

[6] J.N. Moorthy, N. Singhal, *J. Org. Chem*. **2005**, *70* (5), 1926.

[7] A. Pintér, G. Haberhauer, *Eur. J. Org. Chem*. **2008**, (14), 2375.

[8] E. Baloglu, S. Ghosh, M. Lobera, D.R. Schmidt (Tempero Pharmaceuticals, Inc.), WO2013019621A1, **2013**.

[9] I.M. Serafimova, M. Pufall, S. Krishnan, K. Duda, M.S. Cohen, R.L. Maglathlin, J.M. McFarland, R.M. Miller, M. Frödin, J. Taunton, *Nat. Chem. Biol*. **2012**, *8* (5), 471.

[10] H.H. Wasserman, A.K. Petersen, *Tetrahedron Lett*. **1997**, *38* (6), 953.

[11] D.I. Perez, S. Conde, C. Pérez, C. Gil, D. Simon, F. Wandosell, F.J. Moreno, J.L. Gelpí, F.J. Luque, A. Martínez, *Bioorg. Med. Chem*. **2009**, *17* (19), 6914.

[12] A. Baki, A. Bielik, L. Molnár, G. Szendrei, G.M. Keserü, *Assay Drug Dev. Technol.* **2007**, *5* (1), 75

[13] I.G. Salado, M. Redondo, M.L. Bello, N.F. Liachko, B.C. Kraemer, L. Miguel, M. Lecourtois, C. Gil, A. Martinez, D.I. Perez, *J. Med. Chem*. **2014**, *57* (6), 2755.

[14] K. Bettayeb, N. Oumata, A. Echalier, Y. Ferandin, J.A. Endicott, H. Galons, L. Meijer, *Oncogene* **2008**, *27*, 5797.

[15] D.I. Perez, V. Palomo, C. Pérez, C. Gil, P.D. Dans, F.J. Luque, S. Conde, A. Martínez, *J. Med. Chem*. **2011**, *54* (12), 4042.

[16] L. Di, E.H. Kerns, K. Fan, O.J. McConnell, G.T. Carter, *Eur. J. Med. Chem*. **2003**, *38* (3), 223.

[17] A. Avdeef in *Absorption and drug development: solubility, permeability and charge state*, (Ed. A. Avdeef), *John Wiley & Sons,* Hoboken, **2003**, pp. 139-142.

[18] Stardrop™, version 6.2, Optibrium Ltd, http://www.optibrium.com/stardrop/stardrop-adme-qsar-models.php.

[19] T.T. Wager, P. Galatsis, R.Y. Chandrasekaran, T.W. Butler, J. Li, L. Zhang, S. Mente, C. Subramanyam, S. Liu, A.C. Doran, C. Chang, K. Fisher, S. Grimwood, J.R. Hedde, M. Marconi, K. Schildknegt, *ACS Chem. Neurosci.* **2017**, 8 (9), 1995.

[20] C.Aslanidis and P. J.de Jong Ligation-independent cloning of PCR products (LIC-PCR) *Nucleic Acids Research, Vol. 18, No. 20*

[21] W. Kabsch, *Acta Crystallogr, Sect. D.* **2010**, *66*, 125.

[22] A.A. Vagin, M.N.Isupov. *Acta Crystallogr. Sect. D.* **2001**, *57*, 1451.

[23] R. Bhat, Y. Xue, S. Berg, S. Hellberg, M. Ormö, Y. Nilsson, A.C. Radesäter, E. Jerning, P.O. Markgren, T. Borgegård, M. Nylöf, A. Giménez-Cassina, F. Hernández, J.J. Lucas, J. Díaz-Nido, J. Avila, *J.Biol.Chem.* **2003**, *278*, 45937.

[24] P. Emsley, B. Lohkamp, W.G. Scott, K. Cowtan, *Acta Crystallogr. Sect. D*. **2010**, *66*, 486.

[25] G.N. Murshudov, A.A. Vagin, E.J. Dodson, *Acta Crystallogr. Sect. D.* **1997**, *53*, 240.

[26] R.M.C. Di Martino, A. De Simone, V. Andrisano, P. Bisignano, A. Bisi, S. Gobbi, A. Rampa, R. Fato, C. Bergamini, D.I. Perez, A. Martinez, G. Bottegoni, A. Cavalli, F. Belluti, *J. Med. Chem*. **2016**, *59* (2), 531.

[27] T. Halgren, *J. Comput. Chem*. **1996**, *17* (5–6), 490.

[28] M. Totrov, R. Abagyan in *Drug Receptor Thermodynamics : Introduction and Applications*, (Ed: R.B. Raffa), *John Wiley and Sons*, Chichester, **2001**, pp. 603-624.

[29] M. Totrov, R. Abagyan, *Proc. third Annu. Int. Conf. Comput. Mol. Biol. - RECOMB '99*, **1999**,:312.

[30] J.J.P. Stewart, *J. Mol. Model*. **2007**, *13* (12), 1173.

[31] Molecular Operating Environment (MOE). Version 2014.09. Chemical Computing Group (CCG) Inc., Available from: http://www.chemcomp.com.

[32] A. Cuzzolin, M. Sturlese, I. Malvacio, A. Ciancetta, S. Moro, *Molecules*. **2015**, *20* (6), 9977.

[33] a) GOLD Suite, Version 5.2. Cambridge Crystallographic Data Centre: 12 Union Road, Cambridge, UK; b) O. Korb, T. Stützle, T.E. Exner, *J. Chem. Inf. Model*. **2009**, *49* (1), 84; c) G. Jones, P. Willett, R. Glen, A. Leach, R. Taylor, *J. Mol. Biol*. **1997**, 267, 727.

[34] E. Bakhite, A. Abdel-Rahman, E. Al-Taifi, *J. Chem. Res.* **2005**, *3*, 147.

[35] S.A. de Keczer, M.R. Masjedizadeh, S.Y. Wu , T. Lara-Jaime, K. Comstock, C. Dvorak, Y.Y. Liu, W. Berger, *J. Label Compd. Radiopharm*. **2006**, *49*, 1223.

[36] S. Federico, A. Ciancetta, N. Porta, S. Redenti, G. Pastorin, B. Cacciari, K.N. Klotz, S. Moro, G. Spalluto, *Eur. J. Med. Chem.* **2016**, *108*, 529.

[37] G. Rena, J. Bain, M. Elliott, P. Cohen, *EMBO Rep.* **2004**, *5* (1), 60.

[38] J.T. Henderson, M. Piquette-Miller, *Clin. Pharmacol. Ther*. **2015**, *97* (4), 308.

[39] J.L. Mikitsh, A. Chacko, *Perspect. Med. Chem.* **2014**, *6*, 11.

[40] D.I. Pérez, M. Pistolozzi, V. Palomo, M. Redondo, C. Fortugno, C. Gil, G. Felix, A. Martinez, C. Bertucci, *Eur. J. Pharm. Sci.* **2012**, *45* (5), 677.

[41] M.W. Pantoliano, E.C. Petrella, J.D. Kwasnoski, V.S. Lobanov, J. Myslik, E. Graf, T. Carver, E. Asel, B.A. Springer, P. Lane, F.R. Salemme, *J. Biomol. Screening* **2001**, *6*, 429.

[42] L. Schuldt, M.S. Weiss, "Stabilization of proteins for crystallization–how Thermofluor can help" AK1 Biological Structures, Newsletter, March 2010, can be found under http://www.beta-sheet.org/resources/T20-EMBL-Hamburg.pdf

[43] R. Dajani, E. Fraser, S.M. Roe, N. Young, V. Good, T.C. Dale, L.H. Pearl, *Cell* **2001**, *105*, 721.

[44] E.T. Haar, J.T. Coll,D.A. Austen, H.M. Hsiao, L. Swenson, J. Jain, *Nature Struct. Biol.* **2001**, *8*, 593.

[45] M. Aoki, T. Yokota, I. Sugiura, C. Sasaki, T. Hasegawa, C. Okumura, K. Ishiguro, T. Kohno, S. Sugio, T. Matsuzaki, *Acta Crystallogr. Sect. D.* **2004**, *60*, 439.

[46] C.J. Yuskaitis, R.S. Jope, *Cell Signal*. **2009**, 21 (2), 264.

[47] a) Z. Arraf, T. Amit, M.B.H. Youdim, R. Farah, *Neurosci. Lett*. **2012**, *516* (1), 57; b) R.J. Smeyne, V. Jackson-Lewis, *Mol. Brain Res*. **2005**, *134* (1), 57.

[48] a) R.J. Smeyne, V. Jackson-Lewis, *Mol. Brain Res*. **2005**, *134* (1), 57; b) F. Blandini, M.T. Armentero, E. Martignoni, *Park. Relat. Disord*. **2008**, *14*, 124.

[49] C.A. Lazzara, Y.H. Kim, *Front. Neurosci*. **2015**, *9*, 1.

[50] a) F. L'Episcopo, C. Tirolo, S. Caniglia, N. Testa, M.C. Morale, M.F. Serapide, S. Pluchino, B. Marchetti, *J. Mol. Cell. Biol*. **2014**, *6*, 13; b) F. L'Episcopo, M.F. Serapide, C. Tirolo, N. Testa, S. Caniglia, M.C. Mor

SUPPORTING INFORMATION

Author Contributions

Dr Stephanie Federico and Prof. Andrea Cavalli (equal), Prof. Giampiero Spalluto, Prof.Ana Martinez and Dr Paola Storici (supporting): study conception

Dr Sara Redenti (lead), Irene Marcovich, Dr Teresa De Vita, Dr Concepción Pérez, Maicol Bissaro, Prof.Stefano Moro, DR. Paola Bisignano, Dr Giovanni Bottegoni, Dr Stephanie Federico formal analysis and data acquisition

Dr Sara Redenti (lead), Dr Stephanie Federico (supporting): synthesis

Dr Sara Redenti, Irene Marcovich, Dr Teresa De Vita, Dr Concepción Pérez, Dr Rita De Zorzi, Dr Paola Storici, Dr Nicola Demitri, Dr Daniel Perez (supporting), Dr Paola Bisignano, Dr Giovanni Bottegoni, Prof Ana Martinez, Prof Stefano Moro, Prof Giampiero Spalluto, Prof Andrea Cavalli, Dr Stephanie Federico: data curation

Dr Sara Redenti, Dr Teresa De Vita, Dr Paola Storici, Prof Ana Martinez, Dr Paola Bisignano, Dr Stephanie Federico: experimental design

Prof Stefano Moro, Prof Giampiero Spalluto, Prof Andrea Cavalli: funding acquisition

Dr Stephanie Federico (lead), Prof. Andrea Cavalli: project administration

Dr Stephanie Federico and Dr Sara Redenti (equal): writing of original draft